Ontario Hydro

RESEARCH DIVISION

91602
new 82-10

ontario hydro
research division

FLOW DISTRIBUTION AND TUBE VIBRATION IN HEAT EXCHANGERS

Report No 86-329-K

H.L. Anderson
Engineer
Plant Equipment Dynamics Section
Mechanical Research Dept

ABSTRACT

The work described in this report was carried out under the auspices of Canadian Electrical Association as CEA project 118 G 278. CEA Project 118 G 278 was undertaken to study flow distribution and tube vibration in heat exchangers. An experimental program was carried out on a full-size heat exchanger in four test phases of parametric study. Flow induced tube vibration data was used to quantify and develop non-intrusive vibration monitoring techniques for on-line problem evaluation and to study the influence of design features and conditions on the vibration. The results of the study proved the effectiveness of the monitoring techniques and point the way for further development for long-term monitoring for predictive maintenance. The data have provided new insights for the design and operation of heat exchangers with respect to vibration.

job	file	date	report no.
27-524-052	825.4	January 20, 1987	86-329-K

91602
new 82-10

ontario hydro
research division

EXECUTIVE SUMMARY

FLOW DISTRIBUTION AND TUBE VIBRATION IN HEAT EXCHANGERS

H.L. Anderson

The project objective was to investigate flow induced tube vibration in heat exchangers with reference to the following aspects:

(a) Evaluation and development of monitoring techniques for the detection of damaging vibration in operating heat exchangers.

(b) Evaluation of methods for reduction of that vibration by field modification to the exchanger or operating procedure.

(c) Determination of the effect of common design features on the flow distribution and tube vibration in the exchanger.

The experimental program was carried out on a full size heat exchanger, the design of which was modified over four test phases to enable parametric study.

The results obtained in the experimental program proved the accuracy and reliability of the vibroacoustic and microphone monitoring techniques. Developmental work on the techniques showed promise and the results have already been implemented in-service. The data on the tube vibration demonstrated several features of vibration behaviour which should be taken into consideration in the design and operation of heat transfer equipment.

It is recommended that future work be directed to the development of detection techniques for predictive maintenance monitoring over the life of an exchanger.

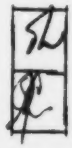

job	file	date	report no.
27-524-052	825.4	January 20, 1987	86-329-K

TABLE OF CONTENTS

		Page
1.0	INTRODUCTION	1
1.1	Historical Background:	1
2.0	DESCRIPTION OF TEST FACILITY	2
2.1	U-Tube Heat Exchanger	2
2.2	Pump and Motor Set	3
2.3	Holding Tank	3
2.4	Flow Control and Monitoring	3
2.5	Piping	4
3.0	EXPERIMENTAL TECHNIQUE AND INSTRUMENTATION	4
3.1	Vibroacoustic Technique	4
3.2	Microphone Technique	6
3.3	In-tube Vibration Monitoring	7
3.4	Pressure Drop Monitoring	9
3.5	Flow Visualization	10
4.0	EXPERIMENTAL PROCEDURE	10
4.1	Phase I	10
4.2	Phase II	13
4.3	Phase III	13
4.4	Phase IV	13
5.0	TEST RESULTS AND CONCLUSIONS	13
5.1	Vibroacoustic Technique	13
5.1.1	Onset of Impacting	13
5.1.2	Two Accelerometer Technique	15
5.2	Microphone Technique	16
5.2.1	Microphone Technique: Impact Tests	16
5.2.2	Microphone Technique: Monitoring With Flow	16
5.2.2.1	Phase I and II Data	17
5.2.2.2	Phase III Tests: Tube Row D Removed	17
5.3	Tube Vibration Data	18
5.3.1	Damping Data	19
5.3.2	In-tube Vibration Data as A Function of Flow	19

5.3.2.1 Phase I Data 20
5.3.2.2 Phase II Data 21
5.3.2.3 Phase III Data 22
5.3.2.4 Phase IV Data 24

5.4 Pressure Drop Data 27
5.5 Flow Visualization 28

6.0 SUMMARY AND RECOMMENDATIONS 29

6.1 Summary 29
6.2 Recommendations for Further Work 29

7.0 ACKNOWLEDGEMENTS 30

REFERENCES 32

TABLES 33

FIGURES 37

ontario hydro
research division

To Dr. D. Mills
Director
Research Division

FLOW DISTRIBUTION AND TUBE VIBRATION IN HEAT EXCHANGERS

1.0 INTRODUCTION

1.1 Historical Background: Flow-Induced Vibration In Heat Exchangers

The nature of the design of shell-and-tube heat exchangers renders elimination of tube vibration impossible. However, the phenomenon may severely limit the life of heat exchangers as fretting wear of the tube walls can lead to tube failure.

In recent years economic factors have placed greater reliability and performance demands on shell and tube exchangers. As a result, the phenomenon of flow-induced tube vibration has seen a marked increase in research activity and subsequent technical publications(1-7). Most of the research activity has been devoted to analysis and definition of the underlying mechanisms of flow-induced vibration. Four major mechanisms defined by the research to date are:

I	Fluid elastic instability:	observed in liquid, gas and two-phase flow
II	Periodic Wake Shedding Resonance:	not observed in two-phase flow.
III	Turbulent Buffeting Excitation:	observed in liquid, gas and two-phase flow.
IV	Acoustic Resonance:	observed in exchangers with gas on the shell side.

Mechanisms I and II will result in short-term failure of the exchanger if the equipment operation is maintained at conditions favourable to such phenomena. Turbulent buffeting (III) generally provides low level excitation which can result in deterioration of the condition of the heat exchanger tubes with

time. Acoustic resonance (IV) can result in tube failures if the acoustic mode in the shell matches that of the tubes. It can also result in unbearably high ambient noise levels and can result in failure of foundations, supports, piping etc. Acoustic resonance is not dealt with in this project.

Owing to the complex mechanical design of shell and tube heat exchangers, most of the research on vibration mechanisms has been performed on idealized, single span tube bundles in air or water test rigs. However, there is a need for research on the manifestation of vibration in full-scale heat transfer equipment with specific reference to the following:

1. Development of techniques to determine the susceptibility of in-service heat exchangers to flow induced vibration.

2. Evaluation of the effect of specific design features on vibration in exchangers.

3. Evaluation of field modifications on the vibration performance of a heat exchanger.

In this project the three aspects outlined above are addressed in an experimental program using a full-scale heat exchanger. The results of the project are discussed in conjunction with the results of a previous experimental program with another heat exchanger design as well as data from experience with operating exchangers.

2.0 DESCRIPTION OF TEST FACILITY

The experimental program was carried out in the Experimental Heat Exchanger Test Facility at Ontario Hydro's Research Division. A photograph of the facility is shown in Figure 1. The major components of the Test Facility are described below.

2.1 U-Tube Heat Exchanger

In order to effect the design changes necessary for parametric study a specially designed heat exchanger was purchased for this project. The exchanger is of a U-tube design with the following features:

(a) Tubes are ferruled into the tubesheet to permit removal of tubes and change of baffle positions. The ferruled end condition did not significantly affect the mechanical properties of the tubes.

(b) Segmented shell to facilitate design changes with minimum of component handling.

(c) Viewing windows in U-Bend end to permit flow visualization.

(d) Compatibility of bundle and shell with existing heat exchanger.

The design details of the heat exchanger manufactured for this project and those of the previous exchanger in the facility are documented in Table I and Figures 2 through 7. The major differences in design between the two exchangers are:

(a) The previous design has an impingement plate at the inlet while the present exchanger does not.

(b) The tube pitch is larger (and the number of tubes smaller) in the present design to accommodate the ferrules.

(c) There is a horizontal baffle in the U-Bend end in the previous exchanger which was omitted in the present design. The purpose of the baffle was to reduce by-passing of the flow around the end of the bundle.

2.2 Pump and Motor Set

The test loop has a 30 kW centrifugal pump and motor with a capacity of 100 L/s. The pump components are 316 SS to avoid corrosion problems. The pump is arranged in the loop for horizontal discharge.

2.3 Holding Tank

The heat exchanger test loop is of a closed-loop design with a 9400 L fibreglass holding tank. Demineralized water is used in the loop to reduce corrosion problems.

2.4 Flow Control and Monitoring

The flow rate through the loop was monitored by a turbine flow meter installed in the loop piping approximately twelve diameters downstream of the pump and approximately twelve diameters upstream of the heat exchanger inlet nozzle.

The flow rate through the loop was regulated with a 30 kW ac speed controller. The speed controller permitted flow control without valves and by-passing which may introduce flow noise and

vibration in the system. The controller is governed by a feedback loop to the flow meter which enables the flow to be held at a specific level.

2.5 Piping

All loop piping components are made of PVC to reduce corrosion. Two PVC gate valves are positioned immediately upstream and downstream of the holding tank to permit isolation of the heat exchanger. In operation these valves are fully open to avoid flow disturbance.

3.0 EXPERIMENTAL TECHNIQUES AND INSTRUMENTATION

The instrumentation used for the experimental program will be documented in conjunction with the technique description.

3.1 Vibroacoustic Technique

The vibroacoustic technique is used for on-line monitoring of tube impacting in shell-and-tube exchangers. The technique is simply a sophisticated "listening" procedure analogous to the use of a stethoscope in medicine.

The impact of a tube on a baffle plate in a heat exchanger imparts energy to the baffle plate which is then transmitted through the exchanger in the form of plate waves. The plate waves are detected on the shell of the exchanger by an accelerometer mounted on the outside wall. The accelerometer is the "stethoscope" of the system. The plate waves can excite a carrier wave such as the accelerometer mounted resonance which will help to amplify the signal.

The frequency range of interest for the vibroacoustic technique is 1 kHz to 10 kHz in the audible range. The audible range is desirable as direct audio monitoring of the impact sounds provides positive feedback for signal authentification. There are drawbacks to audio monitoring in that the signal-to-noise ratio can be severely reduced by other audible phenomena such as flow noise; however, the background noise level can be reduced by judicious filtering and the human ear is extremely sensitive in discerning impacts within the background noise.

The monitoring system used for the vibroacoustic technique is sketched in Figure 8 and described below:

A piezoelectric accelerometer is mounted on the external wall of the shell of the exchanger. The accelerometer can be mounted temporarily by a magnet or more permanently to an electrically isolated stud. The mounted resonance of the accelerometer will

change according to the mounting method and should be determined on installation. The signal from the accelerometer is passed through a charge amplifier which conditions the high impedance accelerometer signal for the low impedance monitoring and analysis instrumentation. The signal can then be tape recorded for further analysis.

The signal is analyzed by three methods:

1. direct audio monitoring (also performed when tape recording in the field)
2. frequency domain analysis
3. time domain analysis

As discussed previously, direct audio monitoring is useful in detecting the presence of impacting in the signal. The most effective band pass filter for reduction of background noise levels is also determined by audio monitoring of the signal while filtering. Experience has shown that band pass filtering to the 1 kHz to 7 kHz range is most effective in reducing high frequency flow noise and lower frequency machinery noise.

Frequency domain analysis may be used in the vibroacoustic signal analysis; however, it is not the powerful technique it is in other vibration monitoring techniques. In the vibroacoustic technique frequency analysis is most useful for determining the accelerometer mounted resonance, machinery frequencies and the range of flow noise frequencies. Occasionally the natural frequency of the impacting tube will be detected in the spectrum but it is a rare occurrence. Tube frequencies are generally below 100 Hz so their acceleration levels are low compared to the order of magnitude higher frequencies of the mounted resonance and flow noise. In addition severe tube impacting is a highly non-linear phenomenon in which the tube impact with the baffle is often random in time. Time domain analysis is the best method for determining impacting frequency.

The signals from the accelerometers can be viewed in the time domain on an oscilloscope. The impacts will appear as bursts of higher amplitude above the constant background noise from the exchanger.

Time domain charting of the signals requires additional signal processing to overcome physical limitations on the pen response on the strip-chart records. Most commercial strip-chart recorders have an upper frequency limit of 50 Hz. In order to chart the audio range signals the data must be full-wave rectified and passed through an envelope detector circuit. Each impact above a specified threshold value will trigger the detector circuit which will drive the recorder to chart the

peak. The strip-chart record of impact peaks can be used to determine the frequency of occurrence of the impacts by a simple count of peaks over a given chart time. The magnitude of the peaks are used as documentation of the state of the problem for reference to previous data.

Time domain analysis is used in the two-accelerometer technique to determine the time delay between one accelerometer detecting the impact and the second detection a distance along the shell. For this analysis a two channel FFT analyzer is used in the instantaneous capture mode.

3.2 Microphone Technique

The microphone technique is used to locate impacting tubes in the bundle. The technique consists of aural monitoring of the sound emitted by each tube as detected by a microphone held in one end of the tube with the other end plugged. The technique has proven highly effective in previous work in locating impacting tubes in large exchangers; eg, the tubesheet of a U-tube exchanger of 2,000 tubes was scanned in one shift with the successful identification of ten problem tubes with severe fretting induced wear that was later identified by eddy-current tests. The tubesheet must be exposed and the tubeside drained for application of the technique, conditions necessary for in-tube work in any outage. In addition, shellside flow at operating rates is required for tube excitation.

In the field the technique is used to reduce the amount of in-tube work required in an exchanger by identifying problem areas. In general a qualitative assessment has proven sufficient. However, quantitative verification is necessary for the further development of the technique. In this project the microphone technique was examined in detail.

The instrumentation used with the microphone technique is extremely simple. An inexpensive microphone connected via an amplifier to a speaker or headphone set comprises the system. In order to adapt the end of the microphone to the tube-ends and achieve a good seal, a rubber battery cable clip cover is fitted over the end of the microphone and inserted in the tube. The other end of the tube is plugged by a rubber stopper.

The laboratory instrumentation set-up for the microphone technique is shown in Figure 9. The field system is portable and battery powered. All components of the field system can be purchased at any retail electronic components supply store.

In analysis of the microphone signals direct audio monitoring and time and frequency domain techniques were used as described

for vibroacoustic technique. A description of the experimental procedure used to study the microphone technique is contained in Section 4.

The hypothesis for the technique is that the impact of a tube on a baffle (or another tube) excites an "organ pipe" mode of the column of air in the tube. It is these "organ pipe modes" which are detected by the microphone. The hypothesis arose from audio monitoring of low frequency "thumping" sounds that were detected by the microphone in tubes which were later verified by in-tube monitoring to be impacting.

A single impact may be viewed as a broad-band excitation to which the air column in the tube responds at its natural frequency. The acoustic modes of the various lengths of tubes in the exchanger have been listed in Table II. The calculations are based on the assumption of closed end conditions at both ends of the tubes.

A series of periodic impacts at the tube natural frequency may force an acoustic mode at that frequency which may be significantly different from the natural acoustic mode frequency. In contrast, where the tube is impacting at a rate close to that of the acoustic mode there may be feedback from the mechanical vibration to produce a strong acoustic signal.

The evaluation of the hypothesis of the microphone technique in this project concentrated on proving that the low frequency signals detected in tubes using the microphone were in fact initiated by impacting. In conjunction with this "proof-of-concept" work the sensitivity of the technique was determined.

3.3 In-Tube Vibration Monitoring

Tube vibration data were obtained using the in-tube biaxial accelerometer system as sketched in Figure 10(a).

The biaxial accelerometer probe design is shown in Figure 10(b). The probe head is made up of two mini-accelerometers which are mounted 90° to each other. The accelerometers have integral preamplifiers which condition the signals at the source and eliminate the effects of low frequency cable motion. The two criteria that had to be satisfied by the probe design were:

(i) Minimum dimensions to permit passage of probe into the U-bend.

(ii) No relative motion permitted between probe and tube when vibration measurement is in progress.

To achieve these two conflicting criteria the probe employs a pneumatic locking mechanism. A cable is pushed out of the probe head at the measurement position to lock the probe in place. The cable is driven by an air cylinder which is located in the probe cable in a position such that the cylinder will not need to pass into the U-Bend of the tube. The total length of the cable between the air cylinder and the accelerometer head is equal to the distance along the tube from the tangent point in the straight leg to the 90° position in the largest radius U-bend. Air is supplied to the cylinder through an air line via a regulator and actuator mechanism housed in the conditioning amplifier box.

In order to document the tube vibration the probe was positioned in the tubes at the mid-span and baffle positions as shown in Figures 3 and 7. The U-Bend motion was measured primarily at the 90° position in the bends.

The orientation of the probe accelerometers relative to the horizontal and vertical axes of the exchanger could not be held constant as the probe was pushed through the tube due to the need for a flexible cable for passage into the U-Bends. For this reason the data for both axes is given.

The system for tube identification in the in-tube work is shown in Figure 2. Because the minimum size of the probe was limited by the accelerometer dimensions the probe could not pass into tubes in vertical rows 6 through 9, the smallest radii tubes.

The acceleration signals from the probe were passed to the instrumentation rack for analysis via the biaxial accelerometer conditioning amplifier box as shown in Figure 10(a). The conditioning amplifier adjusted the gain and impedance of the signals to meet the requirements of instrumentation rack circuitry.

The biaxial accelerometer signal analysis circuitry in the instrumentation rack permitted direct monitoring of the following data:

X(p-p)
Y(p-p)
X(pk)
Y(pk)
Z(pk) $(Z = \sqrt{x^2+y^2})$
Z(rms)

The data was monitored via integration circuits in velocity and displacement as well as acceleration. The integration circuits used Bessel filters to reduce overshoot at extremely low frequencies.

The time domain data was recorded directly on the strip chart recorder or digitally plotted via the dual channel analyzer.

The data was analyzed in the frequency domain using the dual channel FFT analyzer and plotted with the associated digital plotter.

The tube vibration data obtained with the biaxial accelerometer probe system was used for the following purposes:

1. Calibration and verification of microphone and vibroacoustic techniques.

2. Documentation of vibration levels in the exchanger with respect to the effect on vibration of specific design features.

3.4 Pressure Drop Monitoring

Overall pressure drop was measured in the exchanger between the inlet and outlet nozzles. Due to maldistribution of flow in the nozzles average pressure was measured from a ring of four pressure taps positioned around each nozzle. The ring of taps on the inlet nozzle is clearly evident in Figure 1.

Baffle-to-baffle pressure drop was measured from the pressure taps shown in Figures 4 and 7 for the CEA exchanger and the previous exchanger design respectively.

The lines from the pressure taps were connected via manifolds and switches to two Rosemount differential pressure cells, one for 0-50 kPa and one for 0-250 kPa. The two cells were required to cover accurately the range of pressure drops measured in the tests. The panel housing the manifolds, switches and pressure transducers is shown in Figure 1.

Pressure tap position for measurement was selected by the switches on the panel. The transducer signals were routed to the main instrumentation rack shown in Figure 1 where digital read-outs of both overall and baffle-to-baffle pressure drops could be obtained.

3.5 Flow Visualization

In preparation for this project windows were installed diametrically opposite each other in the U-Bend shell segment of the CEA shell. The flow distribution in the U-Bend end was of special concern in this project as very little work had been done in this area.

The flow visualization was achieved by bubbling air into the exchanger through pressure tap 12, into the U-Bend zone (Figure 4). The distribution of the bubbles was monitored by still and motion photography. The process was limited to 60% flow rate; at high flows the bubbles broke up too rapidly to permit tracking of their progress in the U-Bend zone.

4.0 EXPERIMENTAL PROCEDURE

In this section the experimental procedure used in the project will be outlined. The experimental work was carried out in four test phases.

4.1 Phase I: Test Heat Exchanger In The As-Delivered Configuration

i. Tube natural frequencies and damping in quiescent fluid: With tubes empty, using in-tube accelerometers, the natural frequencies and damping of the tubes were determined by impact testing. The entire heat exchanger was excited with an instrumented hammer on the base, tubesheet and shell flanges. The above tests were repeated with the shell side filled.

ii. Determine threshold for tube impacting and monitor performance characteristics: Starting from zero flow the flow was increased in increments of 20 L/s. For these tests, the Hx was instrumented with shell-mounted accelerometers to monitor for tube impacting. At each flow rate, the following parameters were monitored and recorded:

- overall bundle pressure drop
- baffle-to-baffle pressure drop
- water temperature
- blade passing frequency
- shell mounted accelerometer signal.

iii. Location of impacting tubes: At the flow rate at which impacting was first detected, the

impacting tubes were located using a microphone.

Following the location of the impacting tube, the incremental increase in flow rate was continued up to 100% of system flow rate. At each flow step the following parameters were monitored:

- overall bundle pressure drop
- baffle-to-baffle pressure drop
- water temperature
- blade passing frequency
- shell mounted accelerometer signal
- microphone location of impacting tubes.

iv. Characterization of tube vibration: Following completion of steps (ii) and (iii), in-tube monitoring of tubes commenced. The biaxial accelerometer was inserted into each of the tubes identified as impacting. The flow rate was increased in increments of 20 L/s. At each flow rate the tube motion was monitored at each baffle and mid-span location. The tube acceleration, velocity and displacement were recorded in rms, and peak-to-peak format (only one half of each tube was monitored because of symmetry around the vertical centreline). Pressure drop, temperature and blade passing frequency data were monitored after each increment in flow.

At 100% flow, monitoring of selected tubes in all zones of the bundle was performed regardless of whether or not impacting was detected in them.

At positions in which a tube was observed to undergo a large degree of movement, flow sweeps were performed which consisted of monitoring tube displacement continuously as flow rate is increased.

The recorded signals were subsequently analyzed using a dual channel FFT analyzer to obtain power spectra, cross spectra, coherence and phase relationships for the data.

v. Flow visualization in the U-Bend zone was performed at 20%, 40% and 60% design flow. As

previously explained, the break-up of the bubbles was too rapid to permit flow visualization at flows in excess of 60% of full flow.

vi. Development of Vibroacoustic Technique: Developmental work was carried out with the vibroacoustic technique to determine the feasibility of using a time delay technique with two accelerometers to attempt to locate the impacting zone in the bundle.

In a controlled test with no flow in the exchanger, the shell was impacted at the U-Bend end with a suspended weight released from a fixed distance from the shell. The signals from seven accelerometers spaced along the length of the shell were monitored and the time delay for each accelerometer with respect to the accelerometer at the U-Bend determined using the dual channel analyzer.

Measurement of time delay between the axially separated accelerometers with impacting tubes at various flows was performed to test the technique for use in the field.

vii. Study of the microphone technique: In order to quantify the microphone technique developmental work was carried out in addition to the tests described in the previous procedures. The purpose of this work was two-fold:

(i) Proof of concept
(ii) Determination of sensitivity with respect to the vibroacoustic technique.

The response of tubes to a single impact was tested with the exchanger drained and the U-Bends exposed to gain access for impacting. The peripheral U-Bends were impacted once and the response monitored with the microphone at the tubesheet.

With increasing flow in the exchanger, the response of a tube visually observed to initiate impacting was used to check the sensitivity of the microphone with that of the in-tube accelerometer data and the vibroacoustic data.

4.2 Phase II: Vertical Tube-Pass Lane "Dummy" Tubes Removed

Tests (i) to (iv) were repeated with the four dummy tubes in the vertical tube-pass lane removed to determine the effect of opening up the tube-pass lane on flow distribution and tube vibration. The "dummy" tubes were replaced after this test was completed.

4.3 Phase III: Removal of First Tube Row Below the Baffle Edge: Row D

Tests (i) to (iv) were repeated with the tubes in Row D, the row immediately below the lower baffle edges (Figure 2) removed. These Row D tubes were identified in Phase I and II as the most susceptible to vibration and were the first to impact.

With the violently impacting tubes removed the sensitivity of the microphone technique (vii) to lower level impacting was evaluated using vibroacoustic and in-tube accelerometer data.

The tests in Phase III were performed with the tubeholes in the tubesheet plugged but the baffle plate holes left open. The purpose of this procedure is to test a potential field fix. The tube rows were replaced after the test Phase III was completed.

4.4 Phase IV: Six Baffle Configuration

Baffle spacing was increased to 0.592 m (from 0.441 m) to yield a baffle spacing-to-shell inside diameter ratio of 1.2 compared to 0.9 in the as delivered design. The increase in spacing was facilitated by the removal of two baffles. The six-baffle configuration is shown in Figure 11.

Tube D-2 (Figure 2) was removed for these tests. The increased baffle spacing resulted in tube D-2 sagging to touch the shell at the U-Bend end. The impact of tube D-2 on the shell would have dominated all data and was therefore removed. Tests (i) to (iv) were repeated in Phase IV.

5.0 TEST RESULTS AND CONCLUSIONS

5.1 Vibroacoustic Technique

5.1.1 Onset of Impacting

The vibroacoustic work in this CEA project benefitted greatly from the experience with the previous unit-shell exchanger design. The unit shell was made of 304 SS to reduce corrosion problems in the loop although all of our previous development work on the vibroacoustic technique in the field was on carbon

steel shells. The stainless steel shell proved to be completely "dead" from the vibroacoustic viewpoint: tapping on the shell only a few feet from the accelerometer produced little or no response at the accelerometer position. Discussion with the non-destructive testing group of OHRD revealed that the same behaviour is observed in the ultrasonic frequency range and is the result of the structure of the metal. The CEA segmented shell was manufactured of carbon steel to permit study of the vibroacoustic technique.

The vibroacoustic monitoring determined the following thresholds for onset of tube impacting:

Phase I;	as delivered design: flow	24 L/s or 24% max
Phase II;	dummy tubes removed:	26 L/s (26%)
Phase III;	tube row D removed:	29 L/s (29%)
Phase IV;	six baffle configuration:	13 L/s (13%)

Full-wave rectified signals from the accelerometer at the U-Bend end and at the tubesheet end, shown in Figure 12, demonstrate the onset of impacting for the Phase I configuration. This is representative of all tests performed.

Impacting is identified by the appearance of spikes in the signal. In Figure 12 the records indicate that the impacting commenced at approximately 24% of full flow (24 L/s) with the impacting more dominant at the U-Bend end, a dominance that is maintained over the whole range of flow tested.

At the onset of impacting a very small increase in flow resulted in a marked increase in impacting as shown by the records for 24 L/s and 24.5 L/s. The vibroacoustic signal then increased more gradually in magnitude with flow up to 60 L/s. At flows in excess of 60 L/s there was no significant change in the vibroacoustic signal.

The frequency of impacting could be determined by speeding up the strip chart to more clearly define the individual spikes. (In the rectification of the signals the impact spike level is held for 50 ms unless another impact triggers the circuit prior to that time; hence, the square appearance at higher chart speeds).

The frequency of impacting was approximately 14 Hz at low flows, increasing to 19 Hz at higher flows. In-tube monitoring corroborated these observations and demonstrated the effectiveness of the vibroacoustic technique. At 24 L/s tube D-2 was found to vibrate at the U-bend midspan position with a dominant frequency of 13.75 Hz. At higher flow rates the in-tube data revealed vibration at 12 Hz and 19 Hz.

The initiation of vibration at the U-Bend end could be readily observed through the viewing windows. These observations served to clearly define the distinction between onset of vibration and impacting. Tube D-2, the outermost tube in row D, the first row below the baffle edge, could be observed to vibrate at approximately 19 L/s for the Phase I tests. As flow was increased, the amplitude of this vibration increased until impacting on baffle eight could be observed and detected at 24 L/s.

5.1.2 Two Accelerometer Technique

The obvious dominance of impacting in the U-Bend end was used to develop the two-accelerometer technique for locating an impacting zone in a heat exchanger. The time delay between two axially separated accelerometers in detection of an impact at 24.4 L/s is shown in Figure 13.

In the no-flow control test of the two-accelerometer technique the time of detection of the impact was determined for each of the seven accelerometers spaced along the shell. The time delay for each accelerometer was then determined with respect to accelerometer A, the accelerometer at the U-Bend end and closest to the impact. The time delays are plotted in Figure 14. The results show an increase in Δt with increasing distance from the impact. The flanges between segments may enhance this effect; however, a definite increase in Δt was observed between positions B and C on the same shell segment enhancing confidence in the conclusions.

The plate wave velocities determined from these tests were in the range of 1000 m/s to 5000 m/s which is in agreement with data obtained by Bastl and Wach (8).

The results of the time delay tests with flow are plotted in Figure 15. The data revealed an unexpected result: the Δt's between positions A and B were greater than those between positions A and E; furthermore, the time delays between A and D were very much smaller than those measured between either A and B and A and E. The explanation of these observations is that tube impacting was also determined, by the in-tube technique, to be occurring at baffle six, position 12, which is located at accelerometer position D. The signal detected at position E could be either from A or D.

The flow tests indicate that the application of the two-accelerometer technique should be attempted at several

positions along the shell before any conclusions are drawn to take into account multiple impacting sites.

The technique has the potential to assist in locating tube leaks more quickly. This would reduce down-time due to fretting-induced leaks. Although further testing should be performed to verify the application of the technique these results are considered promising.

5.2 The Microphone Technique

In order to quantify the microphone technique and compare its sensitivity to the vibroacoustic technique, the data from the visually-observed impacting tube D-2, from the first two phases of the project, were used. To determine the sensitivity of the technique to lower-level impacting the data from the tests with row D removed, phase III, were used.

5.2.1 Microphone Technique: Impact Tests

The tests to determine the response of the microphone to a single direct impact to the subject tube were performed for both the eight-baffle and six-baffle designs. On examination of the results it was determined that the six baffle design provided a more definitive test as there was a 30% greater separation between the acoustic modes predicted by the length of the tube (Table II) and the mechanical vibration frequencies of the tubes. This greater separation of frequencies helped to clearly define what response was due to the modes in the air column and what was due, if any, to tube vibration.

The frequency spectra of the microphone response to direct impacts in tubes D-2, C-3 and B-4 are shown in Figures 16, 17 and 18 respectively. (Tube D-2 was not removed until it was discovered that it would touch the U-Bend head when replaced after the in-air microphone tests). The order of presentation is in terms of decreasing tube length. In the figures, the response frequency is shown to increase slightly with decreasing length: 20 Hz for D-2; 21 Hz for C-3; 21.5 Hz for B-4. These frequencies are very close to the organ pipes modes predicted for those tubes as listed in Table II. The first mode frequencies of these tubes, tested in air, were in the range of 10.0 to 11.0 Hz, the second mode frequencies monitored in these tubes were in the range of 26 to 28 Hz for the in-air tests.

The results of these tests indicate that the organ-pipe mode was excited in the air column in the tube by the impact. The tube impacts consisted of a single hit at the U-Bend. The vibration, which was not of sufficient amplitude to enable the tube to impact on baffles, was then allowed to decay. The question of

whether the air column response can be modified by violent, continuous impacting of the tube was examined in the flow tests with the microphone technique.

5.2.2 Microphone Technique: Monitoring With Flow

The data from test Phase I and II were used to study the microphone technique in terms of the response of the visually observed impacting tube D-2. The sensitivity of the technique to lower level impacting was tested using the Phase III data in which the row D tubes were removed.

5.2.2.1 Phase I and II Data

The spectrum of the microphone response signal measured in tube D-2 at the onset of impacting, at 24.4 L/s, is shown in Figure 19. The dominant response was at 27.5 Hz. The microphone signal in the time domain is shown in Figures 20 and 21. The signal in Figure 20 has a major frequency component of 27.5 Hz. The occurrence of another impact can be seen in Figure 20 as a higher frequency component "riding" on the lower frequency (27.5 Hz) component of the signal. The higher frequency component is thought to be from the structure-born modes associated with the impact. In order to observe the structure-born vibration, the microphone signal was band-pass filtered from 2 kHz to 7 kHz. The time domain response of the structure-born component of the microphone signal is shown in Figure 21.

The impact bursts detected by the microphone are clearly evident in Figure 21. Three large bursts were captured in the 0.2 s record indicating a frequency of approximately 15 Hz; however, close examination of each large impact burst shows that they are composed of a small leading impact followed by a larger impact signal which decays to a low level prior to the occurrence of the next leading impact signal. The tube is known from the biaxial accelerometer data to have a first mode vibration frequency at 13.75 Hz. The microphone data indicate that two impacts per 13.75 Hz cycle are occurring. The fact that the shell-mounted accelerometer detected a 14 Hz signal at the onset of impacting may be explained by the fact that the small leading impact signal may be damped out prior to reaching the shell-mounted accelerometer.

The sustained low frequency mode of 27.5 Hz excited in the air column of the tube, as shown in Figure 20, is equivalent to the frequency of occurrence of the tube impacts rather than the 22 Hz acoustic mode excited in the air column in the absence of continuous impacting (Figure 17). These observed results are evidence that the air column is in a forced vibration mode in

the presence of continuous excitation. It is possible that the motion of the tube has a coupling or feedback effect on the air column motion.

The microphone technique demonstrated some ability to differentiate between tubes under such conditions. The spectrum of the microphone signal in tube C-3 at 100 L/s is shown in Figure 22. The tube is immediately adjacent to tube D-2. The spectrum shows that the dominant response in tube C-3 was at 20 Hz. From the in-tube data it is known that tube C-3 was impacting at 20 Hz so that the microphone is responding to the excitation of tube C-3. The impacting of tube D-2 is transmitting some signal as shown by the 27.5 Hz peak in the C-3 spectrum.

The microphone technique proved no more sensitive to the onset of impacting in the Phase I and II tests than the vibroacoustic technique. However, with the stainless steel shell exchanger the microphone technique proved to be useful in detecting impacting tubes where the use of the vibroacoustic technique was not feasible. The ability to detect the impacting tubes by the microphone technique provides evidence that the air column in the tube is excited by tube impacting. The tubes detected as impacting by the microphone technique in the original exchanger are identified (in black) in Figure 5.

5.2.2.2 Phase III Tests: Tube Row D Removed

The removal of Row D permitted the study of the sensitivity of the microphone technique to lower level impacting.

At each flow rate increment the tubes were scanned with the microphone to locate impacting tubes. The onset of impacting was detected at 29 L/s, the same threshold detected by the vibroacoustic technique.

Audio monitoring of the microphone signals in the scans again showed the technique to be very sensitive to differences in response between adjacent tubes. Tubes identified as impacting by audio monitoring are shown in Figures 23, 24 and 25 for flows of 31.6 L/s, 60 L/s and 100 L/s respectively. The tubesheet maps in the figures show that the area most susceptible to tube impacting was the periphery of the bundle in the lower baffle windows.

In Figure 25, the results of the 100 L/s scan demonstrate that rattling was detected in all tubes; however, a significant difference in signal could be discerned between those tubes identified as loud and quiet "rattlers". In-tube monitoring

confirmed the aurally interpreted results from the microphone monitoring as will be discussed in the following section.

The microphone monitoring has been shown to be as sensitive as the vibroacoustic technique to onset of impacting. The great advantage of the microphone technique is the sensitivity of the aural interpretation of the signal to differences between adjacent tubes, which permits rapid, accurate scanning of the bundle for detection of problem tubes.

5.3 Tube Vibration Data

5.3.1 Damping Data

Damping data were obtained by impact testing under quiescent fluid conditions. Tube excitation was achieved by a hammer blow to the tubesheet. Tube response was measured at several positions using the biaxial accelerometer.

The results of the damping tests are tabulated in Tables III and IV for the 8-baffle (Phases I to III) and 6-baffle (Phase IV) configuration respectively.

The mechanical and hydrodynamic coupling inherent in a liquid-filled heat exchanger demand that extreme care be exercised in the evaluation of the damping data. The only data points used for the damping determination were those which met the following criteria:

(a) excitation was low enough to produce a linear response; ie, no impacting of the tube on the baffle was present nor was the excitation sufficient to produce hydrodynamic coupling between tubes.

(b) for logarithmic decrement analysis, the time trace was composed of a clean, single frequency response.

The logarithmic decrement technique was used for most of the data; however, this data was checked using the half-power technique.

There was no significant difference between the 8-baffle and 6-baffle data. The data indicates that a value of $\delta = 0.1$ for water on the shellside is a reasonable assumption for analytical work. However, damping in tube arrays is an extremely complex phenomenon that is very difficult to measure or predict. In the application of damping data to analysis, the origin of that data should be determined and the values used with caution.

5.3.2 In-tube Vibration Data as a Function of Flow

5.3.2.1 Phase I Data

The in-tube data confirmed the microphone survey results. The highest vibration levels were detected in tubes D-2, C-3 and B-4 in the lower baffle windows.

Sustained tube impacting initiated in the as-delivered design at 24 L/s (24% full flow). As noted in previous sections tube D-2 which was identified as the first tube to impact, was observed to be unstable prior to initiation of impacting. Unfortunately, the flow control system did not permit steady control of the flow at low enough levels to determine the onset of instability in tube D-2. Signal analysis problems arose at flow rates above 24% full flow with tube D-2, as the violent impacting overloaded the integration circuits. Consequently, it was not possible to fully characterize the displacement behaviour of tube D-2.

Velocity spectra of tube D-2 at the 90° position in the U-Bend at 24 L/s revealed a dominant response at 13.75 Hz with lower peaks at 12 Hz and 27.5 Hz as shown in Figure 26. The 13.75 Hz and 27.5 Hz peaks were in agreement with the vibroacoustic and microphone data at this flow rate. At 100 L/s the dominant response was at 12 Hz and 20 Hz. The 20 Hz peak was in agreement with the vibroacoustic data.

There was no significant difference observed between the two orthogonal mode frequencies in the U-Bend indicating that in a liquid the differences in stiffness between the in-plane and out-of-plane axes in the bend of the tube are not significant due to the coupling in the liquid.

The peak-to-peak displacement data for tube B-4 are plotted in Figures 27 and 28. The data for tube B-4 is typical of that for tubes D-2 and C-3. The displacement of tube B-4 was greatest in the U-Bend end, reaching values greater than 50% of the outer diameter peak-to-peak and 40% tube o.d. in Z-rms displacement. The tube motion consisted of several cycles of relatively low level motion building up to large displacements for several cycles before dying down to repeat the pattern.

The same tubes were most susceptible to vibration in the previous fixed tubesheet design; however, the displacements in the previous design were an order of magnitude lower, the maximum displacement in the U-Bend reaching only 6% of tube o.d. The natural frequencies of the tubes in the original design were similar to those in the present exchanger, Phases I to III, since the baffle spacing is nominally the same.

The difference in vibration susceptibility between the previous design and the present design could be related to several "small" details of bundle design as outlined below:

(a) The present design is a "fuller" bundle with a larger outer tube limit (OTL) which places the most susceptible tubes closer to the shell in a high velocity by-pass stream.

(b) The previous design had incorporated several features to block peripheral by-pass flow around the bundle. The by-pass blocking features used in the original bundle were:

(i) Three full length sealing strips on each side of the bundle to block the bundle-shell by-pass stream.

(ii) A sealing strip-type baffle in the head at the U-Bend end to prevent flow from by-passing around the U-Bends between the tubes and the shell.

The impingement plate incorporated at the inlet of the previous heat exchanger design did not help reduce vibration levels. Displacement in tube A-5, immediately adjacent to the edge of the baffle plate in the previous heat exchanger, was 25% greater in the inlet span than the levels measured in tube B-4 in an equivalent position in the present exchanger. This data reinforces a growing belief that impingement plates may not be effective in reducing vibration levels because they create problems for tubes adjacent to the edges of the plate.

The susceptibility of tubes to vibration in the peripheral areas of the present heat exchanger was emphasized by examination of the displacement of tubes in the centre of the bundle. The displacements in tube M-5, which are shown in Figures 29 and 30, indicate that the maximum displacement was less than 2% tube OD.

5.3.2.2 Phase II Data

Impacting initiated in the Phase II tests with the vertical tube-free lane open at 26% of full flow compared to the 24% full flow onset in the Phase I tests. The delayed onset was due to reduced flow around the tube bundle as a result of increased by-pass flow through the open vertical lane. The by-passing to the tube-free lane was reflected in reduced pressure drop performance which will be discussed in 5.4.

The peripheral tubes in the lower baffle window were again the tubes most susceptible to vibration. As in the Phase I tests tube D-2 was the first tube to impact, again with such force as to prohibit accurate displacement measurement. The data from tubes B-4 and C-3 will be presented to demonstrate the behaviour of susceptible tubes.

Vibration velocity has become a standard measurement to determine the severity of the vibration experienced by a particular system. The limits of acceptance for heat exchanger tubes, as determined by Ontario Hydro are:

75 mm/s peak for fatigue only.
33 mm/s peak in the presence of impacting (9).

The z-peak velocity data for tube C-3 as a function of position in the tube are shown in Figure 31. The z-peak velocity levels exceed both limits at flows in excess of 40 L/s. As in the Phase I tests the levels are highest at the U-Bend.

The z-RMS displacement for tube C-3, as plotted in Figure 32 corroborated the velocity data. Tube C-3 was impacting so violently at 100 L/s that displacement records for that flow were impossible to obtain. The displacement exceeded 2% tube o.d. rms in the U-Bend zone at flows in excess of 40 L/s. Data for tube B-4 was similar to that for tube C-3.

The unstable response in the U-Bends of the peripheral tubes in the lower baffle windows was reflected in the velocity spectra of tubes C-3 and B-4 as shown in Figures 33 and 34 respectively. The sharply defined response, at 19.5 Hz for tube C-3 is indicative of instability. A broad band response typical of turbulent buffeting is shown in Figure 35 for tube A-9.

The removal of the dummy tubes resulted in a slightly delayed onset of impacting and slightly reduced vibration levels in the more susceptible tubes. These results were expected with the opening of the central tube-free lane for by-pass flow, thereby reducing by-pass flow around the periphery of the bundle. However, the effects of opening the central lane were not significant. The tubes adjacent to the tube-free lane, eg, tube A-9, did not experience significantly higher vibration as a result of the increased flow.

5.3.2.3 Phase III Data

With the removal of tube Row D, impacting did not begin in the bundle until 29% of full flow. Again the U-Bends of the peripheral tubes in the lower baffle windows were the most susceptible to vibration.

The first tube to impact in the Phase III configuration was tube C-3. Z-RMS displacement at the 90° position of the bend in tube C-3 is plotted as function of flow rate in Figure 36. From the Figure 36 data it can be observed that instability began at approximately 26 L/s; however, tube amplitudes were not sufficient to cause impacting until 29 L/s.

The decrease in amplitude at 45 L/s as shown in Figure 36 has been observed in other investigations (10) and has been attributed to a change in frequency caused by fluid coupling effects. The frequency response measured in tube C-3 is plotted in Figure 37. Although the data is sparse, the frequency drop between 40 and 60 L/s corresponds to the drop and subsequent rise in amplitude between 40 and 60 L/s observed in Tube C-3. Between 60 and 80 L/s the displacement amplitude remained constant while the dominant frequency response varied from 12 Hz at 60 L/s to 19 Hz at 70 L/s to 12 Hz at 80 L/s. No displacement data could be taken at 100 L/s due to the impacting overloading the circuits. The frequency response was measured at 100 L/s in velocity. Two modes at 16 Hz and 19.5 Hz, were observed at 100 L/s. The two mode response is in agreement with other researcher's data at maximum response amplitudes (10).

The z-peak displacement data for tube C-3 are plotted as a function of position in the tube in Figure 38 to provide information on the location of impacting along the tube. The data shows that the tube was impacting at baffles 3 and 5 at flows in excess of 40 L/s. The plot of tube C-3 z-peak velocity in Figure 39 shows that the velocities exceeded the limits of acceptance at flows in excess of 40 L/s. The data in Figure 39 is very similar to that for the Phase II tests documented in Figure 31.

One of the most interesting observations in the Phase III test was made in documenting the behaviour of tube C-5, immediately adjacent to tube C-3. Tube C-5 was found to undergo a significant increase in amplitude in the U-Bend at flows between 30 and 50 L/s as documented in Figure 40 in a plot of z-RMS displacement with respect to flow for the 90° U-Bend position. The sudden increase in amplitude between 25 and 30 L/s and the sudden drop between 45 and 50 L/s are suggestive of a structural resonance with a periodic flow phenomenon whose frequency matches that of the tube at approximately 40 L/s. The phenomenon described is similar to that of vortex shedding resonance observed on isolated tubes; however, in tube bundles it is often referred to as periodic wake shedding resonance. (The ratio of $fnDo/V_{gap}$ for tube C-5 would be 0.6 based on a 60° entrance velocity or 0.34 for a 30° entrance velocity orientation, assuming 100% cross-flow; the actual flow fraction could be as low as 50% which would raise the $fnDo/V_{gap}$ to

unity). Regardless of the details of the mechanism, the fact that such behaviour has been observed in a full scale tube bundle is significant in that the reduction of flow rate from 100% to reduce vibration levels would not be an appropriate action to take in this case. It could bring the exchanger into the resonance regime. The phenomenon was also observed in the Phase IV tests.

The Phase III tests were used to test the sensitivity of the microphone technique to low level impacting. Tube R-9, which is adjacent to the vertical lane with the dummy tubes was identified as rattling at 60 L/s (Figure 24) and strongly impacting at 100 L/s (Figure 25). The displacement data indicated that the tube was impacting at baffles 2 and 4 at 100 L/s. The z-peak velocity records for this tube are plotted for each flow as a function of position in Figure 41. The velocity levels measured at 100 L/s at baffles 2 and 4 were in excess of the allowable limits for impacting tubes.

In summary, the removal of the fourth tube row did not significantly affect the vibration characteristics of the bundle. However, as a consequence of the removal of the tubes most susceptible to vibration the flow rate at which impacting began was 29 L/s compared to 24 L/s in the original design and 26 L/s in the Phase II tests.

5.3.2.4 Phase IV Data

The removal of two baffles and the consequent increase in baffle spacing to 0.59 m from 0.44 m resulted in a substantial change in the susceptibility of the heat exchanger to tube vibration. (Tube D-2 was removed from this configuration because it sagged onto the end bell wall).

As noted in Section 5.1.1 impacting began at 13 L/s, a full 45% lower than the threshold of 24 L/s for the as-delivered heat exchanger (present) design. The first tube to impact in the 6-baffle design was tube B-4, Figures 42 and 43.

The behaviour in the U-Bend of tube B-4 at low flows is documented in Figure 42. Tube B-4 was observed to undergo significant motion in the U-bend prior to the onset of impacting. The visual observation was confirmed by the in-tube data in Figure 42 where the U-Bend z-RMS displacement was approximately 7% of tube O.D. at 12.6 L/s just before the onset of impacting.

The z-RMS response of the U-Bend in tube B-4 over the full range of flow is documented in Figure 43. From Figure 42 it appears that instability onset occurred, in the U-Bend at approximately

12.8 L/s. In Figure 43 the displacements are shown to have risen quite quickly up to 20% of tube O.D. at 21 L/s. The response dropped between 21 and 24 L/s which may be attributed to a change in mode of vibration as shown in the frequency plot in Figure 43.

At flows in excess of 30 L/s the displacement increased steadily with flow. The rate of change of displacement increased at flows in excess of 50 L/s. The response of tube B-4 from the 8-baffle Phase I data has been included in Figure 43 for comparison. The 6-Baffle response was shown to be higher at the lower flows than the 8-baffle but at the highest flows the same maximum displacement was reached.

The response of tube C-3 for the 6-Baffle design is documented in Figures 44 to 47. Tube C-3 did not experience the rate of increase in displacement at low flows as did tube B-4 as shown by comparison of Figures 44 and 42. While tube C-3 displacement did increase rapidly from 0.38% o.d. at 12 L/s to 1.5% o.d. at 14 L/s, the increase is not on the same order as for tube B-4 which went from 0.9% o.d. at 11.8 L/s to 7.6% o.d. at 12.6 L/s. The trend to a slower increase in displacement in tube C-3 continued as flow rate increased above 20 L/s. In comparing Figure 45 with Figure 43 the increase in displacement at the lower flows in tube C-3 occurred at a slower rate than experienced in tube B-4. At 50 L/s, however, the rate of change did increase for tube C-3 with maximum displacement of the same order as that in Tube B-4.

The RMS displacement in tube C-3 at 100 L/s is plotted as a function of position in the tube in Figure 46. The corresponding Z-peak velocity response is plotted in Figure 47. The displacement plot indicates that impacting was occurring at all baffles supporting the tube while the velocity levels were well above the limits of acceptance.

The U-Bend frequency response for tubes B-4 and C-3, contained in Figures 43 and 45, respectively were very similar. The frequencies were lower than those for the 8-baffle configuration, by a factor of 0.6 to 0.85 as expected for the longer tube spans in the 6-baffle design. The general trend was to increasing frequency with increasing flow rate; however, in each case after an initial increase in frequency with flow the frequency dropped suddenly at approximately 50 L/s. This flow rate also marked a change in the rate of increase of the displacement. The general trend to increasing frequency with flow was also observed in the vibroacoustic data (Figure 12).

The response of tube D-4, immediately above tube B-4 in the bundle is similar to that of B-4 as shown in Figure 48. The

U-Bend midspan z-RMS displacement at low flows, increased from 0.31% o.d. at 11.8 L/s to 6.3% o.d. at 14.8 L/s. The onset of the rapid increase in displacement occurred at the same flow as in the case of tube B-4 (Figure 42).

In the microphone survey of the tubes, tube A-9, the bottom tube in the bundle was found to be impacting at flow in excess of 50 L/s. In previous tests this tube was found to experience low level vibration. During the in-tube monitoring of phase IV, documented in Figures 49, the tube was found to exhibit behaviour similar to that observed in tube C-5 (Figure 40) in the Phase III tests; ie, the tube behaviour at the tangent line position was consistent with periodic wake shedding resonance. As documented in Figure 49, the tube experienced a sudden rise in vibration amplitude at 45 L/s, followed by a sudden drop in amplitude at 70 L/s. The amplitude rise was very dramatic, from a value of 1.5% tube O.D. to a maximum of 12% tube O.D. over a flow range of 10 L/s.

The vibration in tube C-5 in the Phase IV tests is documented in Figure 50. In comparison with the Phase III data (Figure 40) the response of the 6-baffle configuration was dominated by the instability phenomenon rather than the passage through a resonance peak. However, over the flow range of 14 L/s to 20 L/s there was some evidence that the tube did pass through a resonance peak. The data in the low flow range was replotted in Figure 51 in order to examine the response in detail. The tube displacement did rise fairly rapidly from 0.9% tube O.D. at 14 L/s to 4.6% of tube O.D. at 19 L/s, falling again to 1.3% tube O.D. at 25 L/s. The fact that the observed rise in amplitude at low flows was well removed from the significant increase in amplitude of 45 L/s indicated that the two phenomena were separate.

The frequency of the tube changed most dramatically during the occurrence of the resonance phenomenon as shown in Figure 50; this observation was in agreement with the concept that a significant change in the vibration level is accompanied by a change in frequency.

The occurrence of the periodic resonance phenomenon in a heat exchanger is significant in that, as previously mentioned, reduction of flow rate may not remove the danger of damaging tube vibration. In addition, this phenomenon was observed well away from the inlet area which is in contrast to the previously held belief that the inlet would be the only area of concern with respect to periodic resonance.

In summary, the six baffle configuration proved to be more susceptible to tube vibration at the lower flows than did the

8-baffle design. However, the location for the most susceptible tubes remained unchanged by the increase in baffle spacing. The tests demonstrated that a periodic resonance phenomenon can exist in a bundle in a zone well removed from the inlet area. The Phase IV data, as in the other phases, confirmed the results of the non-intrusive techniques.

5.4 Pressure Drop Data

Pressure drop data relative to flow are displayed in Figures 52 and 53. Overall pressure drop is shown for each phase of the tests and compared to the tests on the previous fixed tubesheet exchanger. The curves all exhibit a $\Delta p \alpha Q^{\beta}$ relationship, with an average value of β for all curves of 2.05.

The pressure drop was greater in the previous fixed-tubesheet design than in the present design. This higher pressure drop was due to the following factors:

(i) Higher tube count, smaller pitch.
(ii) Presence of flow-directing baffle in the U-Bend head which was absent in the present design.
(iii) Impingement plate at inlet, absent in the present design.

The data from the four test phases were all similar. The Phase II (dummy-tubes removed) and the Phase IV (6-baffle design) tests exhibited the lowest pressure drops. The Phase II and IV observations were expected since these two configurations were significant departures from the as-delivered design; however, the difference in pressure drop behaviour between all phases of the testing was not significant, indicating that most of the pressure drop across the exchanger took place in areas that remained essentially unchanged; eg, the tube layout, the baffle windows and the inlet and outlet zones were not significantly changed by the modifications.

A plot of cumulative pressure drop across the tube bundle for the Phase I design is shown in Figure 54. Comparison of the pressure drop between taps 2 and 12 in Figure 54 with the overall pressure drop for the Phase I design plotted in Figure 53 demonstrates that the pressure drop across the bundle accounted for between 60 and 75% of the Δp across the exchanger. The same behaviour was observed in all phases tested. The negative pressure drop measured between taps 2-3 and 2-4 at low flows is most likely due to the existence of separated flow in the region of the taps. The differences in the pressure between tap 2 and taps 3 and 4 were extremely small so that any slight alteration would adversely affect the pressure drop. Deeper into the bundle the total pressure loss

would increase, thus reducing the effect of the localized separated zones. At higher flows the susceptibility to flow separation will be reduced.

5.5 Flow Visualization

The flow visualization in the U-Bend zone confirmed that a large fraction of the flow from the last baffle window was by-passing around the end of the bundle; that is, a high velocity flow stream was passing around the area most susceptible to vibration, the largest U-Bends. In the fixed tubesheet bundle the horizontal baffle in the U-Bend at the horizontal centre line would have blocked a large portion of this by-passing flow, thus accounting for the reduced vibration level in the fixed tubesheet design.

Some photographs from the series taken during the flow visualization tests are shown in Figure 55. The flow range of 20 L/s to 60 L/s was covered. Above 60 L/s the bubbles dispersed too quickly to permit observation of flow.

In the tests, air bubbles injected into the flow at the pressure tap in the last baffle window were used for flow visualization. Increased numbers of bubbles in a given area was an indication of preferential flow path. Increased elongation of the bubbles was an indication of increasing velocity.

The photograph at 20 L/s shows a low flow with the bubbles clearly defined and distinct with the major portion passing around the outside of the bundle on the left of the photo and through the centre tube-free lane to the right in the photo.

At 40 L/s the by-passing flow around the outside of the bundle was clearly marked by the high density of bubbles, particularly at the bottom of the bundle where the flow exited from the baffle window. The elongation of the bubbles in this zone indicated a higher velocity. There appeared to be more flow passing through the bundle as shown by the increase in bubbles in the bundle area; however, there still appeared to be some by-passing through the tube-free lane.

The elongation of the bubbles in the lower bundle by-pass zone was greatly increased at 60 L/s. The velocity in the by-pass flow around the bundle appeared to decrease toward the horizontal centre-line of the bundle as evidenced by the reduction in the elongation of the bubbles. This drop in velocity correlates well with reduced vibration of the peripheral U-Bends in the area of the horizontal centre-line compared to that in tubes at the bottom of the bundle close to the baffle window. Increased flow through the bundle proper can

be detected from the increased bubble density and elongation of the bubbles through the bundle.

6.0 SUMMARY AND RECOMMENDATIONS FOR FURTHER WORK

6.1 Summary

The project investigated flow induced tube vibration phenomena in a full size heat exchanger, assessed techniques for detection of that vibration and evaluated techniques for vibration reduction by design modifications.

The results of the project are summarized below:

1. The in-tube vibration data obtained have shown the vibroacoustic and microphone monitoring techniques to be reliable and accurate methods for the detection of tube impacting in an operating heat exchanger.

2. Development of work on the use of a two-accelerometer vibroacoustic technique for the location of impacting zones in a bundle showed promise and is currently being employed in the field.

3. The in-tube vibration data have demonstrated the effects that changes in the design of a bundle can have on tube vibration in that bundle. These results indicate that an important factor in bundle design is the local flow distribution in areas of high vibration susceptibility.

4. The in-tube data have demonstrated that tubes in zones other than the inlet region can be susceptible to a form of periodic resonant excitation. This observation has implications for cases where flow reduction is implemented to avoid an instability problem. Such a reduction could bring the tube bundle into a flow regime where it is susceptible to the resonant excitation.

6.2 Recommendations for Further Work

During this project emphasis was focused on the techniques for the detection and quantification of tube vibration in a full size heat exchanger. An expansion of the role of the monitoring techniques for use in predictive maintenance programs is an area of increasing interest. It is recommended that the non-intrusive techniques introduced in this project be evaluated

with respect to their application to monitoring tube vibration over time for detection of increased wear and determination of the optimum time for eddy current examination. If the non-intrusive techniques can be proven to be accurate for this application, costly outages either forced by undetected problems or required for unnecessary eddy-current examination could be avoided.

Monitoring for predictive maintenance has proved to be cost-effective for rotating machinery. An evaluation and development program is necessary to determine whether on-line monitoring techniques could achieve similar benefits for flow-induced vibration damage in heat exchangers.

7.0 ACKNOWLEDGEMENTS

The successful completion of this project could not have been achieved without the aid of the following:

- W.P. Sutherland and M. Valcic of Nuclear Systems Department of Ontario Hydro who did the preliminary design work for the exchanger.

- J. Robinson of Muirhead Engineering whose effort and attention to detail in the construction of the "one-off" design exchanger was instrumental in the success of the program.

- G. Bakker, J. Lindsay and M. deMontmorency of Ontario Hydro Research who designed, built and repaired most of the instrumentation used in the project.

- K. Buck of Ontario Hydro who photographed the flow visualization work.

- N. Andrews of Nova Scotia Power and Light and L. Foote of Newfoundland and Labrador Hydro, technical advisors for the project whose support and comments aided in the successful completion of the project.

- A. Kingsley and the CEA who provided the opportunity to conduct this study and were extremely supportive over the course of the project.

Approved by:

G.J. Clarke
Manager
Mechanical Research Dept

Prepared by:

H.L. Anderson
Engineer
Plant Equipment Dynamics Section

Reviewed by:

T. Loewen
Supervising Engineer
Plant Equipment Dynamics Section

HLA:llg

REFERENCES

1. Proceedings of the IUTAM-IAHR Symposium on Practical Experiences with Flow Induced Vibrations, Ed.: Naudascher and Rockwell, Springer-Verlag, Berlin, 1980.

2. "Proceedings of the Third Vibration in Nuclear Plant Conference, Keswick 1982", The British Nuclear Energy Society, London, 1983.

3. S.S. Chen, 1981 ASME Design Engineering Technical Conference, Hartford, Connecticut, Papers 81-DET-21 and 81-DET-22. "Instability Mechanisms and Stability Criteria of a Group of Circular Cylinders Subjected to Cross-Flow; Part I: Theory; Part II: Numerical Results and Discussion".

4. H. Tanaka and S. Takahara, "Fluid Elastic Vibration of Tube Array in Cross-Flow", Journal of Sound and Vibration, 1981, 77 (1), pp 19-37.

5. Proceedings of: "Flow-Induced Vibration in Heat Exchangers", Winter Annual Meeting of the American Society of Mechanical Engineers", 1970, ASME, N.Y..

6. Proceedings of the IUTAM-IAHR Symposium, Karlsruhe, 1972, Flow Induced Structural Vibrations, ed E. Naudascher, Springer-Verlag, New York, 1974.

7. "Flow-Induced Heat Exchanger Tube Vibration - 1980", ed J. Chenoweth, J. Stenner, The American Society of Mechanical Engineers, New York, Publication #600182.

8. W. Bastl, D. Wach, "Experiences with Noise Surveillance Systems in German LWRs", Progress in Nuclear Energy, Vol 9, 1982.

9. H.L. Anderson, "Bruce NGS 'B' - Main Moderator Heat Exchanger Tube Vibration: An Engineering Assessment and Test Specification", Ontario Hydro Research Division Report #82-123-K.

10. D. Weaver and D. Koroyonnakis, "The Cross-flow Response of a Tube Array in Water - A Comparison with the Same Array in Air", presented at the ASME Pressure Vessel and Piping Conference, Orlando, Florida, June 27 - July 2, 1982. Publication #H00220.

Table I

HEAT EXCHANGERS DESIGN DATA

Item		Original	CEA
Tube	- material	304 SS	304 SS
	- number	146	98
	- o.d.	15.88 mm	15.88 mm
	- i.d.	13.4 mm	13.4 mm
	- str. leg length	3.65 m	3.65 m
	- pitch	20.64 mm	25.4 mm
	- pattern	rotated triangular	rotated triangular
Shell	- material	304 SS	Carbon steel
	- o.d.	0.508 m	0.508 m
	- i.d.	0.489 m	0.489 m
	- length	4.14 m	4.14 m
	- flanged sections	2	7
Baffles	- number	8	8
	- type	single-segmental	single-segmental
	- cut; orientation	25% horizontal	25% horizontal
	- tube hole	16.3 mm	16.3 mm
	- tube-to-baffle clearance	0.42 mm (diam)	0.42 mm
	- tube-tubesheet joint	rolled and welded	ferruled
Impingement plate		127mmx127mmx6.35mm	no
Flow directing baffle in U-Bend head		263.5mm lgx9.5mm th	no
Nozzles; orientation		vertical	vertical
	size (inlet & outlet)	0.203 m	0.203 m

Table II

CALCULATED ACOUSTIC MODE FREQUENCIES IN TUBING
(Hz)

Tube	f_1	f_2	f_3	f_4	f_5	f_6	f_7	f_8
D-2	21.96	43.9	65.8	87.8	109.8	131.8	153.7	175.7
C-3	22.16	44.3	66.5	88.6	110.8	133.0	155.1	177.3
B-4	22.4	44.7	67.0	89.4	111.7	134.1	156.4	178.8
I-1	21.8	43.5	65.3	87.0	108.8	130.6	152.3	174.1
Z-9	23.4	46.8	70.2	93.6	117.0	140.4	163.8	187.2

Table III

DAMPING DATA - 8 BAFFLE CONFIGURATION

Tube	Position	Air			[1]Water		
		Direction	Freq	δ	Direction	Freq	δ
D-1	1-m				X	14	0.14
					Y	14	0.08
	2-b				X	14	0.1
					Y	14	0.1
	10-b				X	14	0.09
					X	14	0.08
					Y	14	0.04
	12-m				X	14	0.09
	15-m				X	26	0.05
	UB-m				X	14	0.09
					Y	14	0.04
C-3	2-b	X	44	0.14			
		Y	36	0.07			
	7-m	X	63.1	0.07			
		Y	203	0.04			
	UB-m	X	63.1	0.07	X	15.6	0.16
		Y	91.3	0.05	Y	15.6	0.08
	3-m				X	15.6	0.3
					Y	15.6	0.32
R-9	8-b	X	59.4	0.08	X	50	0.08
		Y	99.4	0.07	Y	16	0.18
L-6	3-m				X	15.6	0.3
P-5	3-m				Y	15.6	0.6
	U-bend				X	11.25	0.70
O-6	3-m				Y	25.625	0.22
						15.6	0.6
W-2	3-m				X	19.375	0.2
					Y	15.6	0.4
	UB				Y	25.625	0.18

Notes: [1] Only dominant response direction recorded in water.
m - midspan location
b - baffle location

Table IV

DAMPING DATA - 6 BAFFLE CONFIGURATION

Tube	Position	Dir'n	Air		Water		
			Freq	δ	Dir'n	Freq	δ
		X	10	0.05			
D-2	UB-m	Y	10	0.05			
C-3	UB-m	X	10.125	0.1	X	9.0	excessive
		Y	10.125	0.09	Y	9.0	coupling
B-4	UB-m	X	11.0	<0.01	X	10.0	excessive
		Y	11.0		Y	10.0	coupling
Z-9	6				X	9.75	low excit'n
					X	9.75	0.1
	6				Y	34.0	0.06
	6				Y	80	0.4
	TL	X	42.5	0.2	Y	13	0.04
		Y	89	0.3	Y	36.2	0.7
					X	30	0.6
					X	80	0.3
W-2	UB	X	:80	very low			
		Y	:80	0.08			
R-9	TL	X	89	0.27			
		Y	425	0.16			

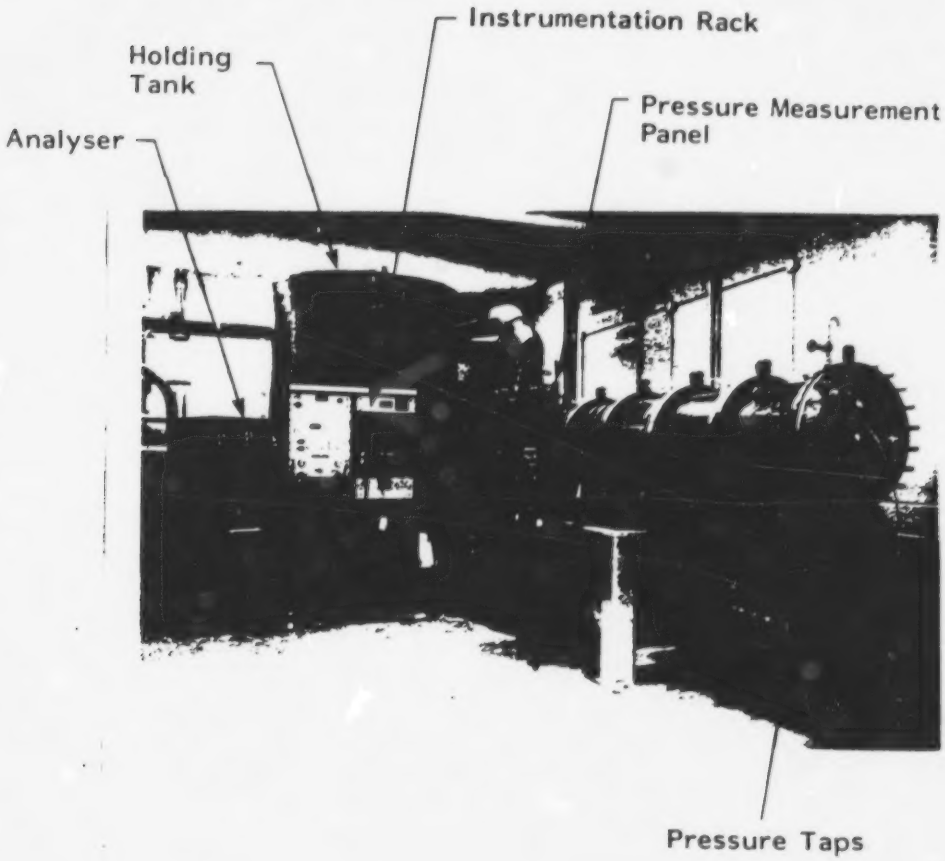

Figure 1: Heat Exchanger Test Facility with CEA Heat Exchanger

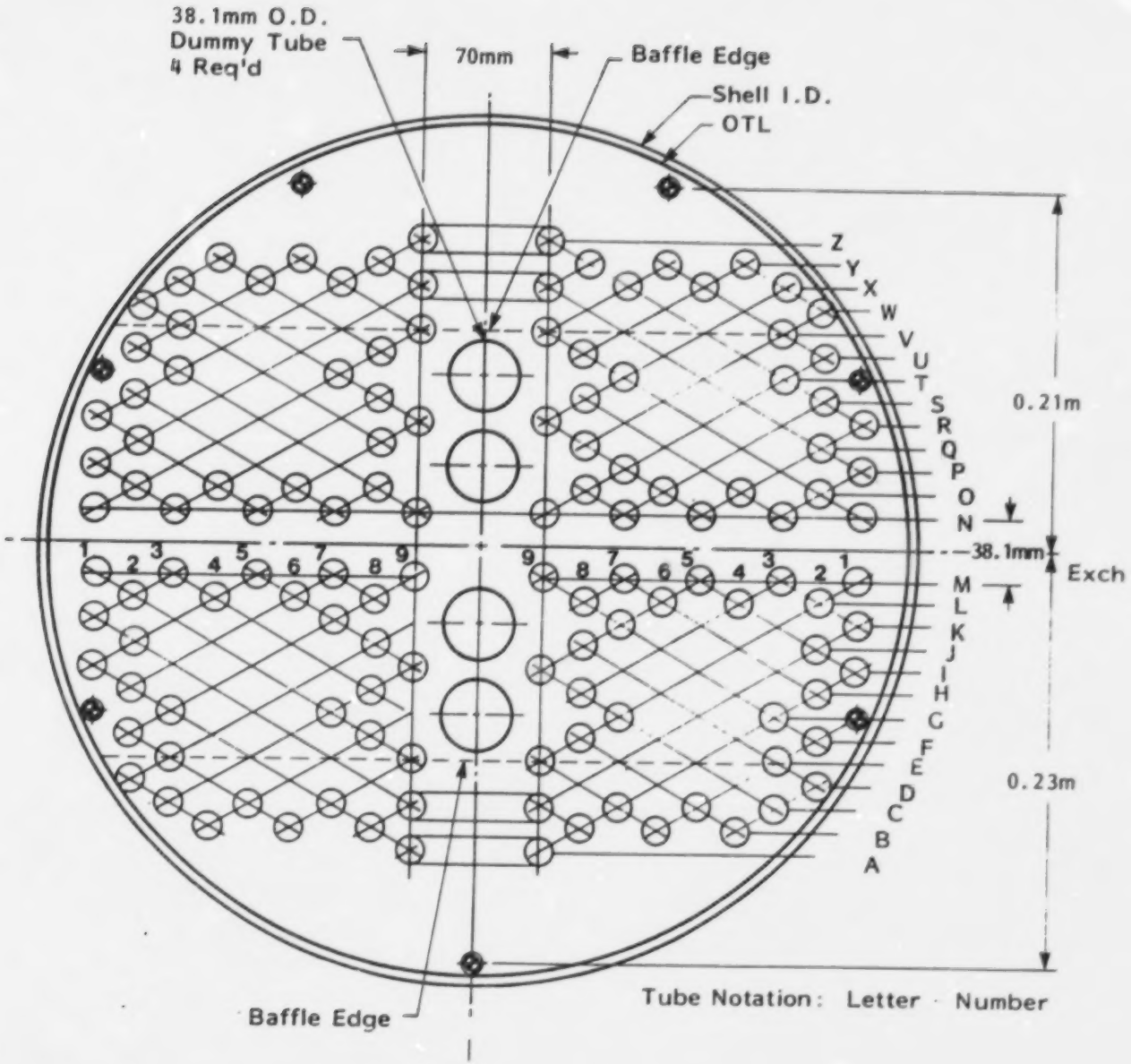

Tube Layout

Pitch: 25.4mm
O.D. 15.89mm
I.D. 13.4mm

Figure 2: CEA Exchanger

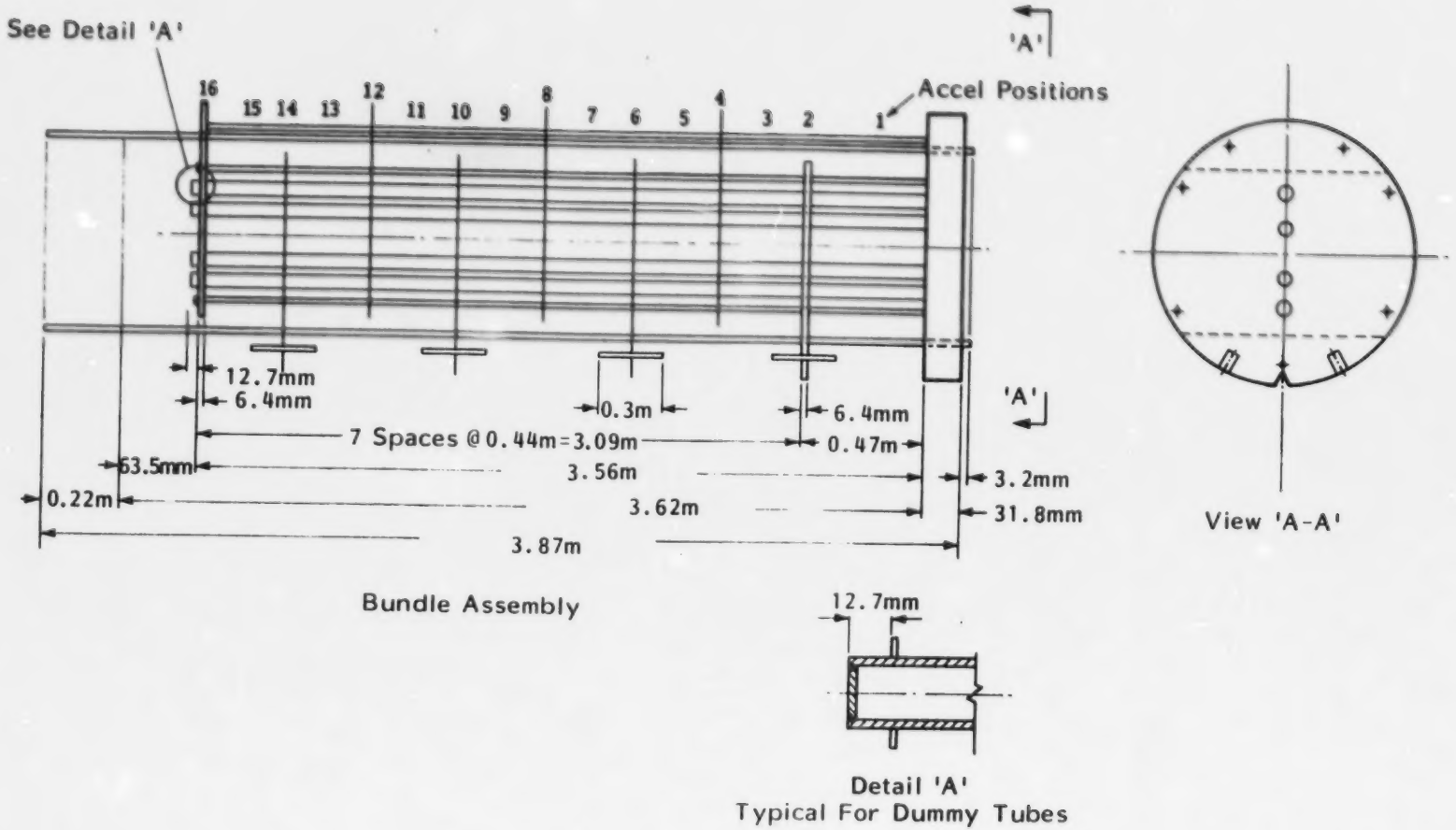

Figure 3: Baffle Spacing CEA Exchanger, as Delivered

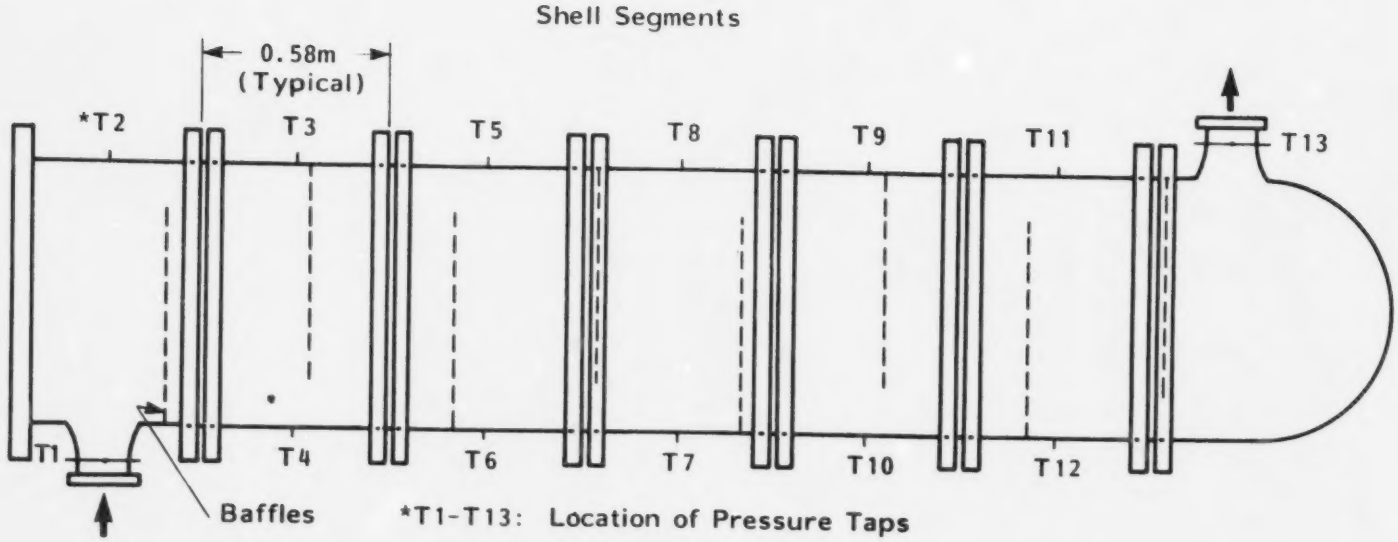

Figure 4: CEA Heat Exchanger Shell

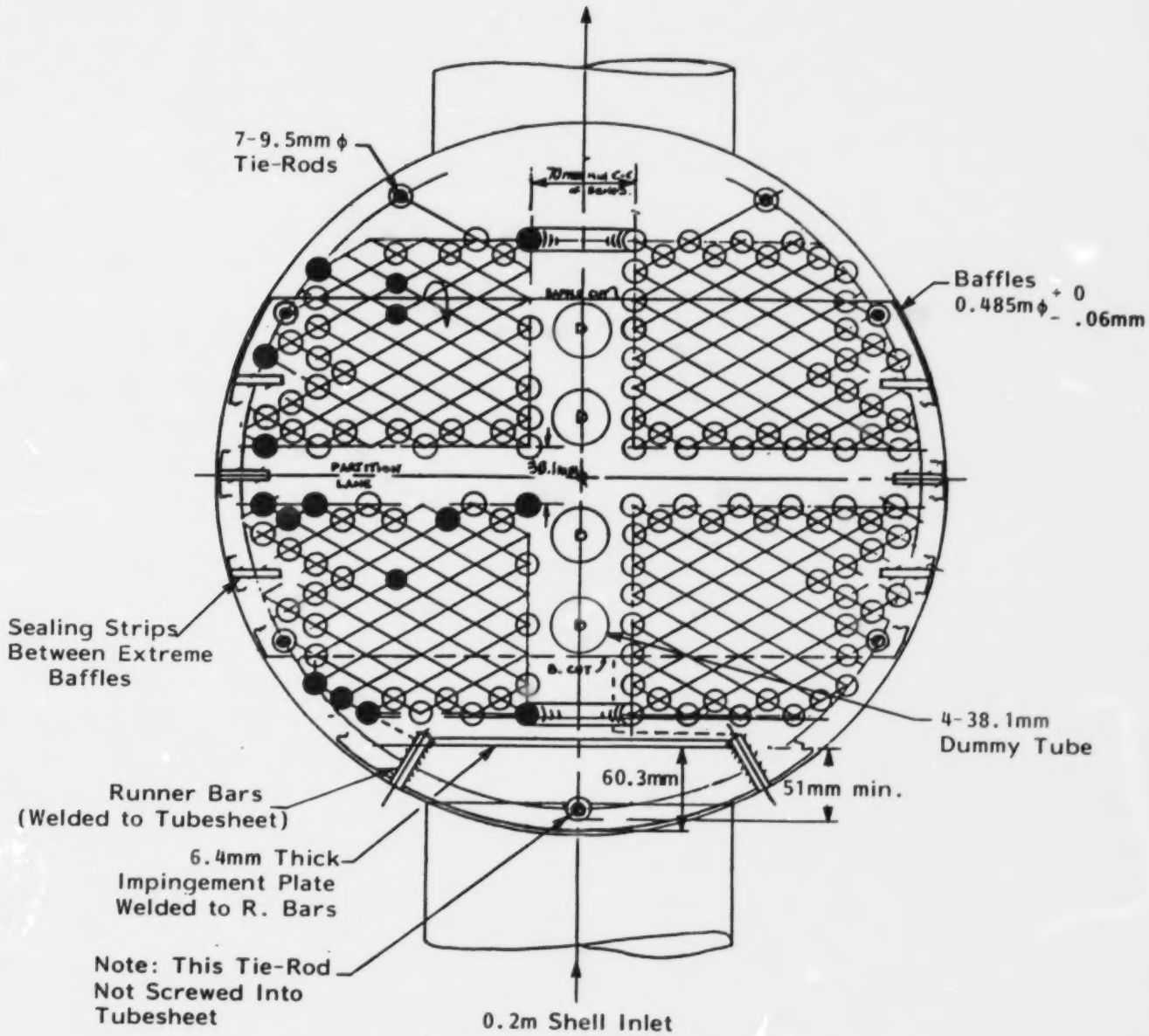

Figure 5: Tube Layout for Original Heat Exchanger

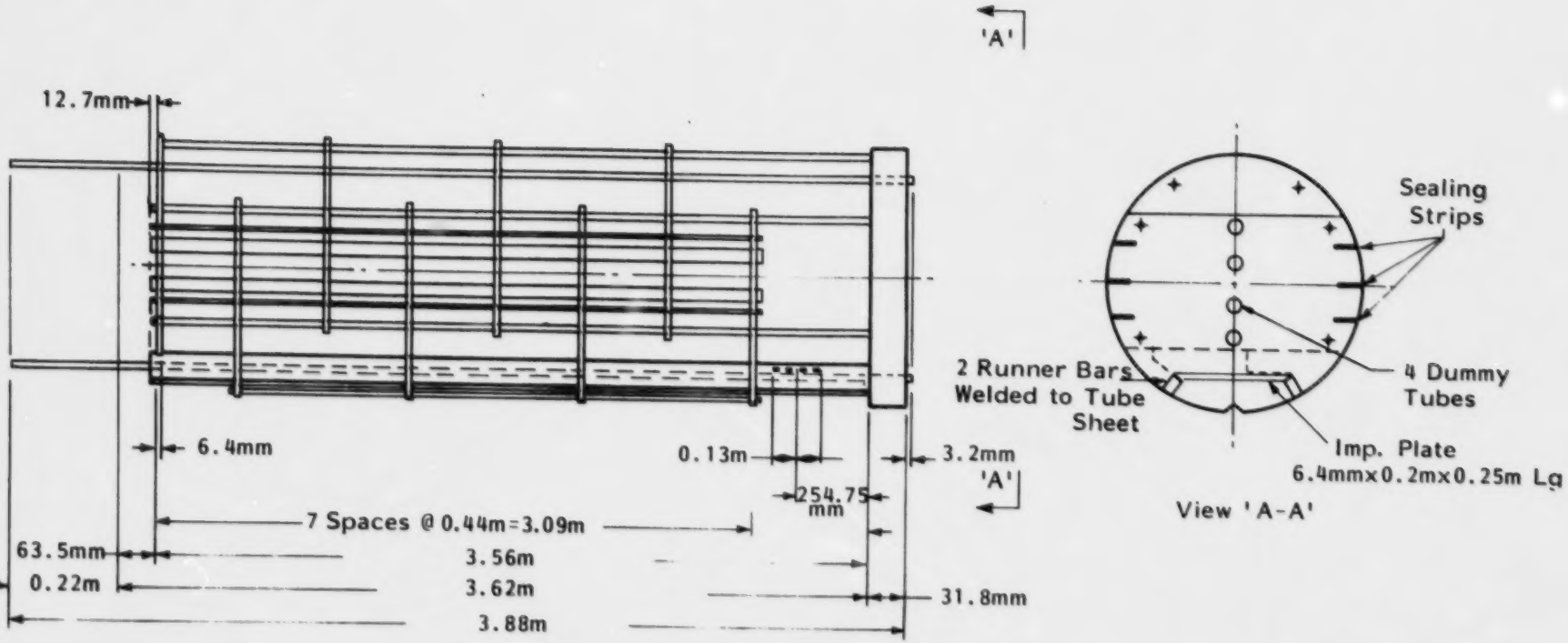

Figure 6: Bundle Assembly, Original Exchanger

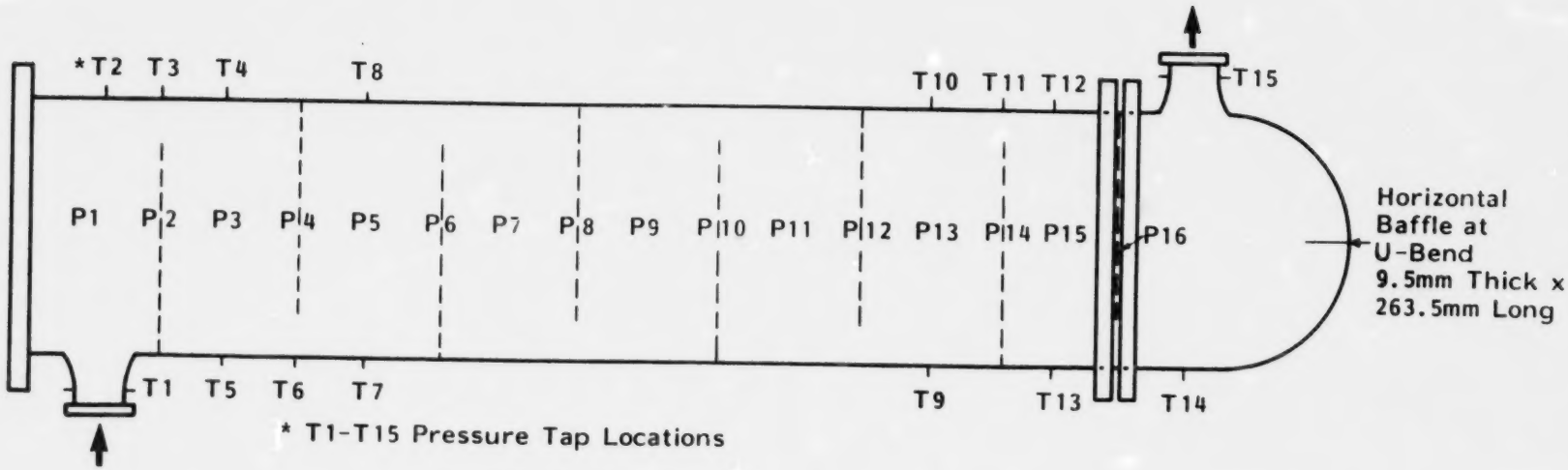
*T2 T3 T4 T8 T10 T11 T12 T15
P1 P2 P3 P4 P5 P6 P7 P8 P9 P10 P11 P12 P13 P14 P15 P16
T1 T5 T6 T7 T9 T13 T14
* T1-T15 Pressure Tap Locations
Horizontal Baffle at U-Bend 9.5mm Thick x 263.5mm Long

Figure 7: Original Heat Exchanger Shell

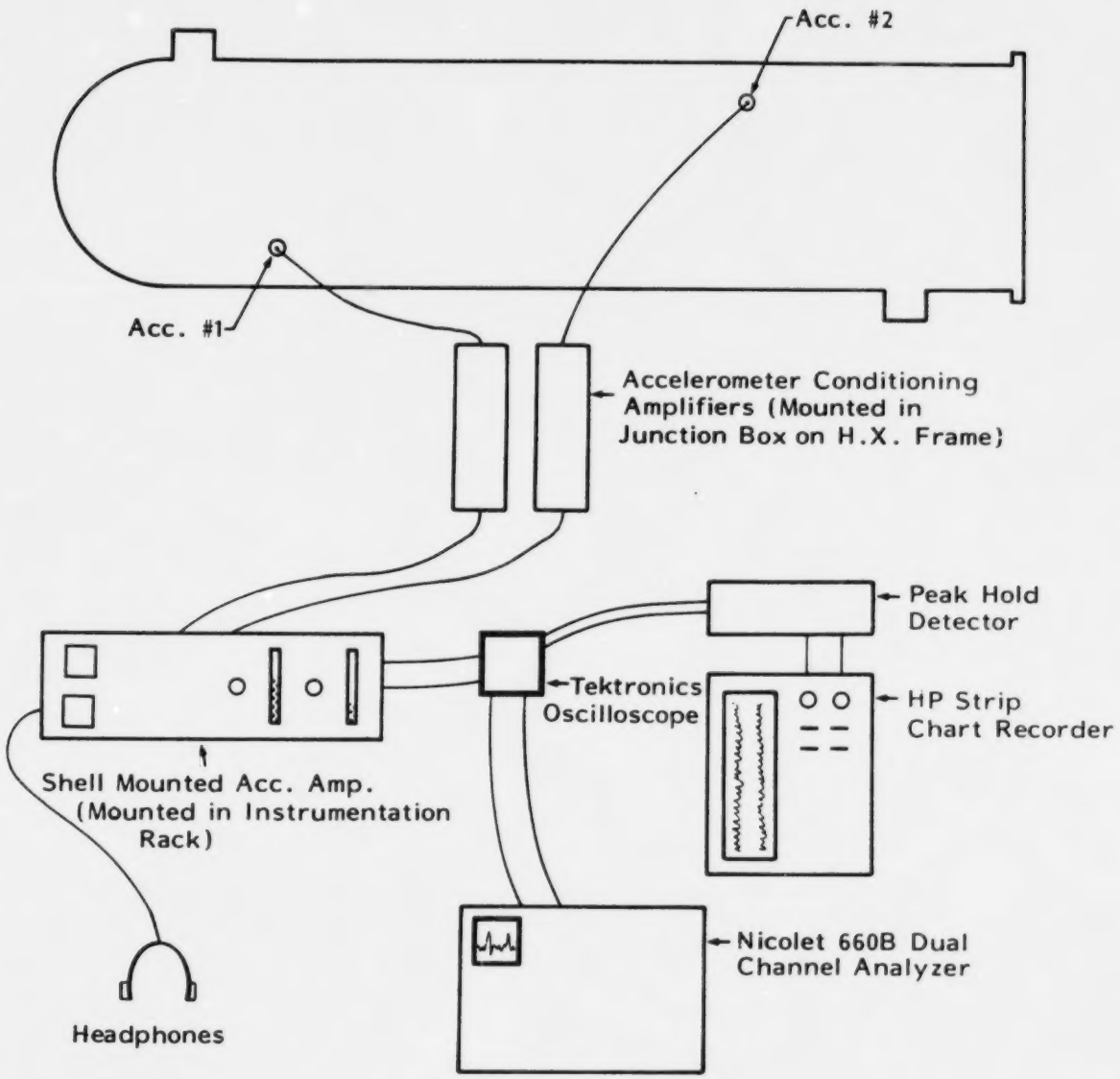
Acc. #2
Acc. #1
Accelerometer Conditioning Amplifiers (Mounted in Junction Box on H.X. Frame)
Peak Hold Detector
Tektronics Oscilloscope
HP Strip Chart Recorder
Shell Mounted Acc. Amp. (Mounted in Instrumentation Rack)
Nicolet 660B Dual Channel Analyzer
Headphones

Figure 8: Vibroacoustic Instrumentation

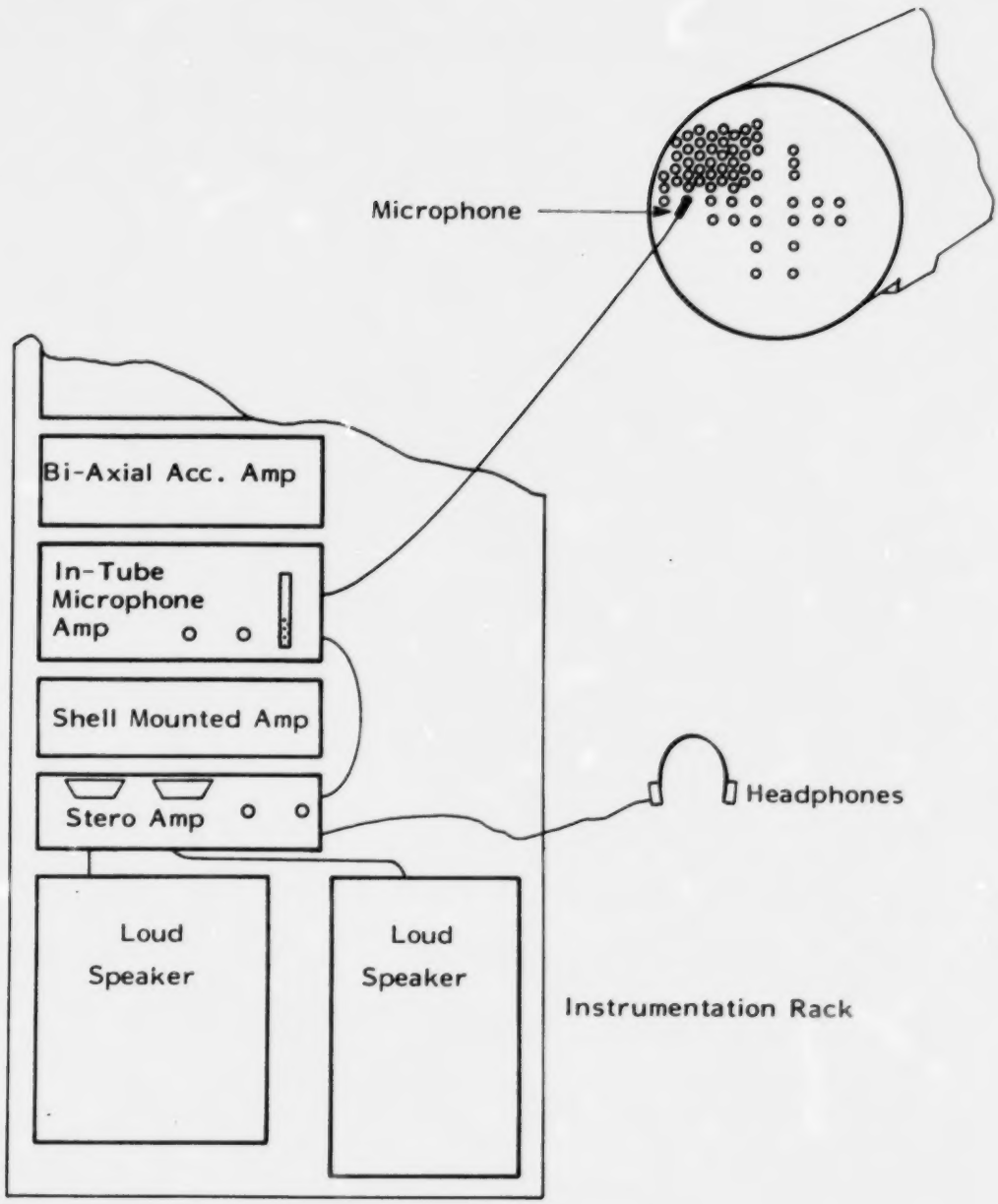

Figure 9: Microphone Technique Instrumentation

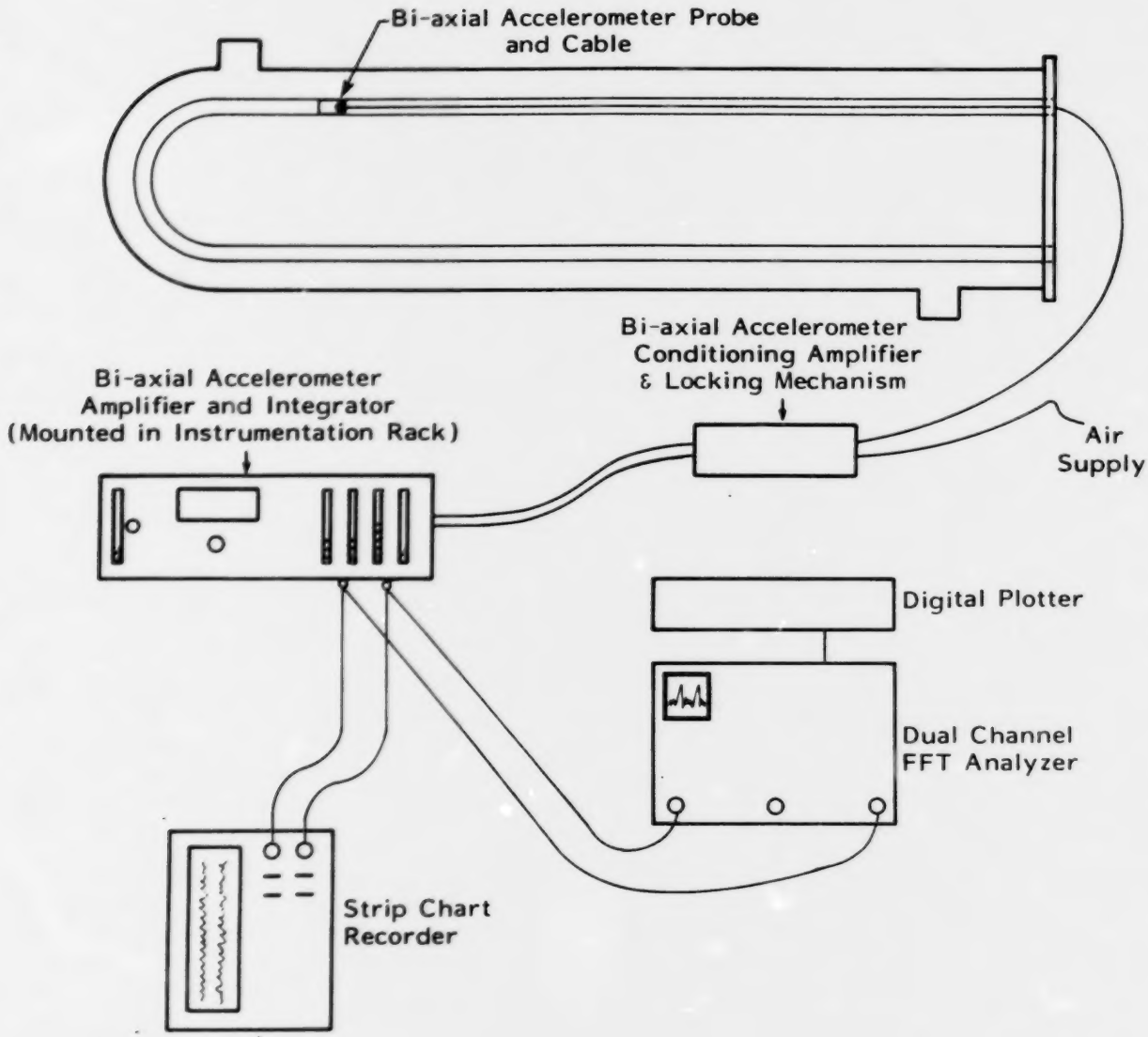

Figure 10(a): Biaxial Accelerometer System

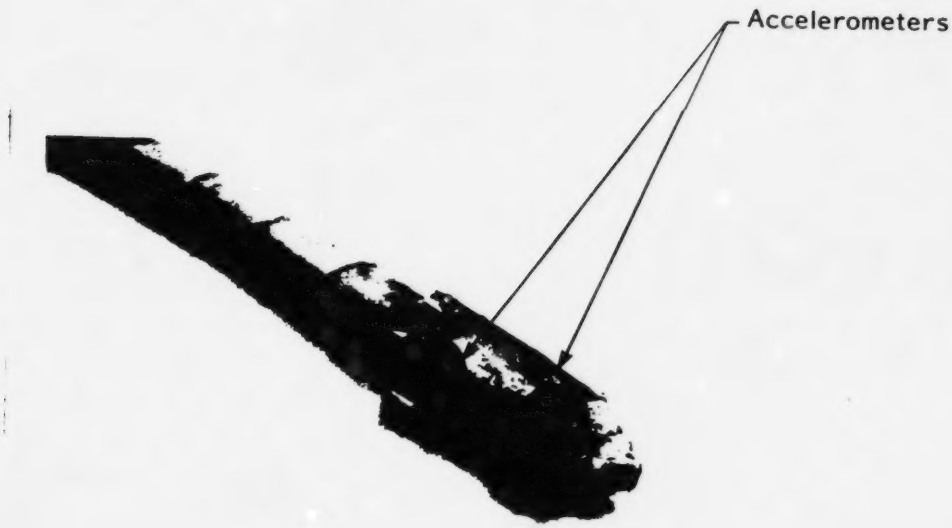

Figure 10(b): Biaxial Accelerometer Probe Head

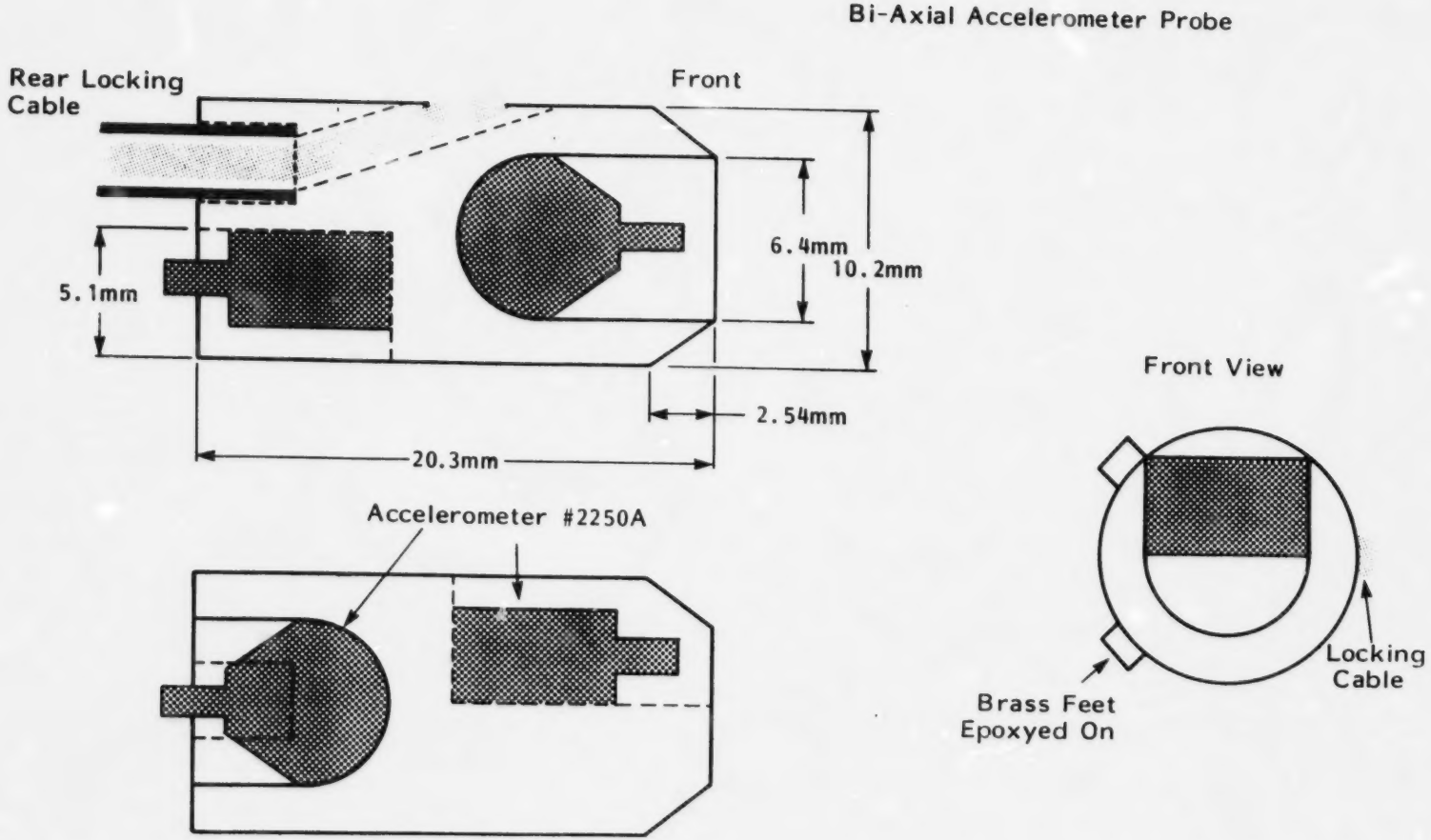

Figure 10(b) con't: Biaxial Accelerometer Probe Head

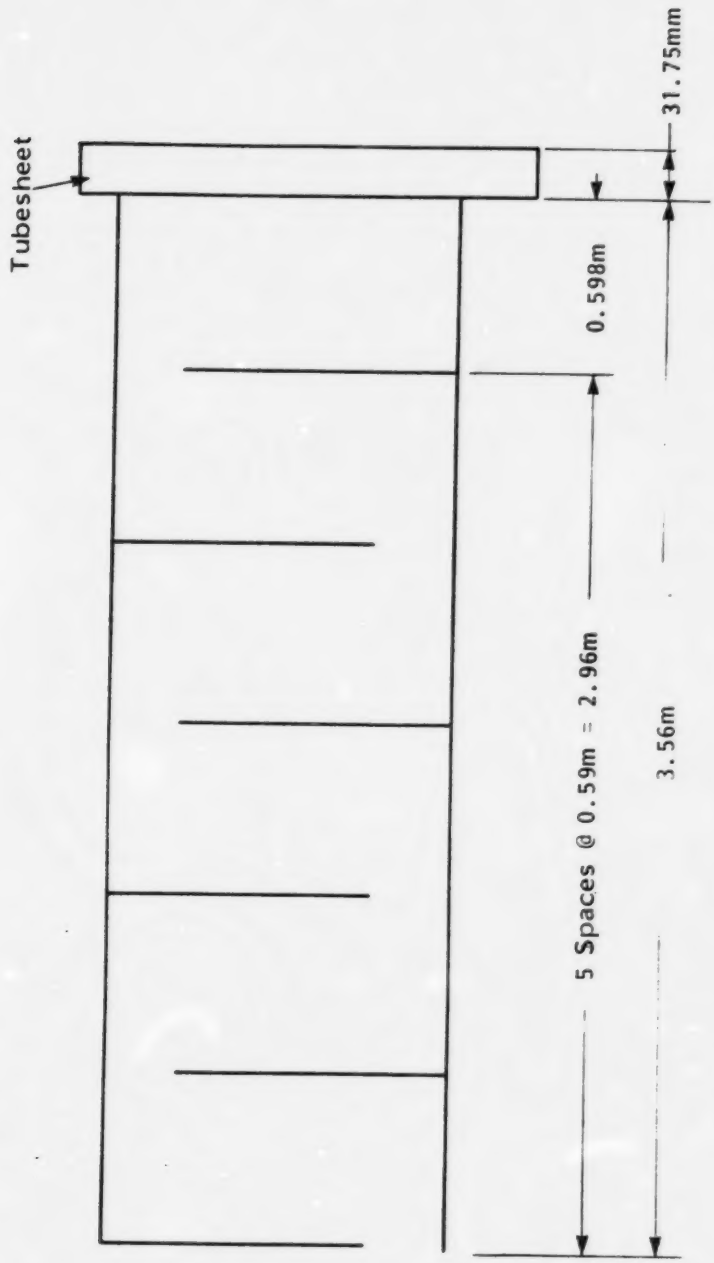

Figure 11: Spacing for Phase IV 6 Baffle Configuration

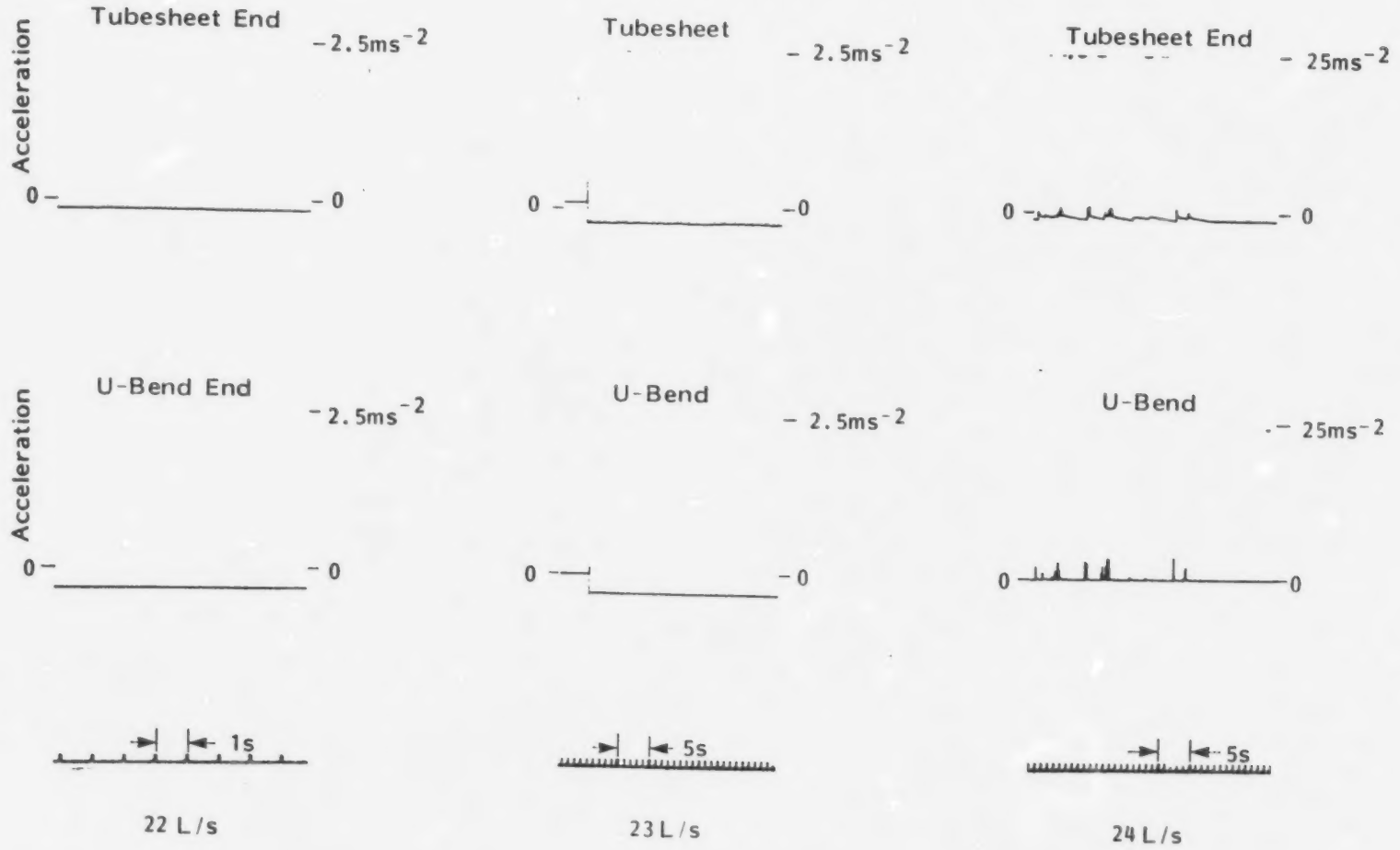

Figure 12: Full-Wave Rectified Signals for the Phase 1 Configuration

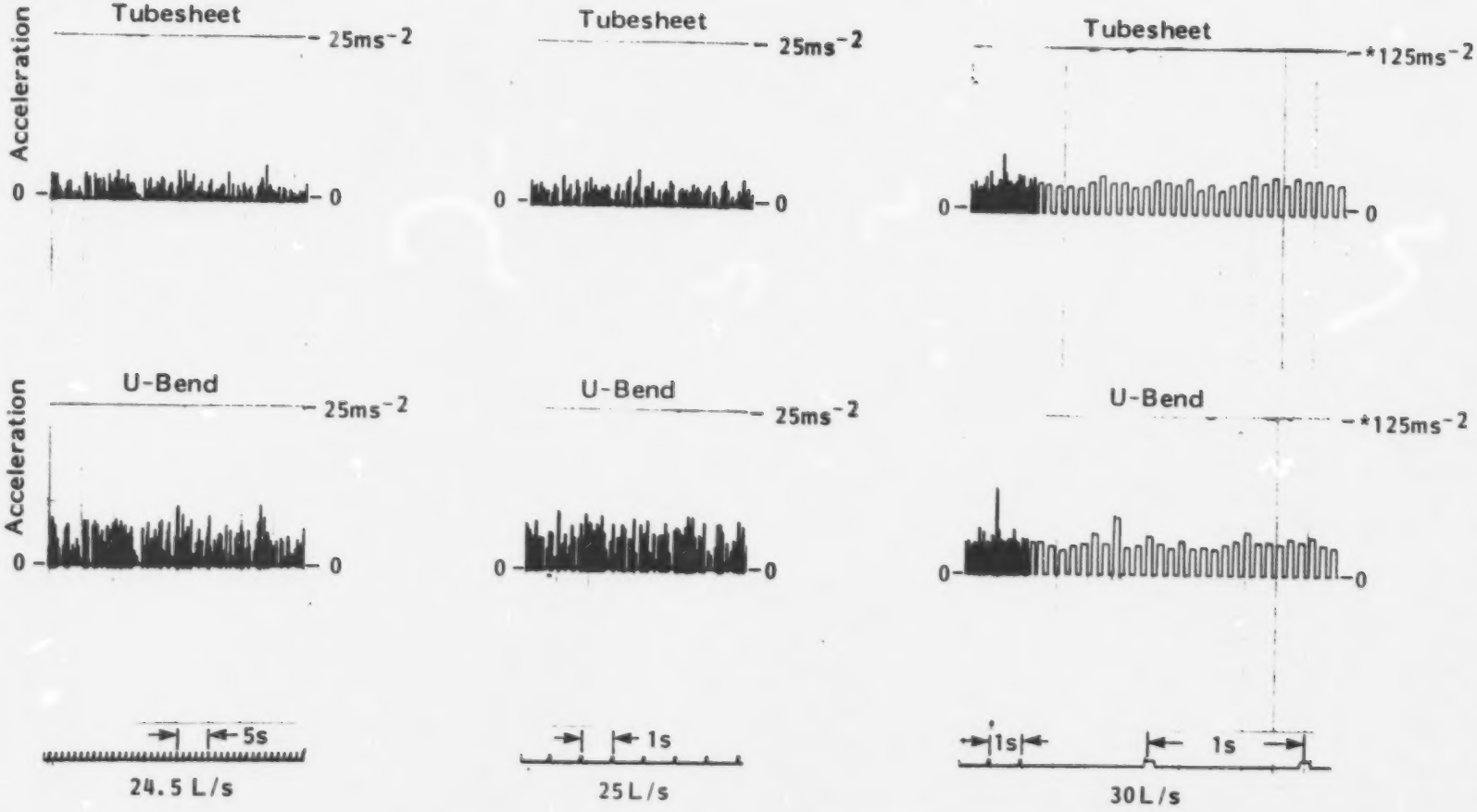

Figure 12: Continued

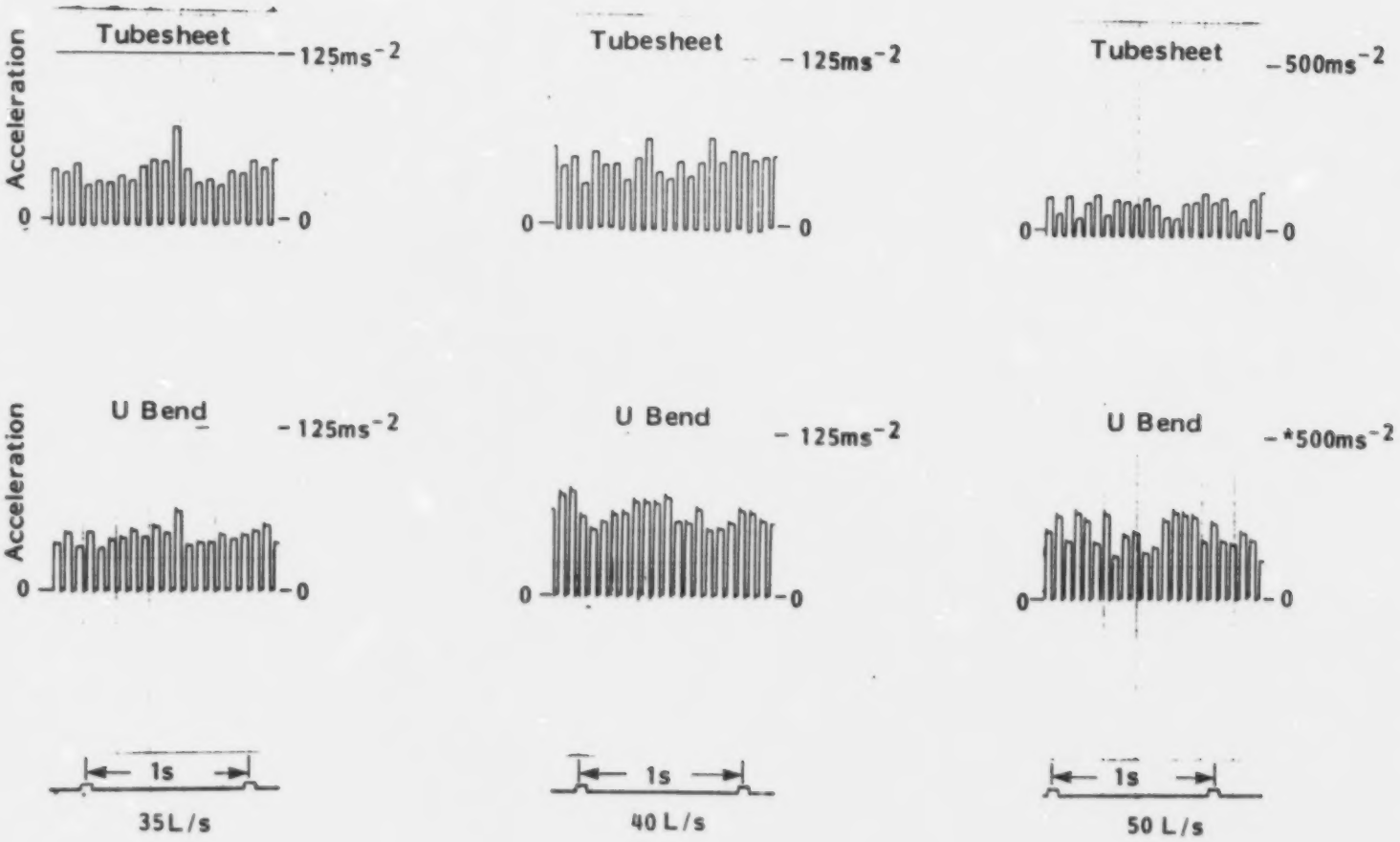

*Change of Scale

Figure 12: continued

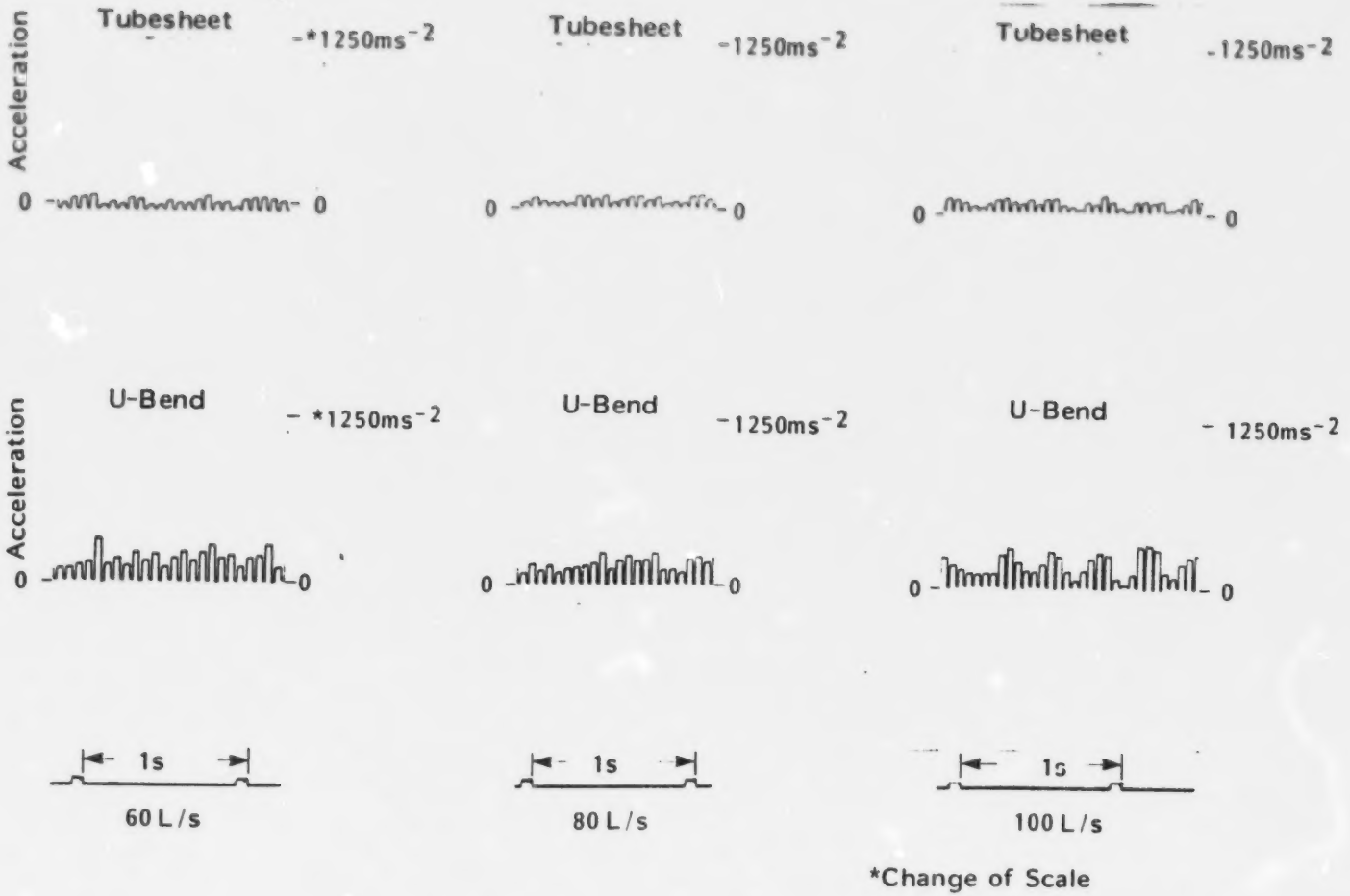

Figure 12: Continued

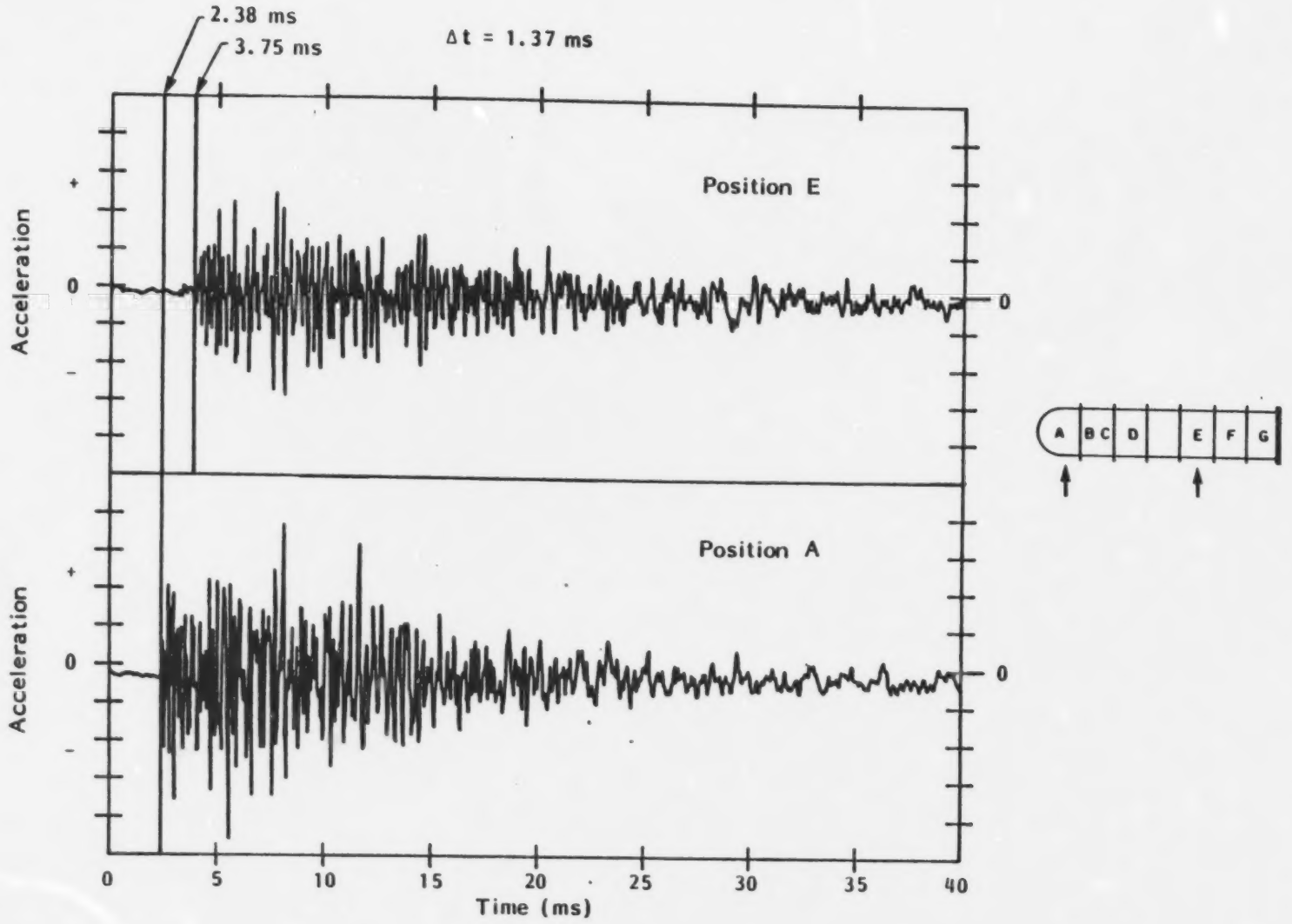

Figure 13: Time-delay for Observation of Impact at 24 L/s

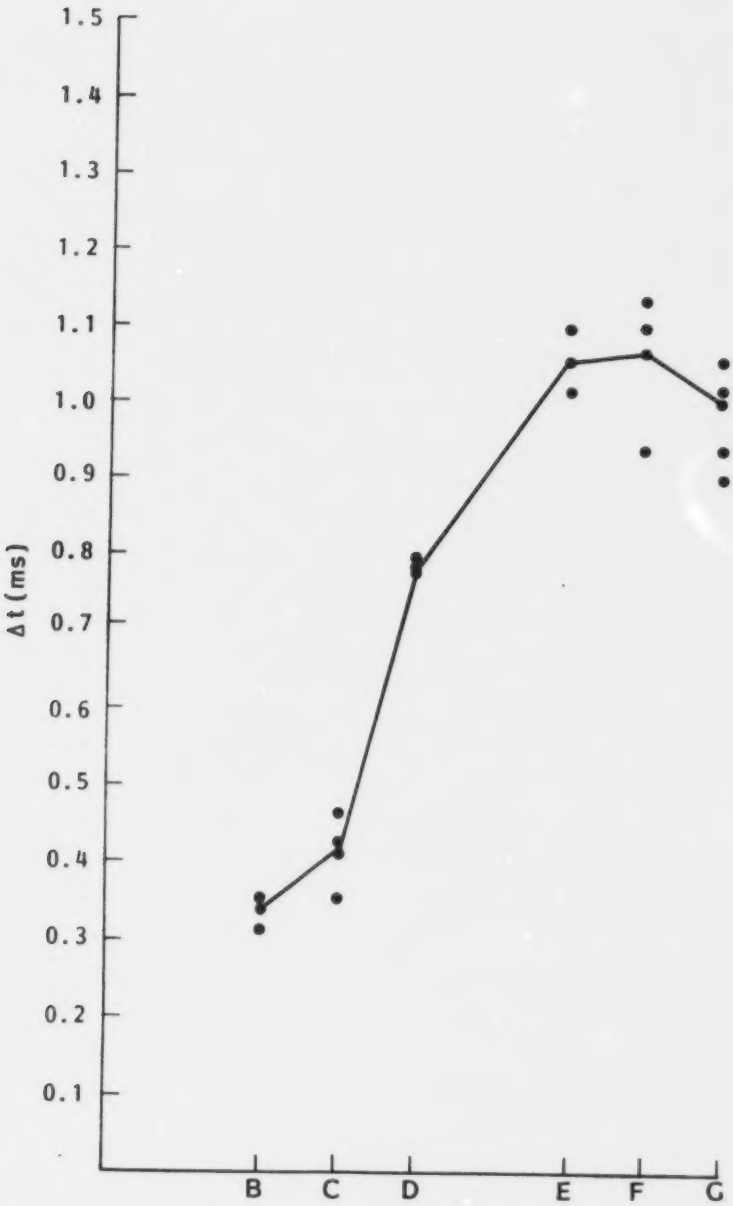

Figure 14: Controlled Impact Tests

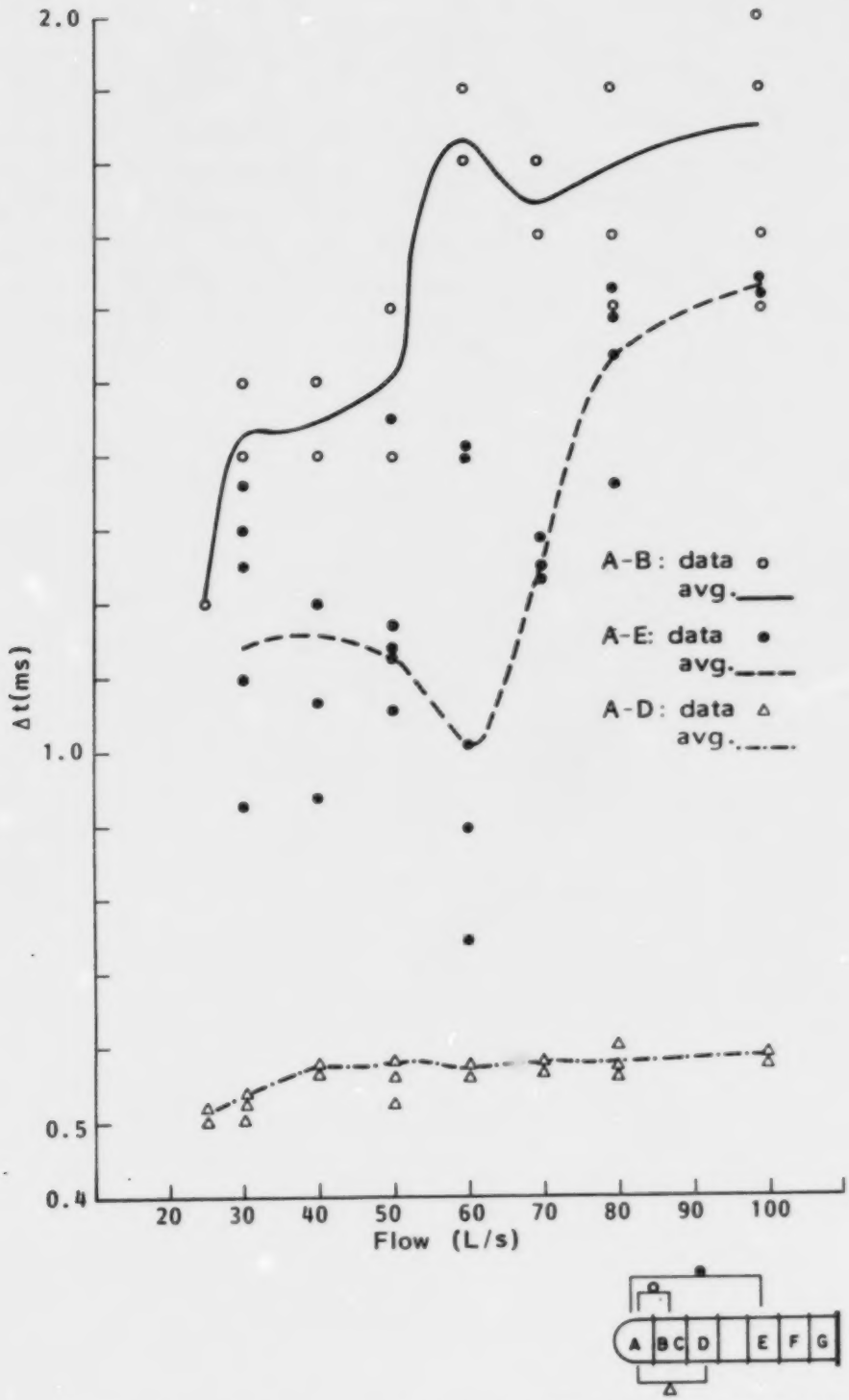

Figure 15: Δt vs Flow Rate for the Vibroacoustic Technique As-delivered Design

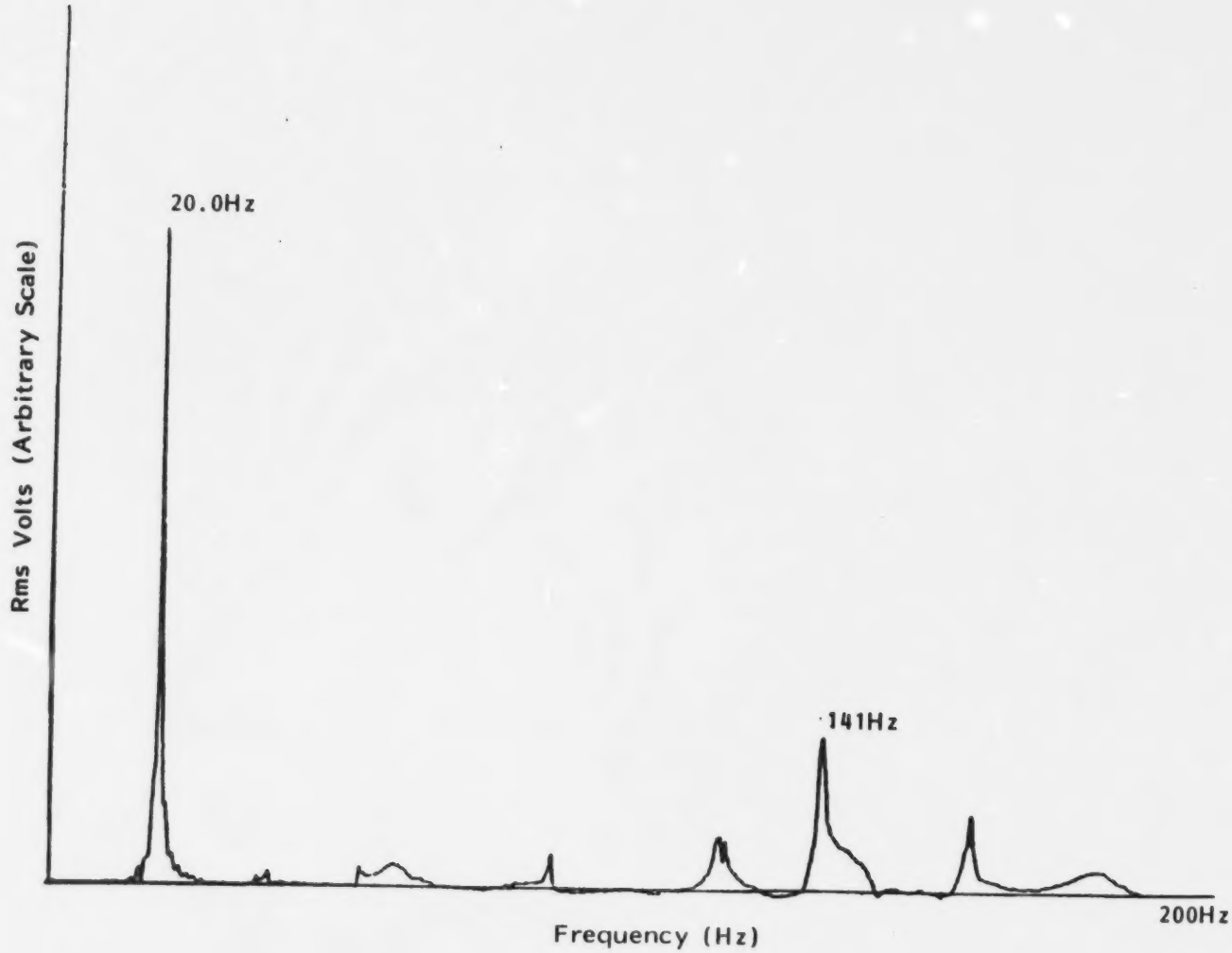

Figure 16: Impact test of Microphone Technique:
Tube D-2; 6-Baffle Configuration

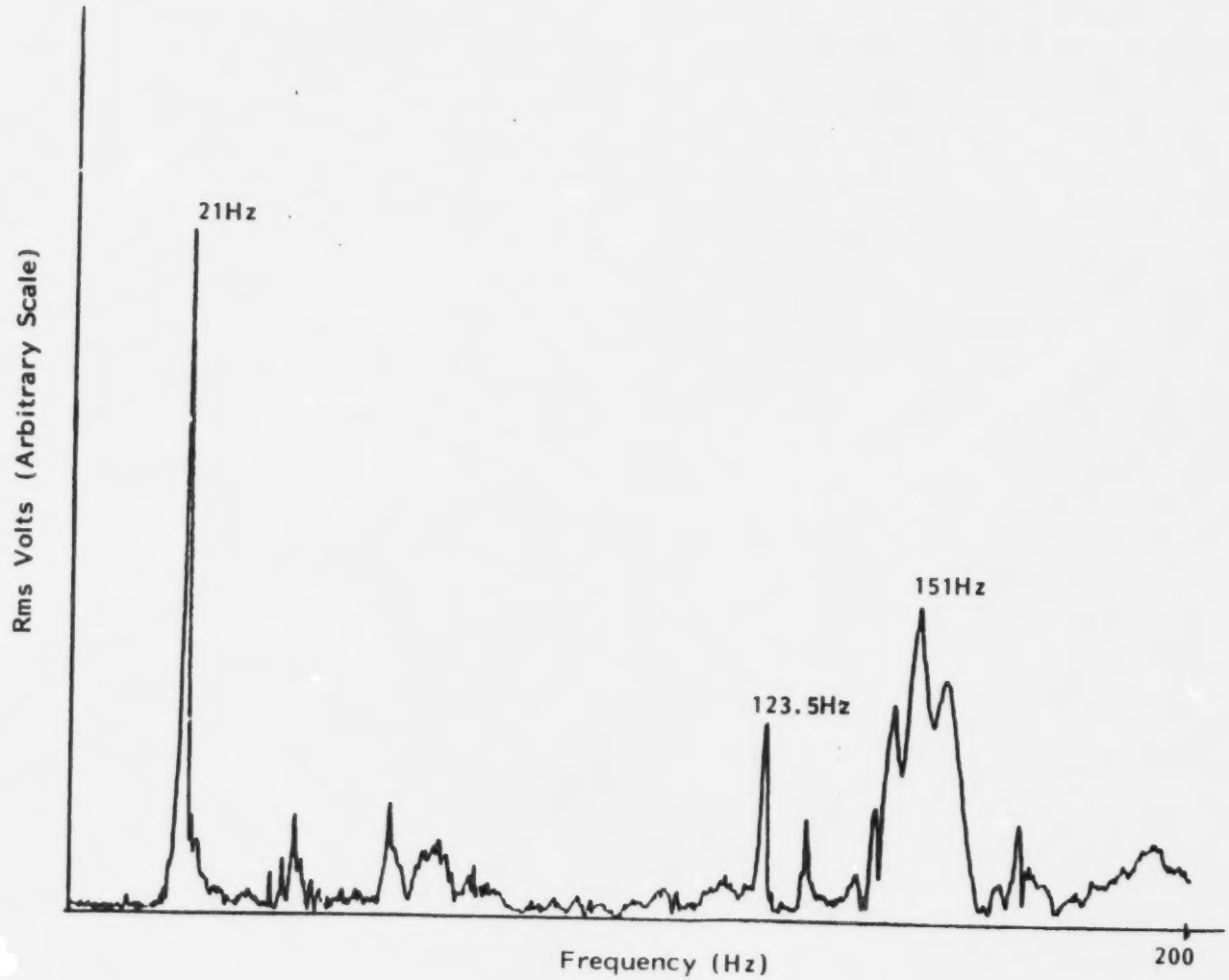

Figure 17: Impact Test of Microphone Technique: Tube C-3; 6-Baffle Configuration

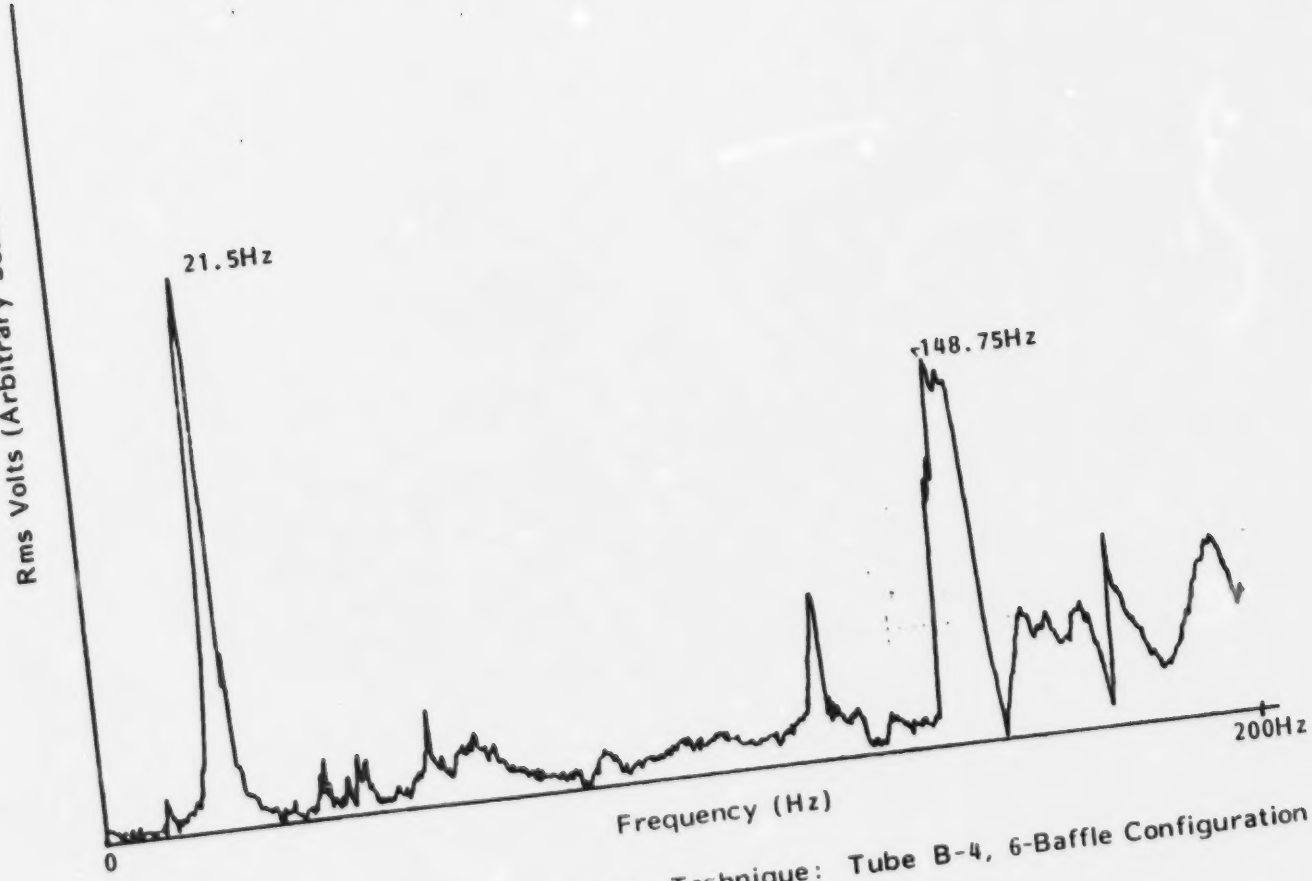

Figure 18: Impact Test of Microphone Technique: Tube B-4, 6-Baffle Configuration

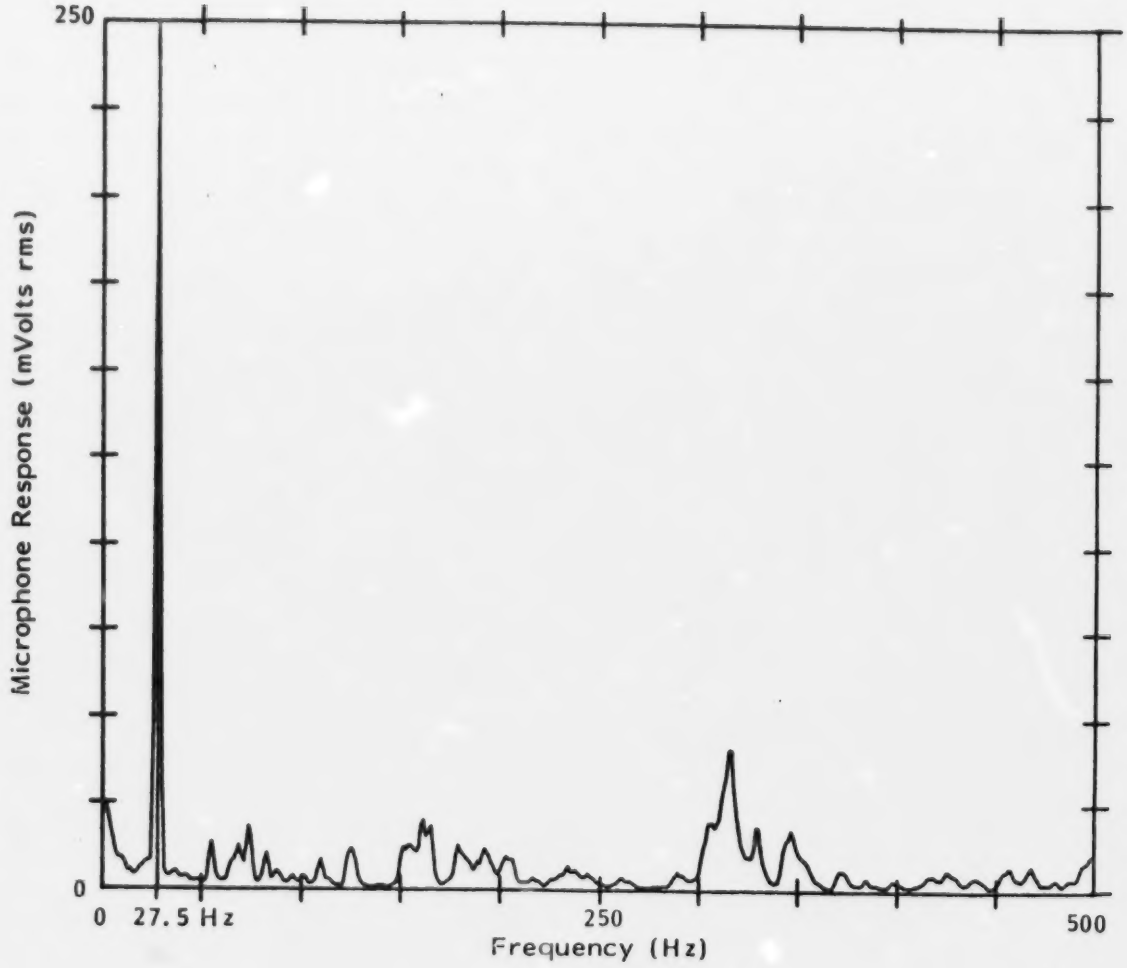

Figure 19: Phase I Microphone 24.4L/s Onset of Impacts Tube D-2

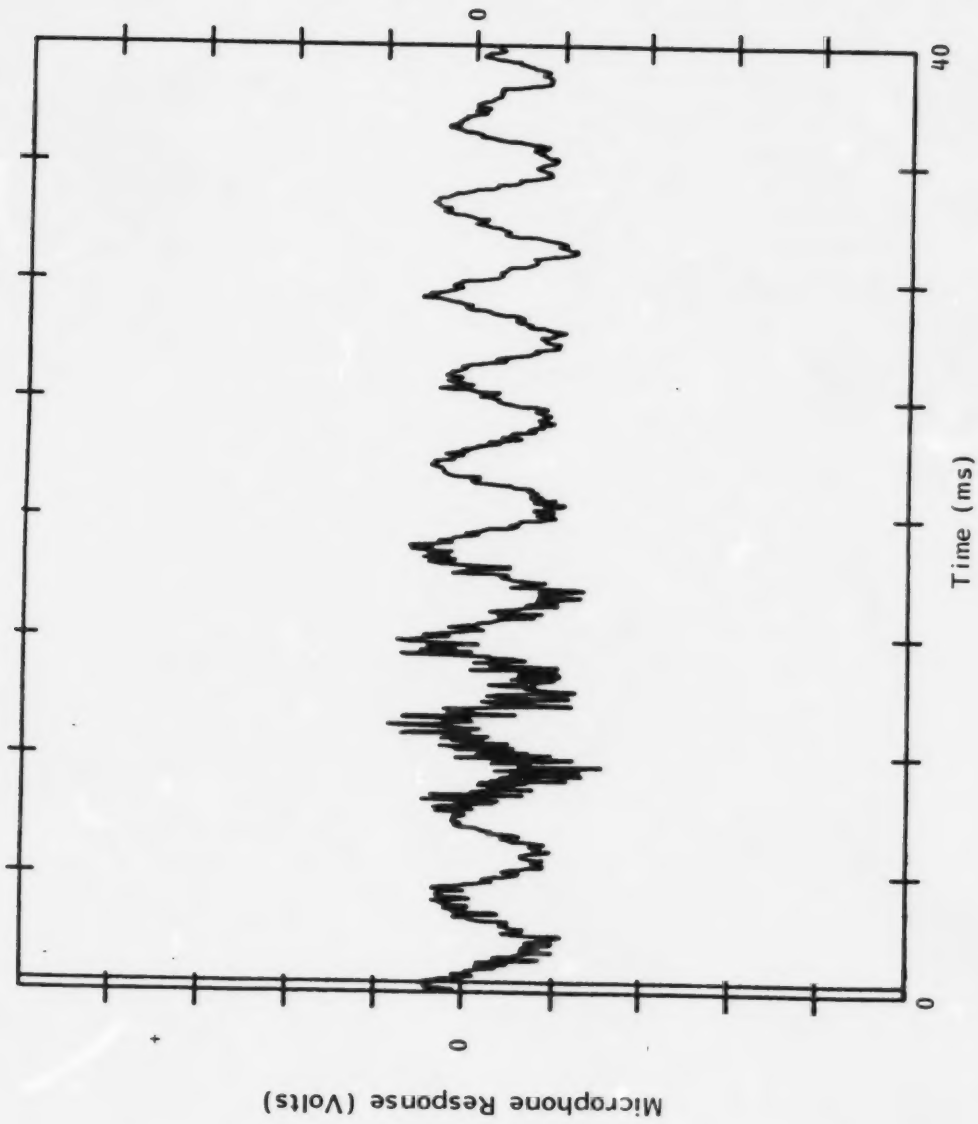

Figure 20: Phase I Microphone 24.4L/s Onset of Impacts Tube D-2

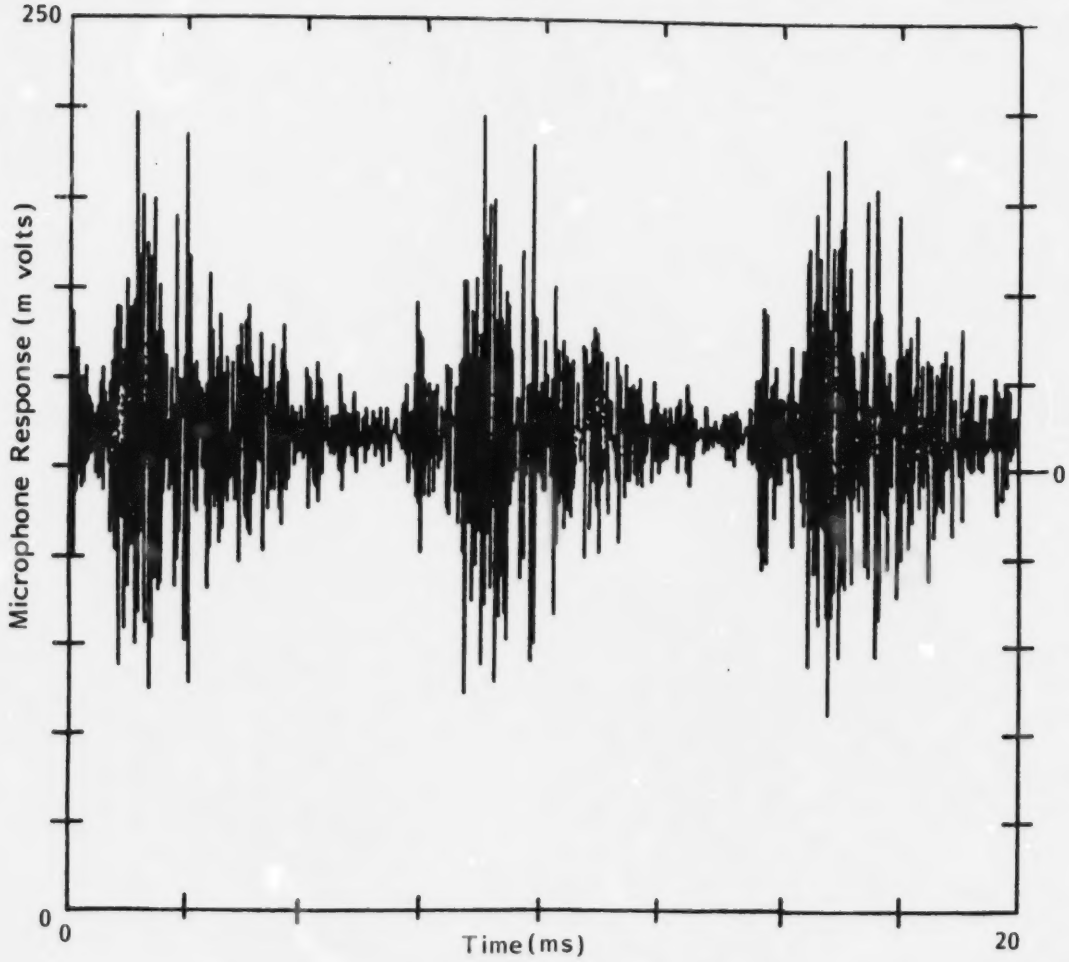

Figure 21: Phase I Microphone 24.4 L/s Onset of Impacts Tube D-2
Bandpass Filtered: 2kHz to 7kHz

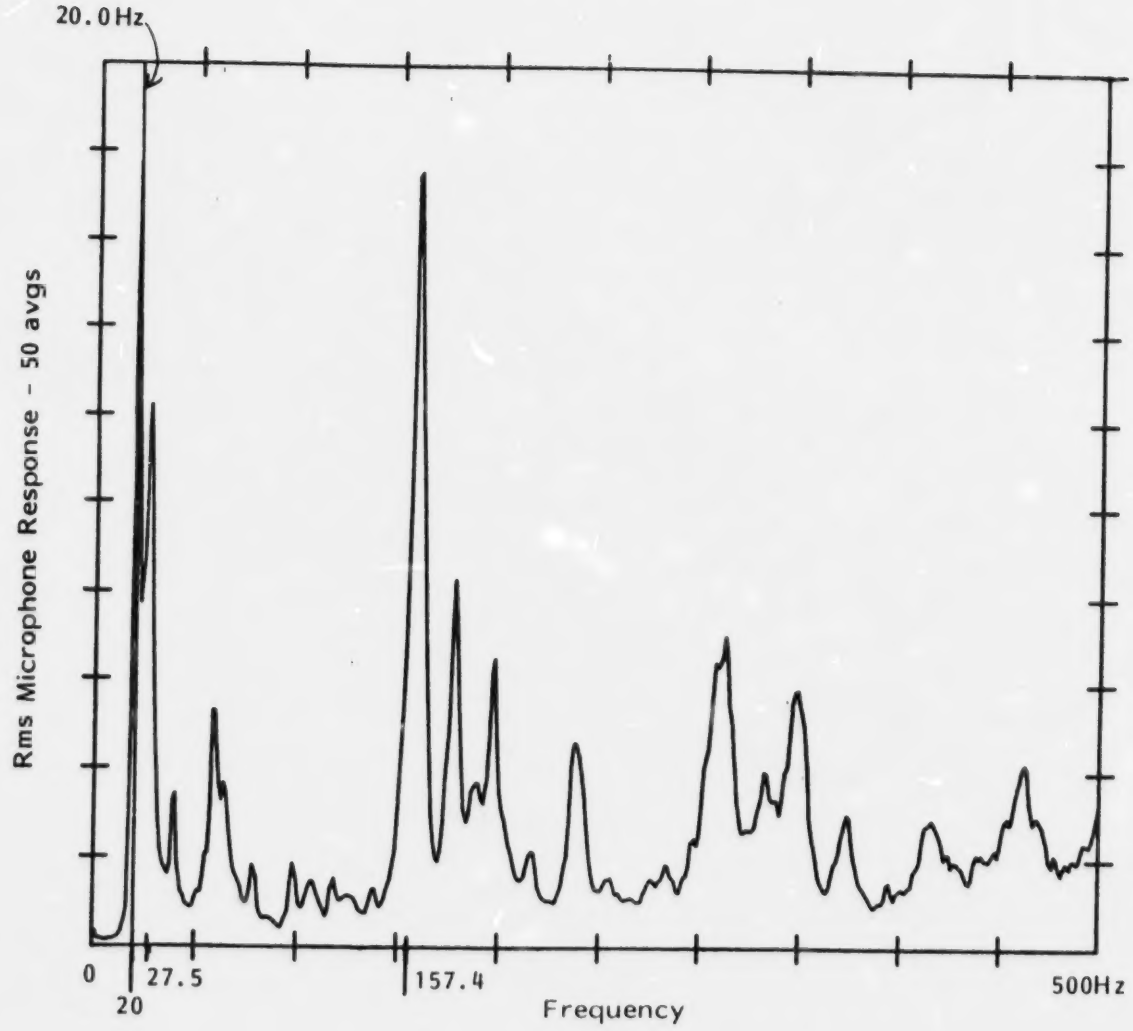

Figure 22: Phase I Microphone 99.9 L/s Tube C-3

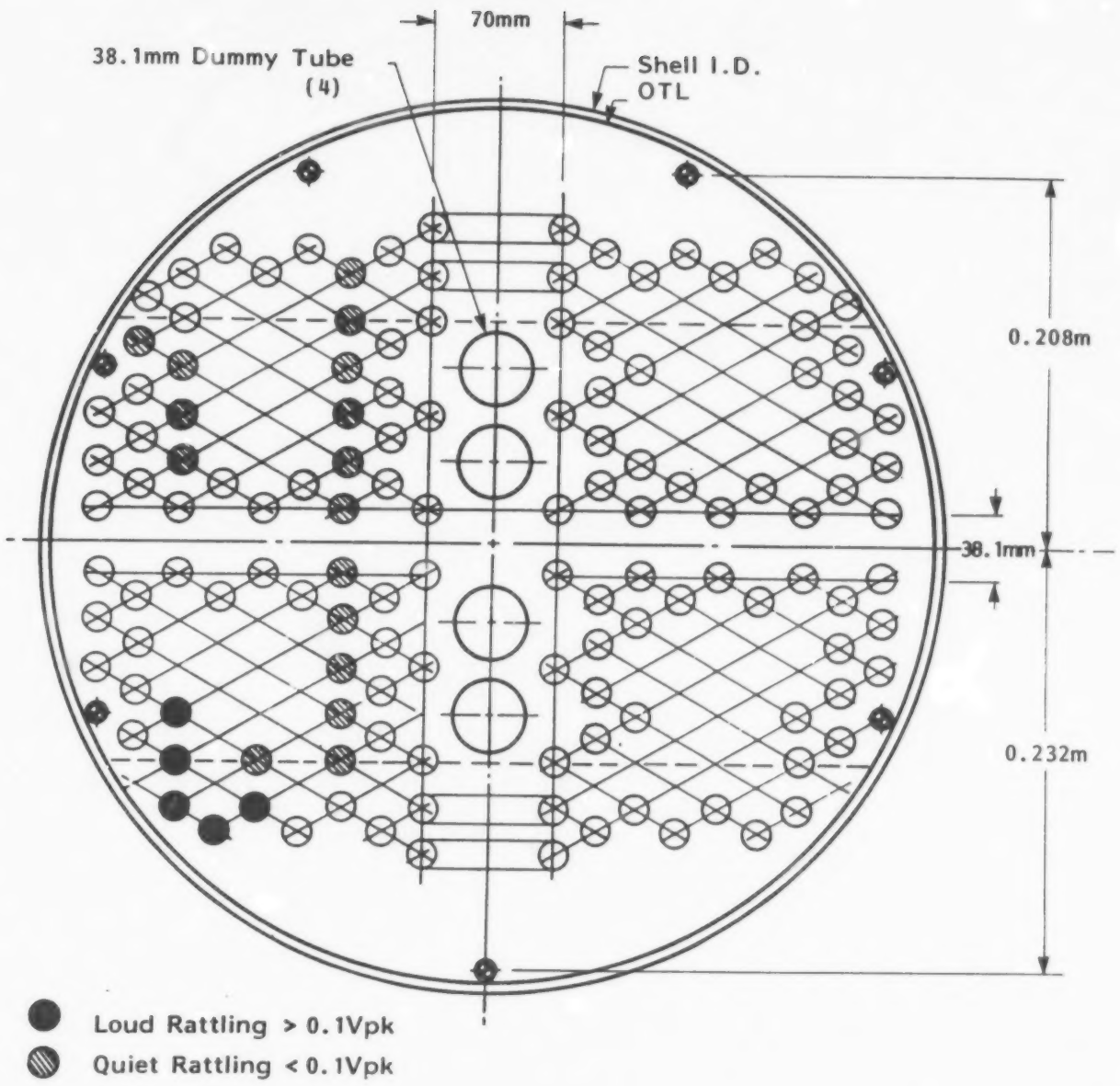

Figure 23: Microphone Tests Tube Row D Removed, 31.6 L/s

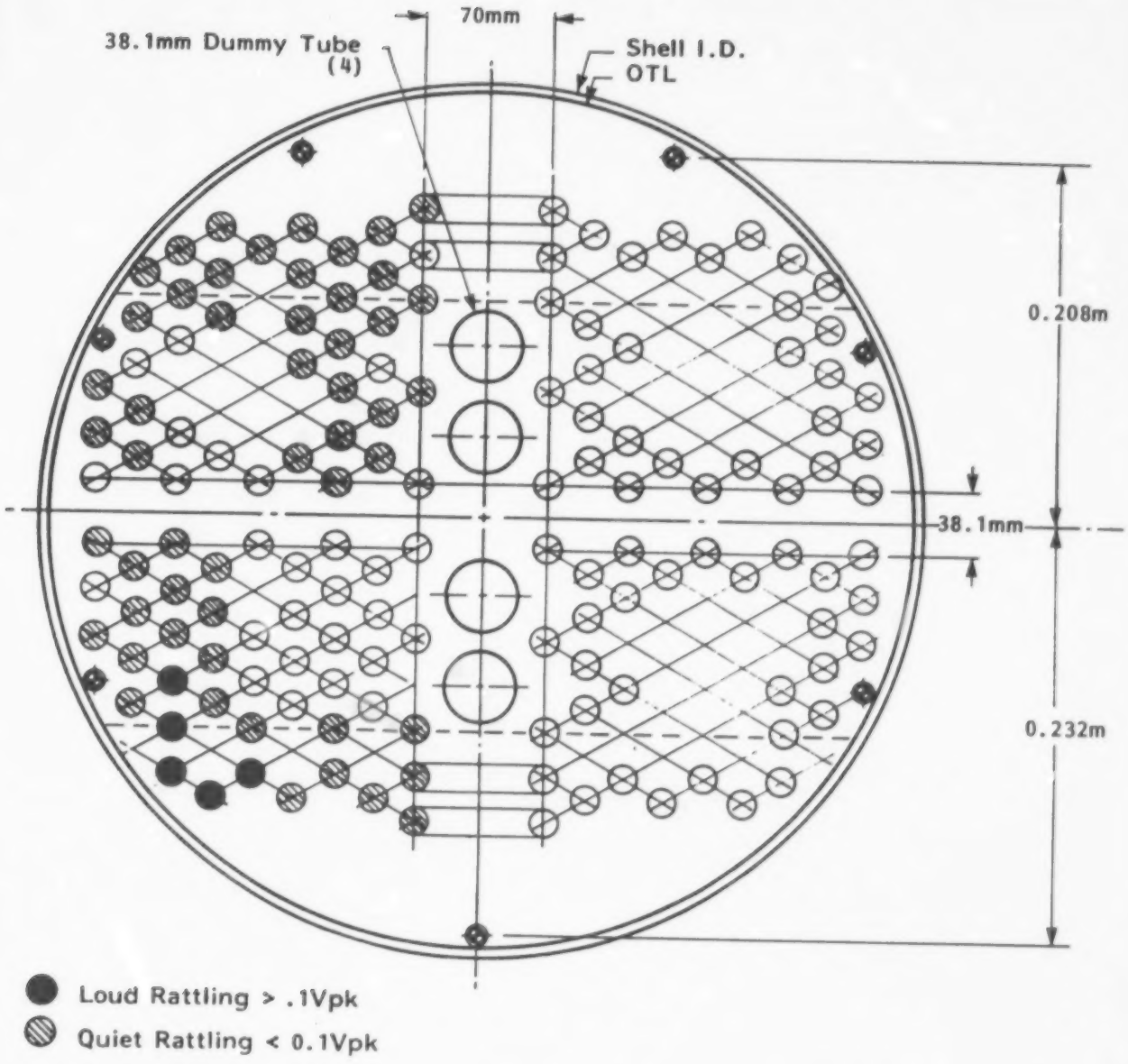

Figure 24: Microphone Tests Tube Row D Removed, 60 L/s

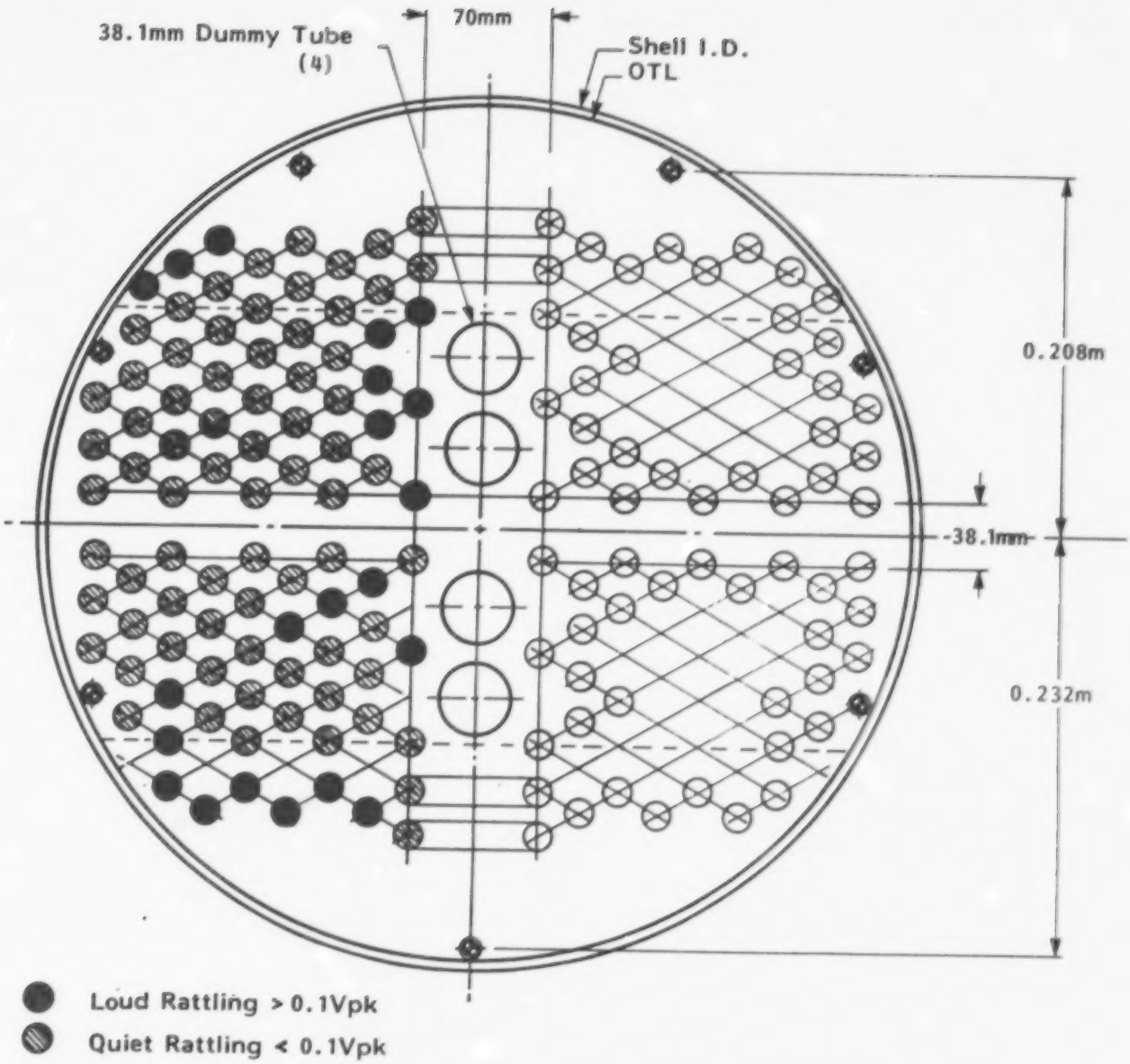

Figure 25: Microphone Tests Tube Row D Removed, 100 L/s

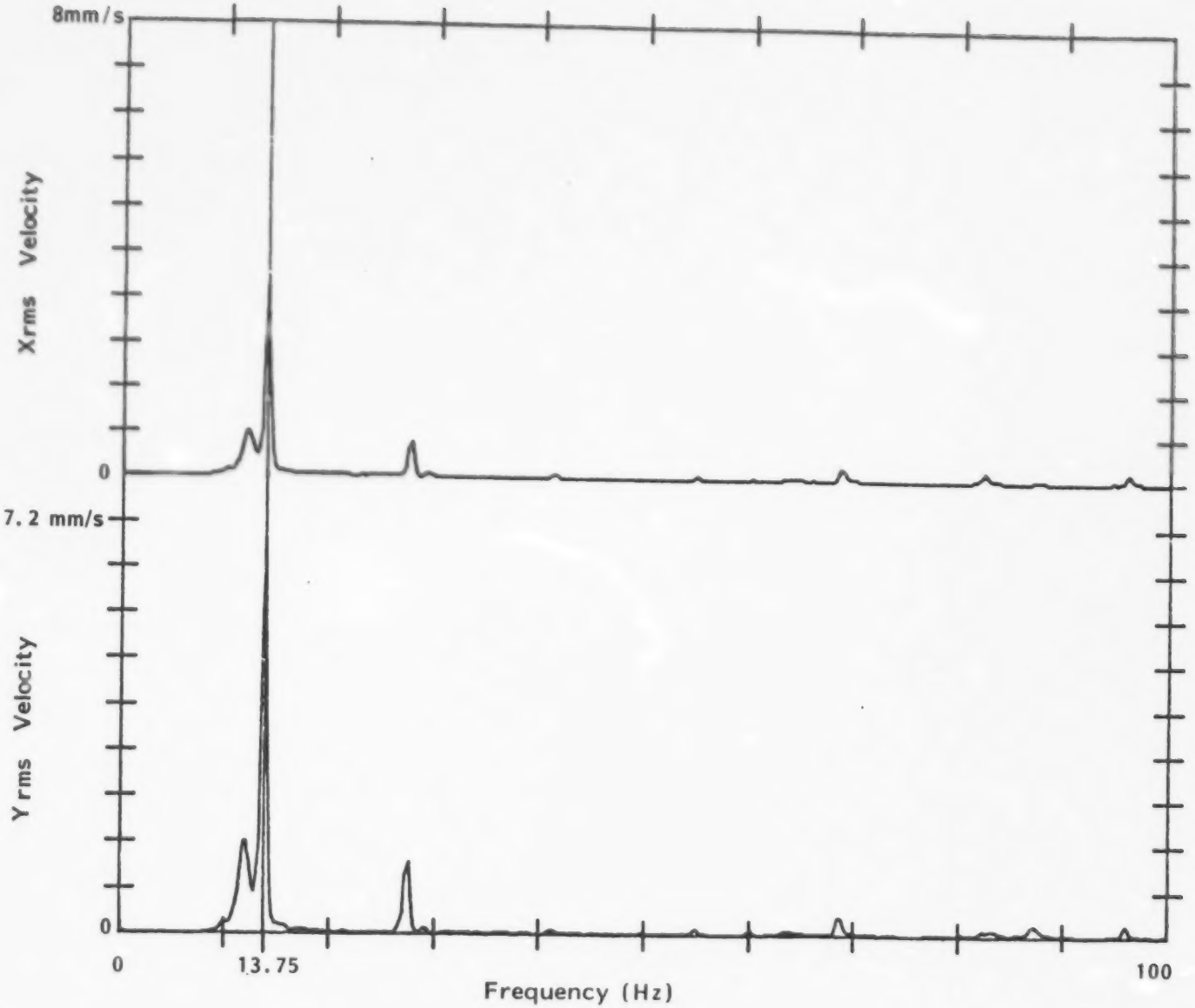

Figure 26: Phase I
Tube D-2, RMS Velocity Spectra for 90° U Bend Position at 24 L/s

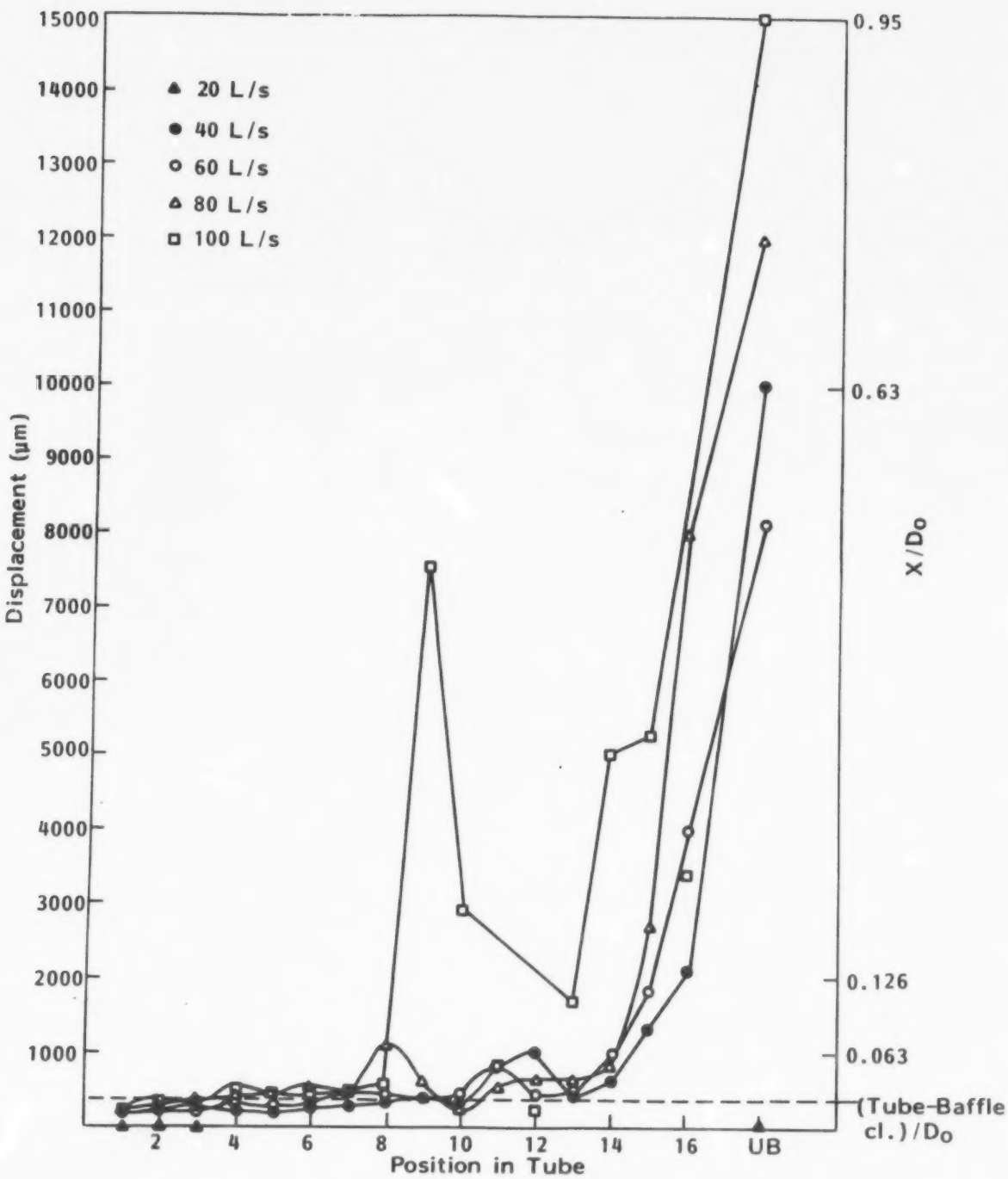

Figure 27: Phase I
Tube B-4 Xp-p Displacement

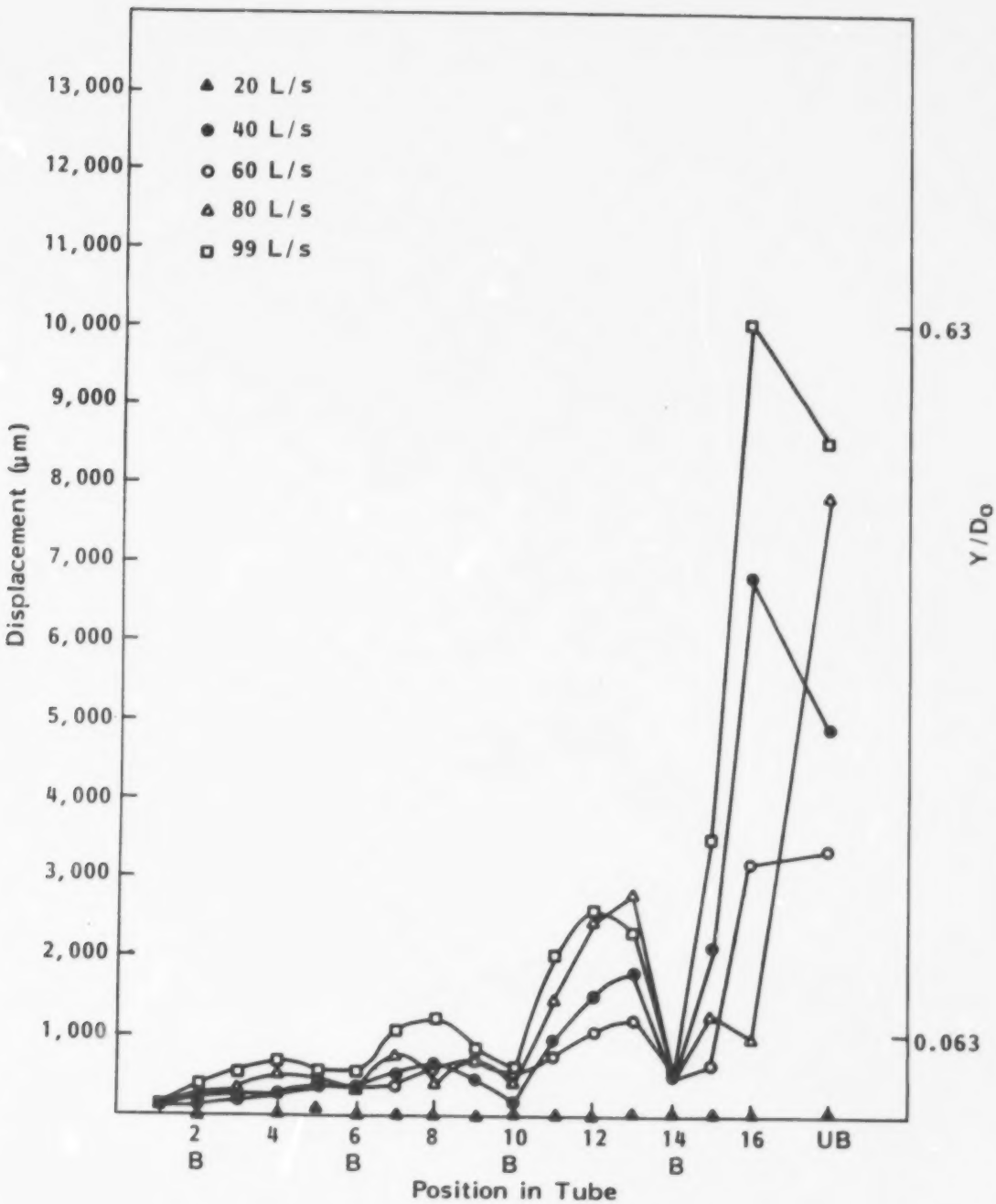

Figure 28: Phase I
Tube B-4 Yp-p Displacement

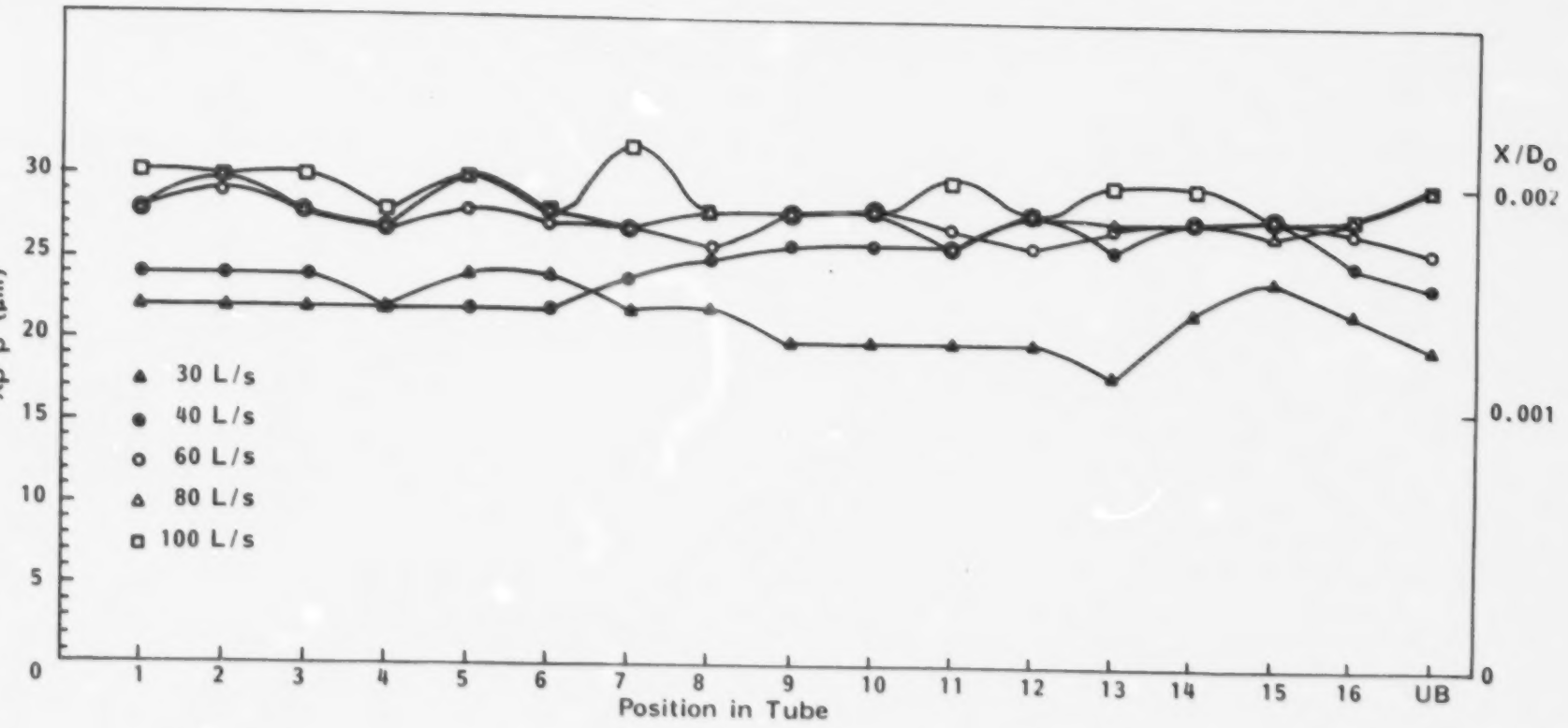

Figure 29: Phase I
Tube M-5 Xp-p Displacement

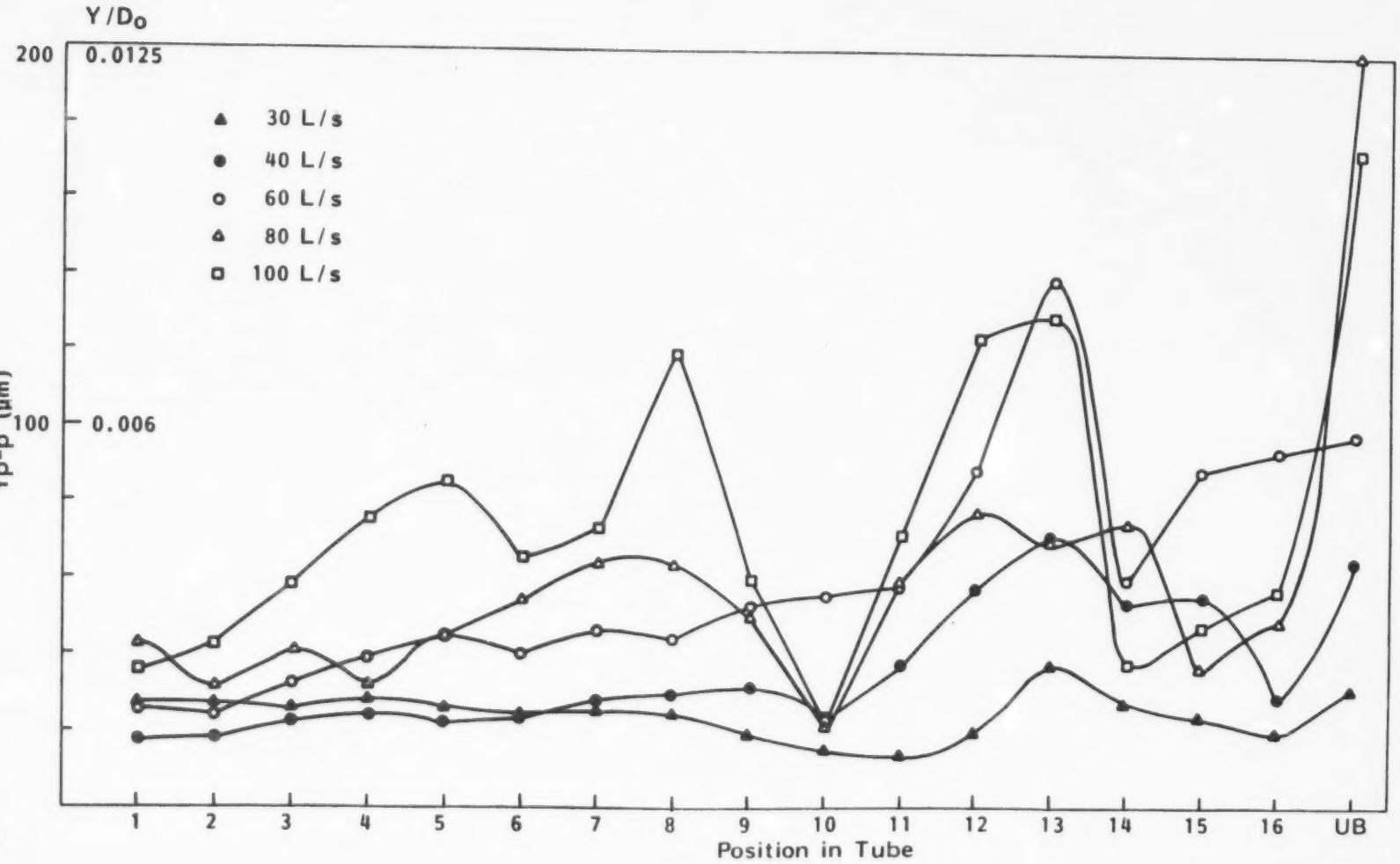

Figure 30: Phase I
Tube M-5 Y p-p Displacement

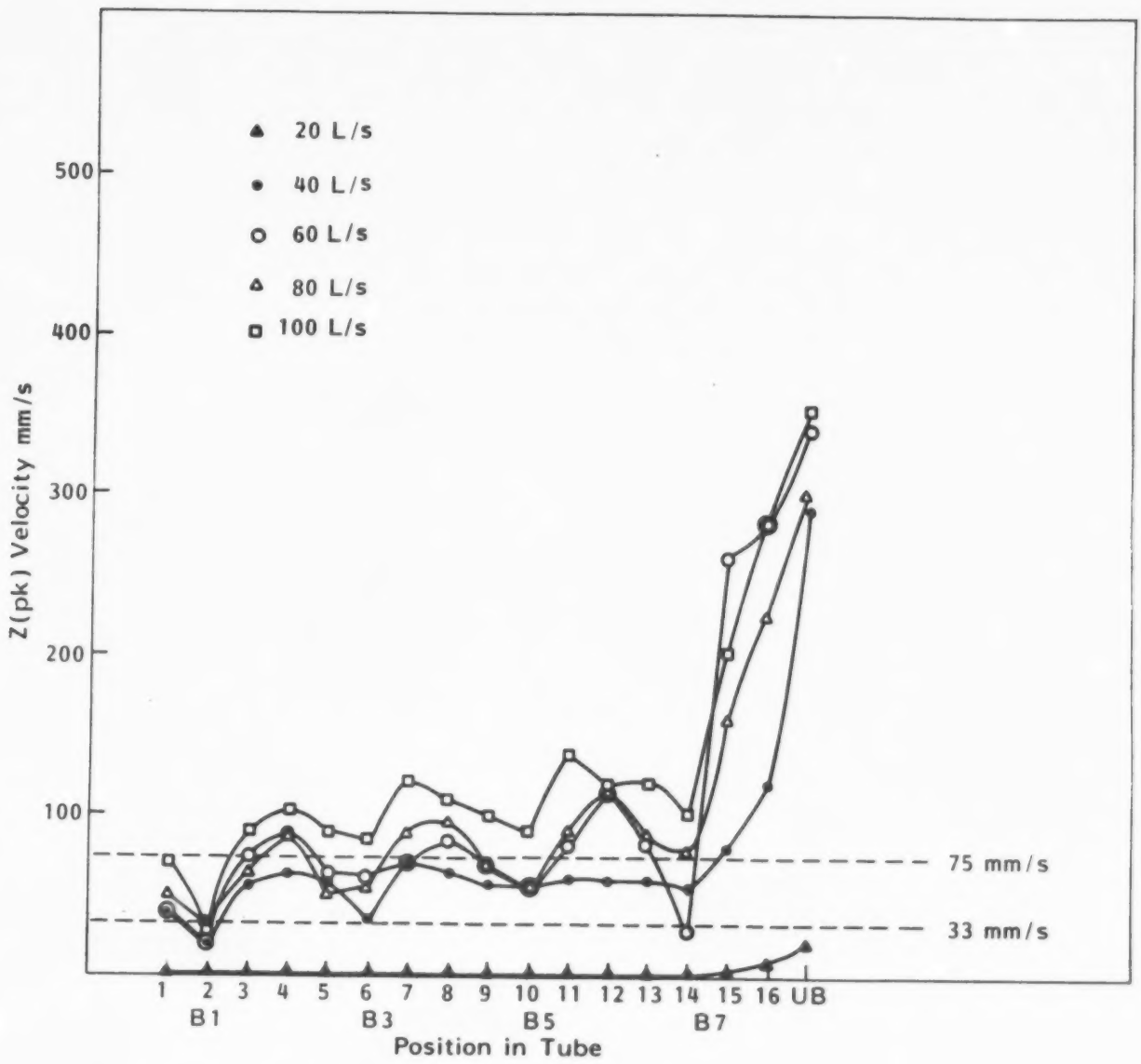

Figure 31: Phase II Dummy Tubes Removed
Z(pk)Velocity vs Position for Tube C-3

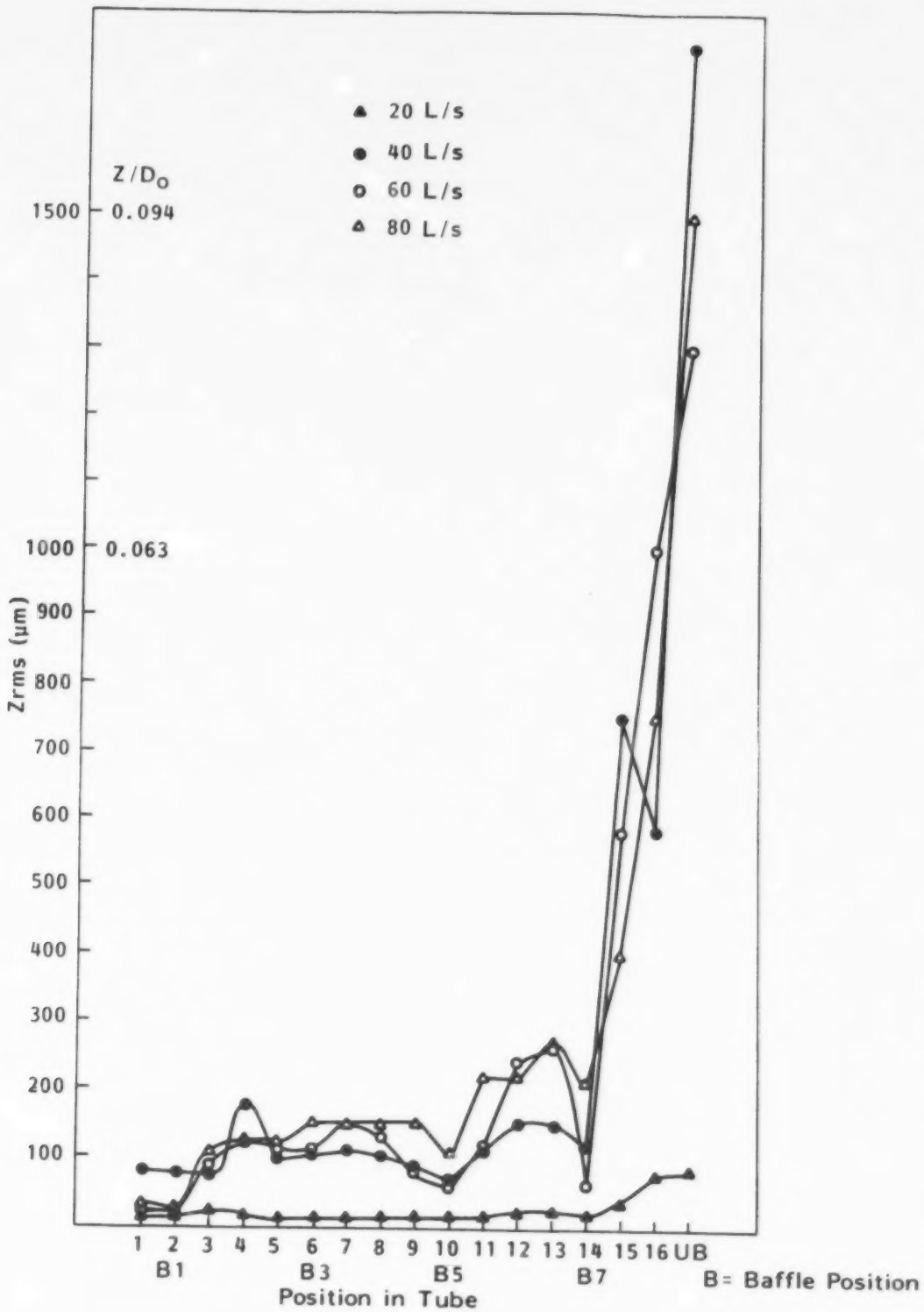

Figure 32: Phase II Dummy Tubes Removed
Zrms Displacement vs Position in Tube C-3

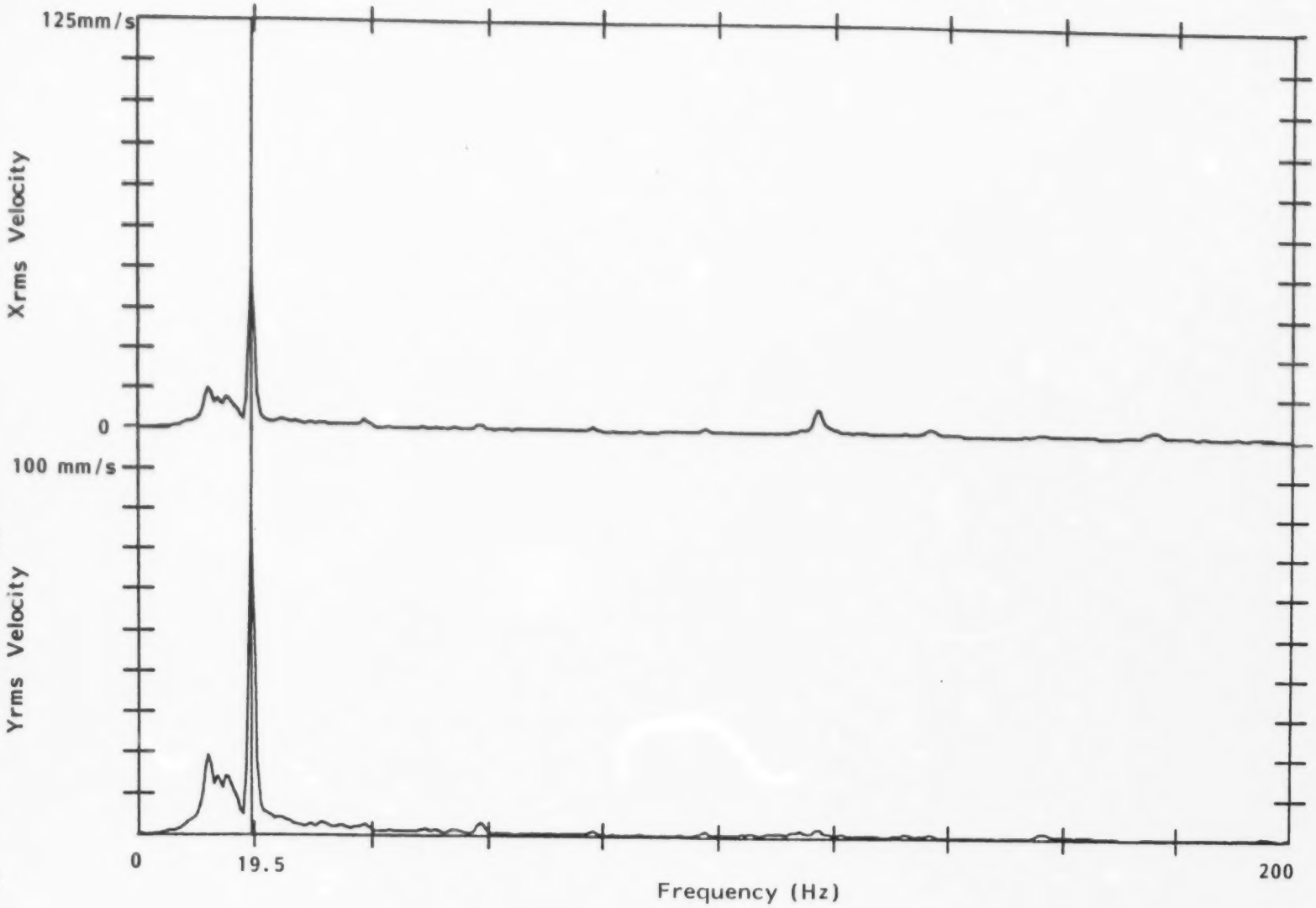

Figure 33: Phase II Dummy Tubes Removed
RMS Velocity Spectra for Tube C-3 90° in U Bend at 100 L/s

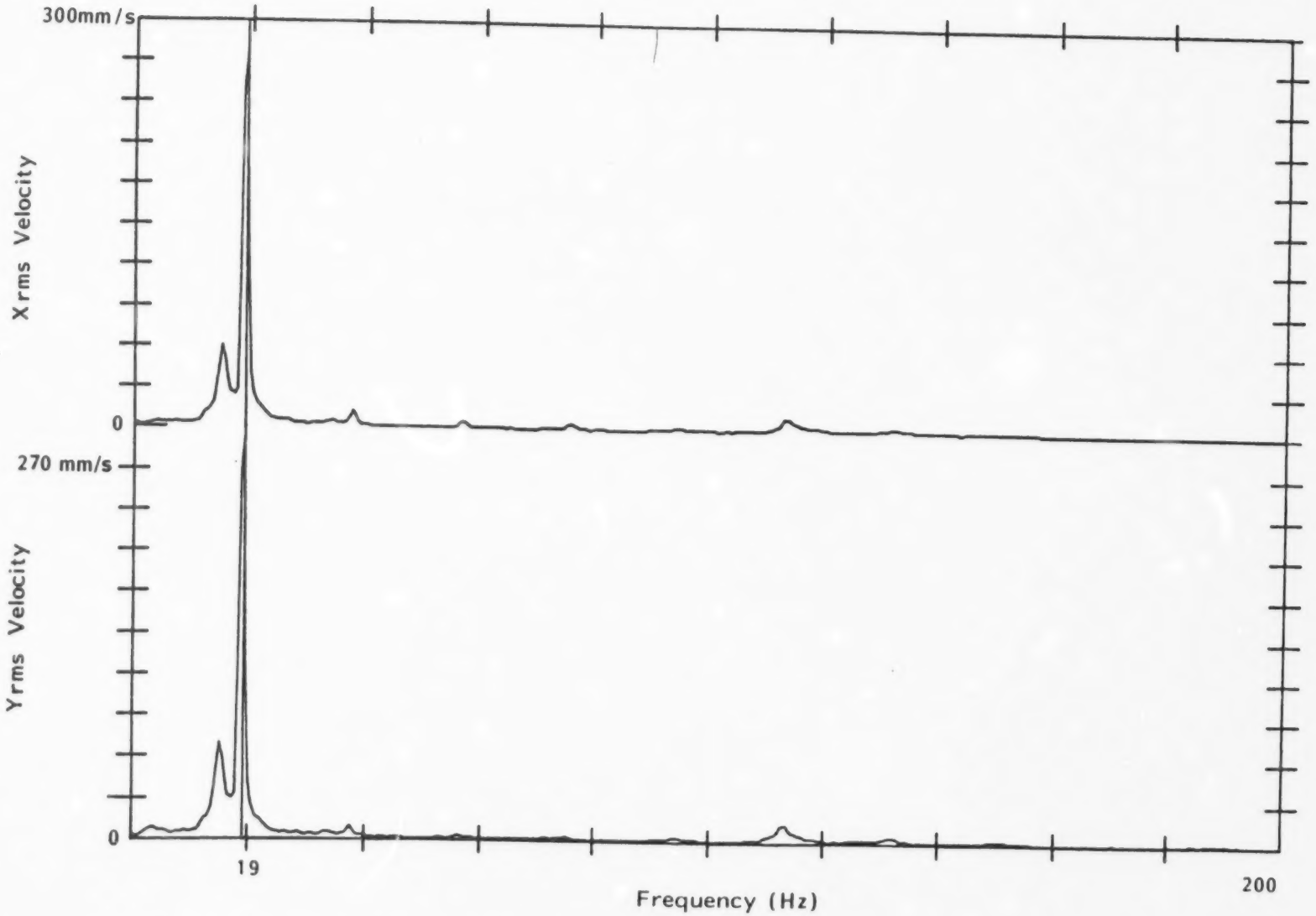

Figure 34: Phase II Dummy Tubes Removed
RMS Velocity Spectra for Tube B-4, 90° in U Bend at 100 L/s

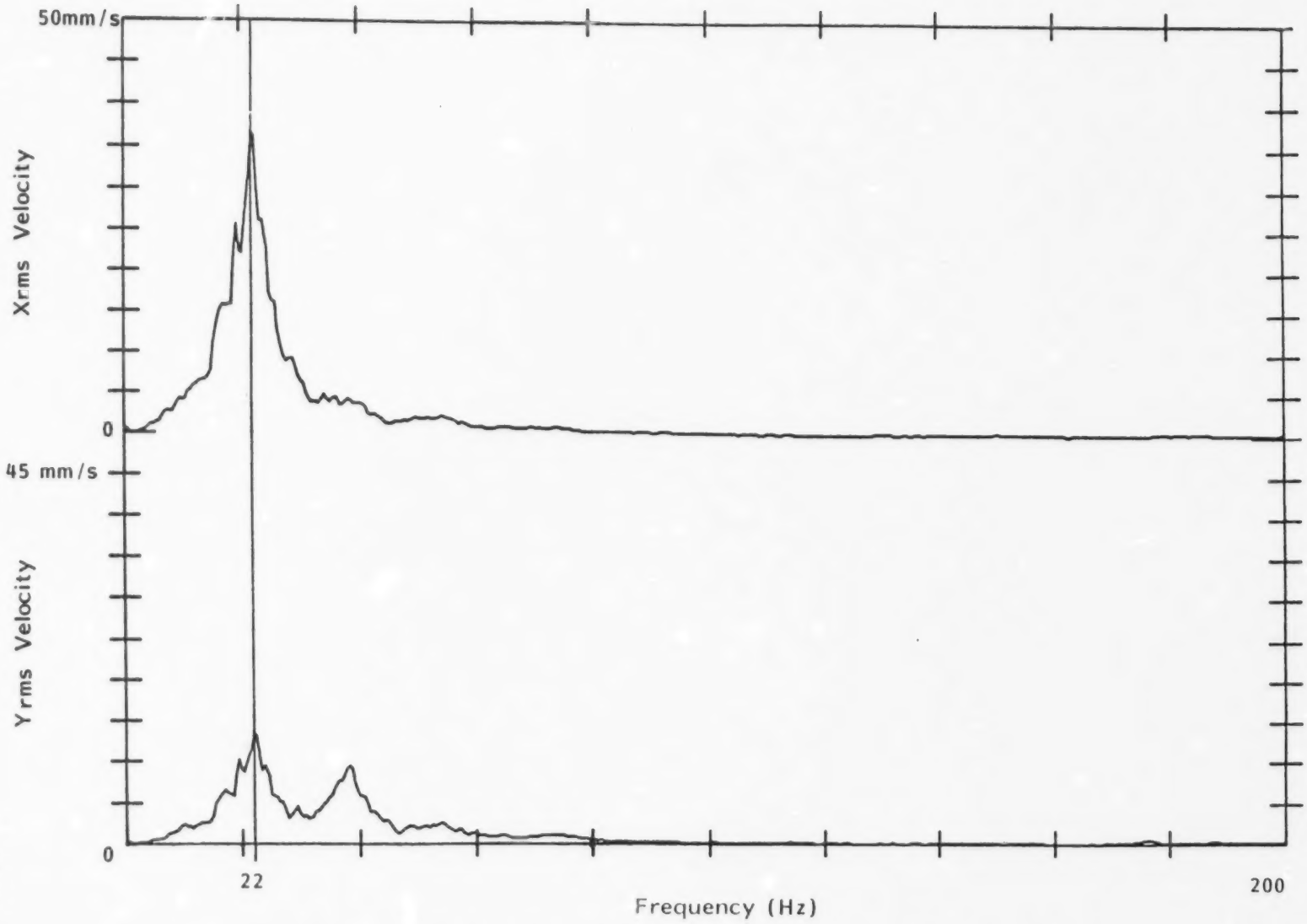

Figure 35: Phase II Dummy Tubes Removed
RMS Velocity Spectra for Tube A-9 at the Tangent Line Position at 100 L/s

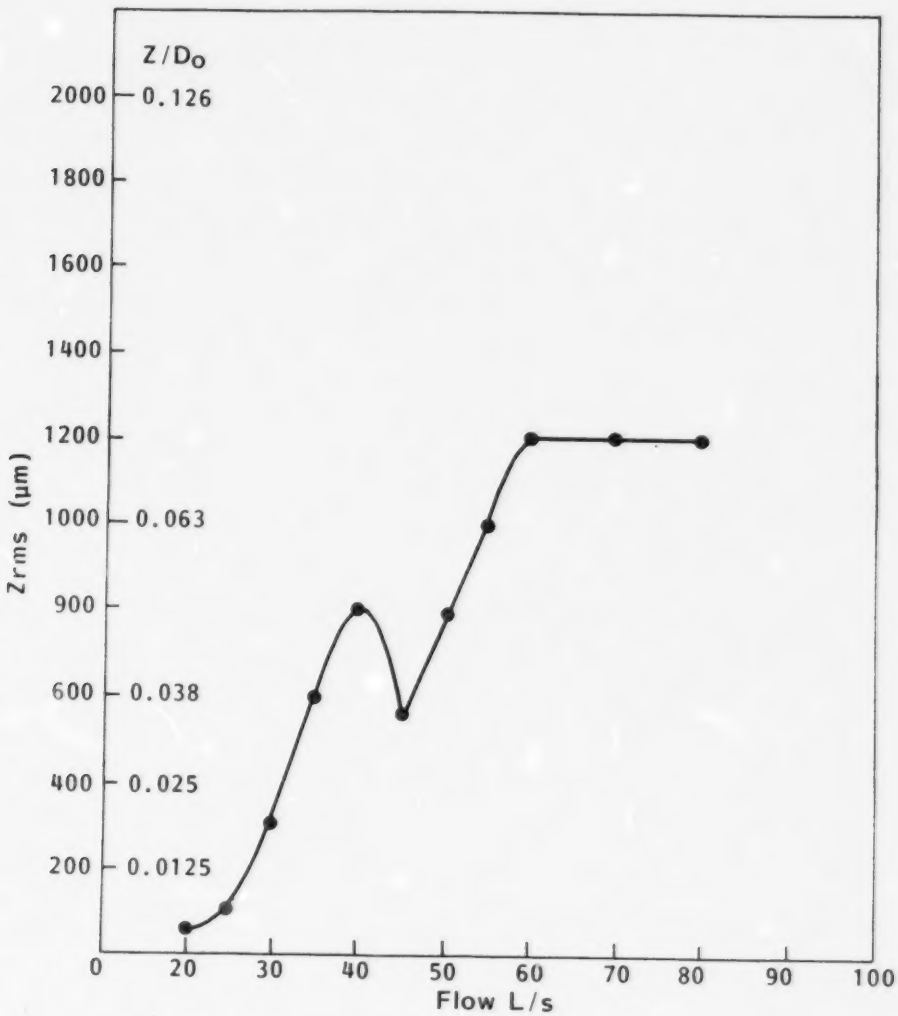

Figure 36: Phase III Tube Row D Removed
Tube C-3 U Bend RMS Displacement vs Flow

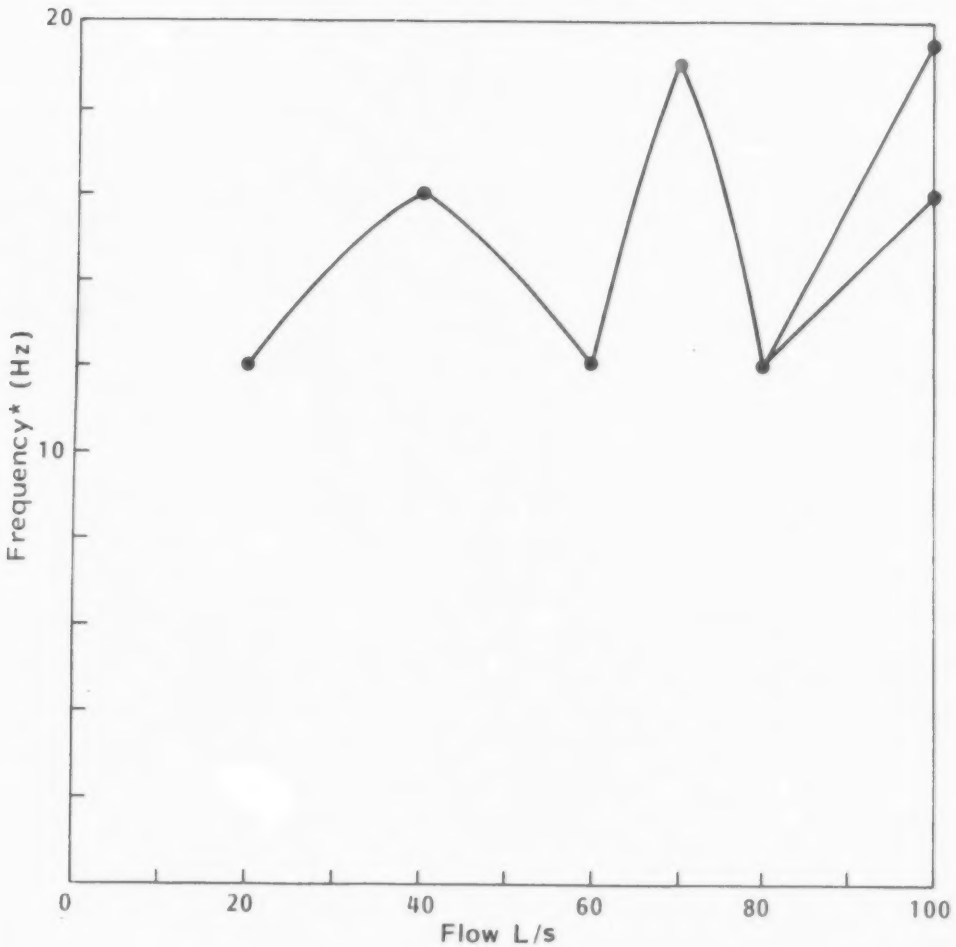

* X & Y Response at same Frequency

Figure 37: Phase III
Tube C-3 Frequencies Measured in the U Bend Over a Range of Flows

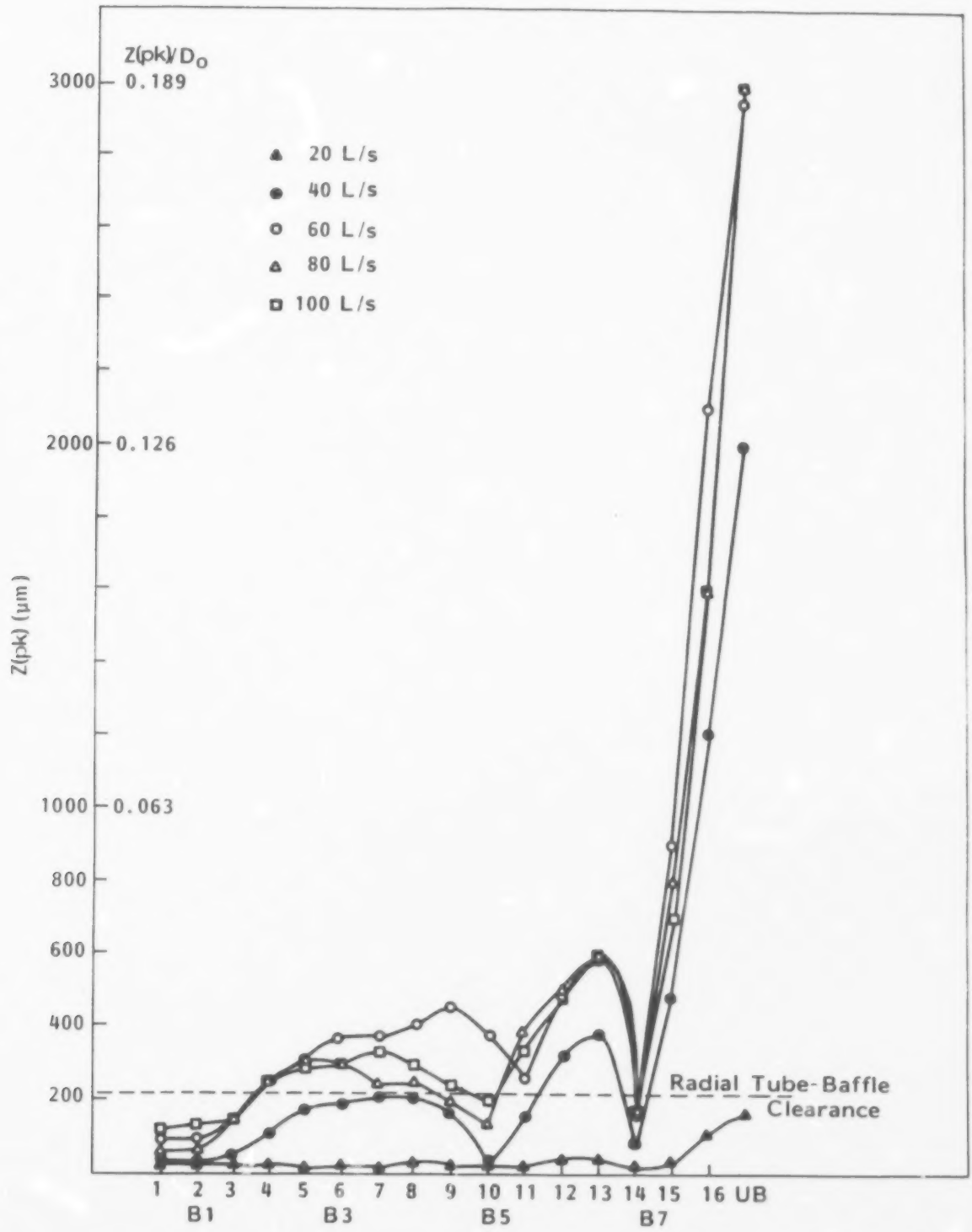

Figure 38: Phase III Tests
Tube C-3 Z(pk) Displacement vs Position for all Flows

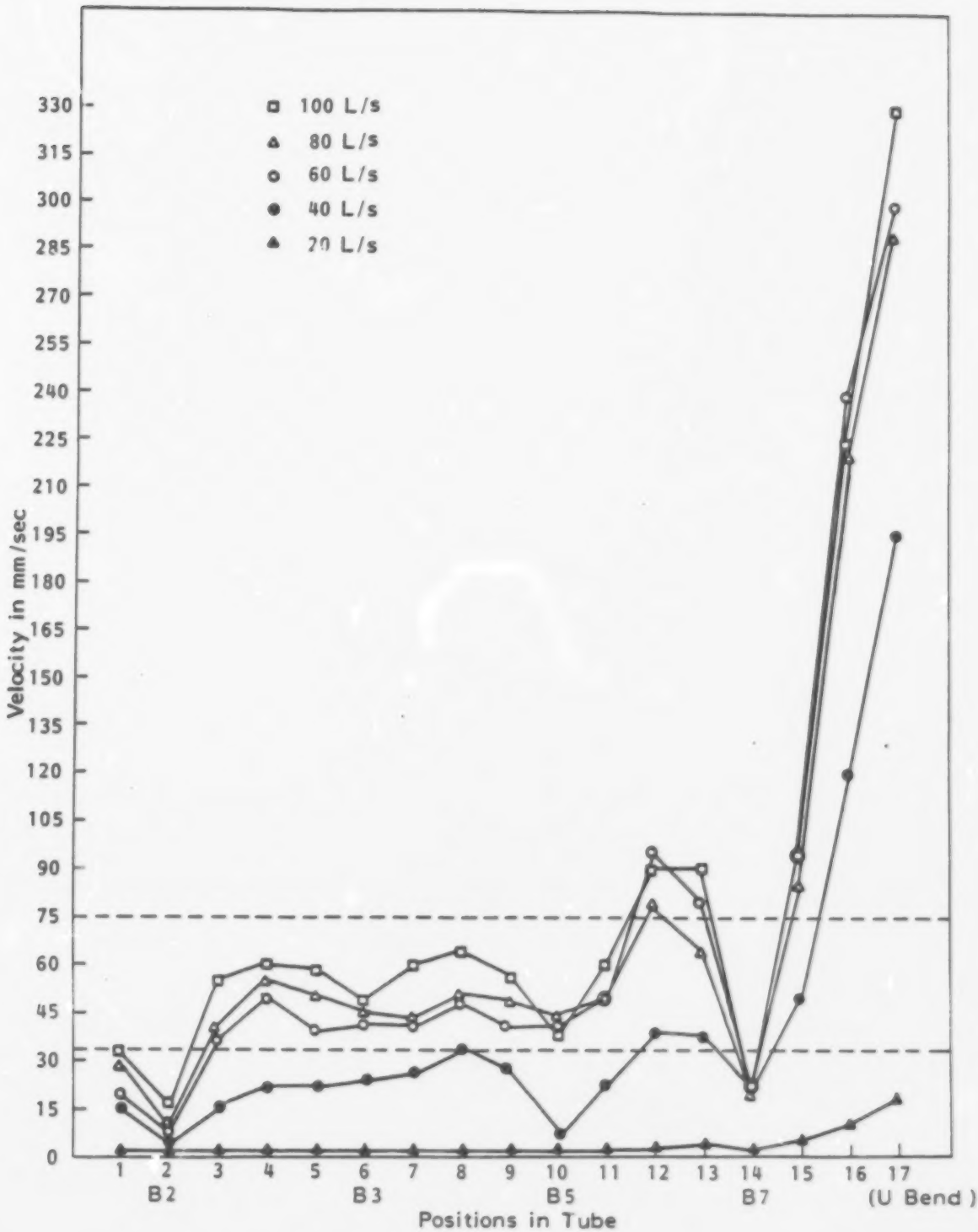

Figure 39: Phase III Tests
Tube C-3 Z Peak Velocity as a Function of Position

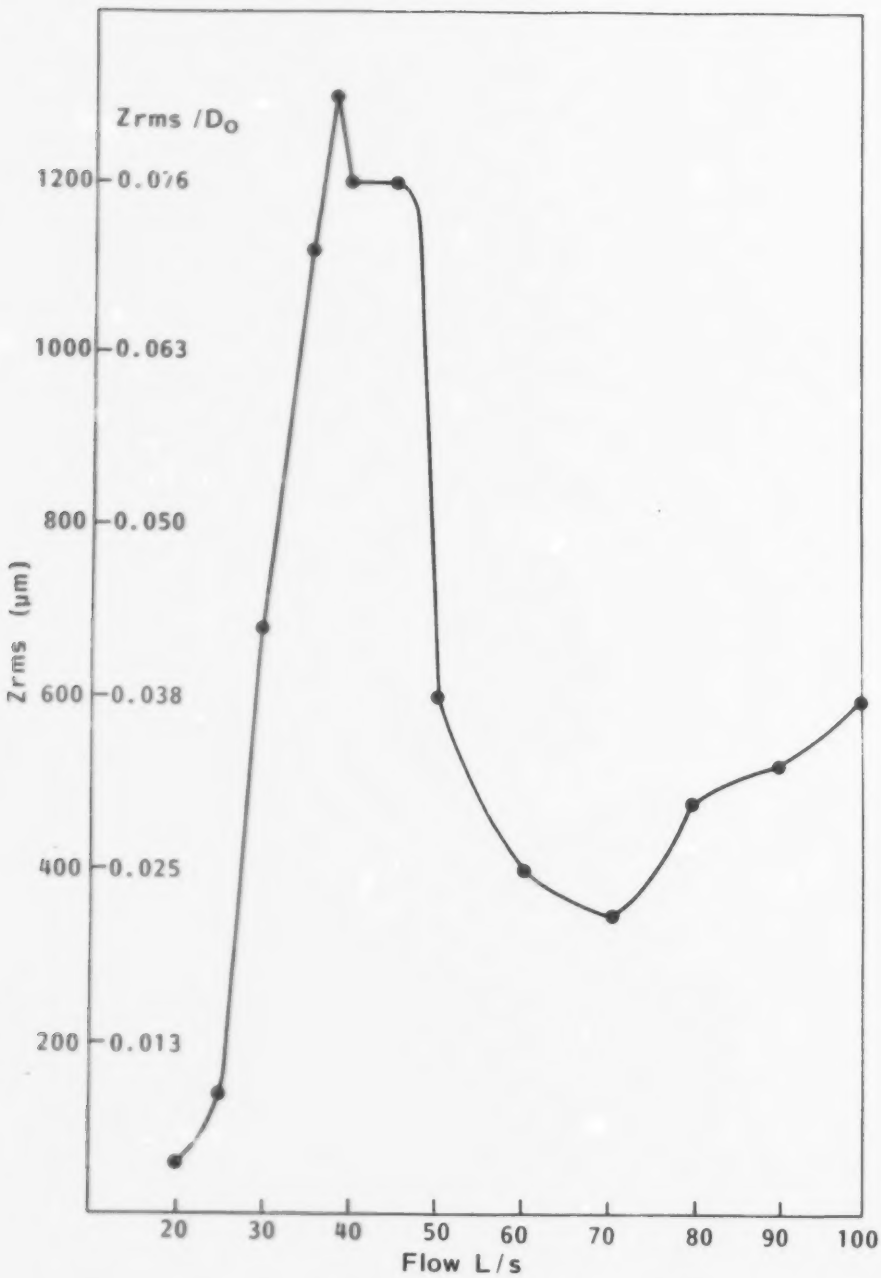

Figure 40: Phase III
Tube C-5 ZRMS Displacement vs Flow in the 90° U Bend Position

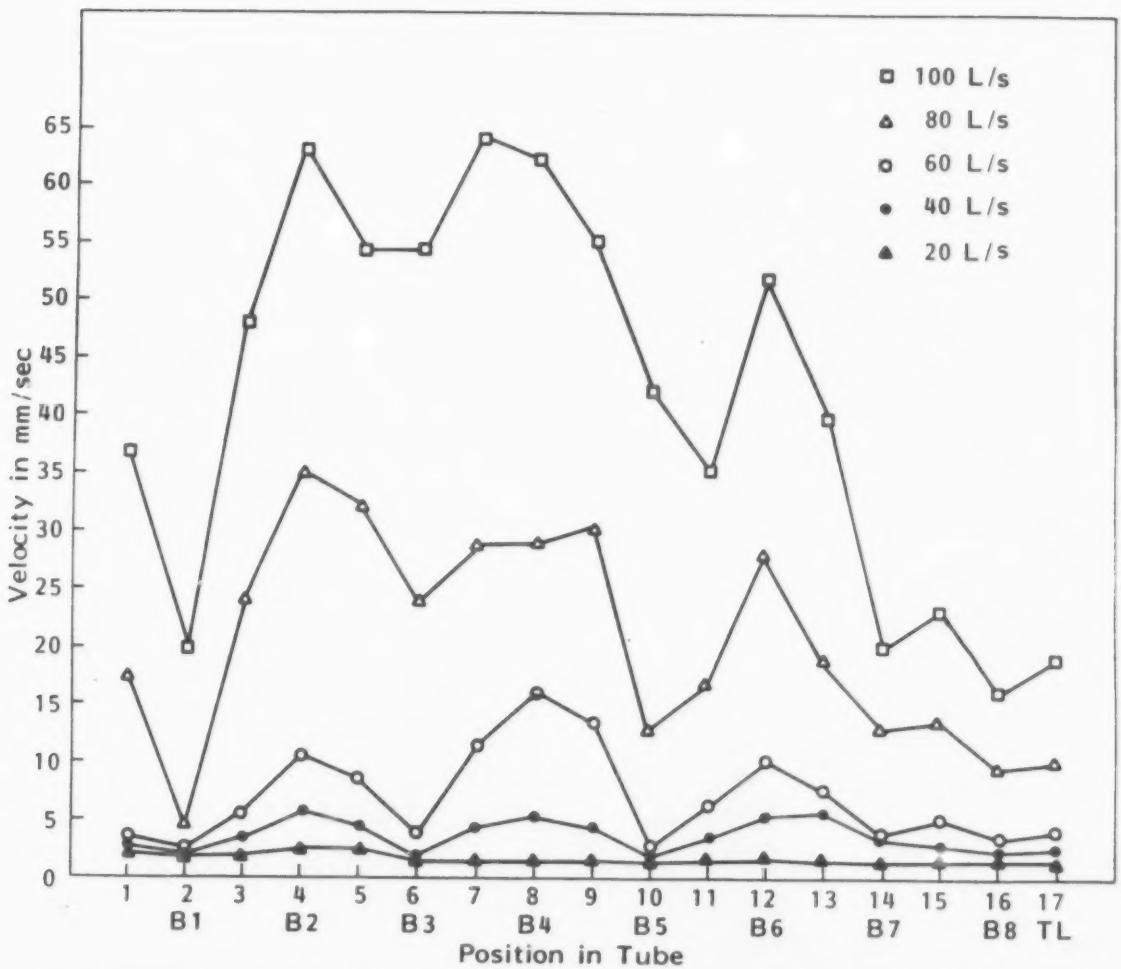

Figure 41: Phase III
Tube R-9 Z Peak Velocity from Strip Chart Records

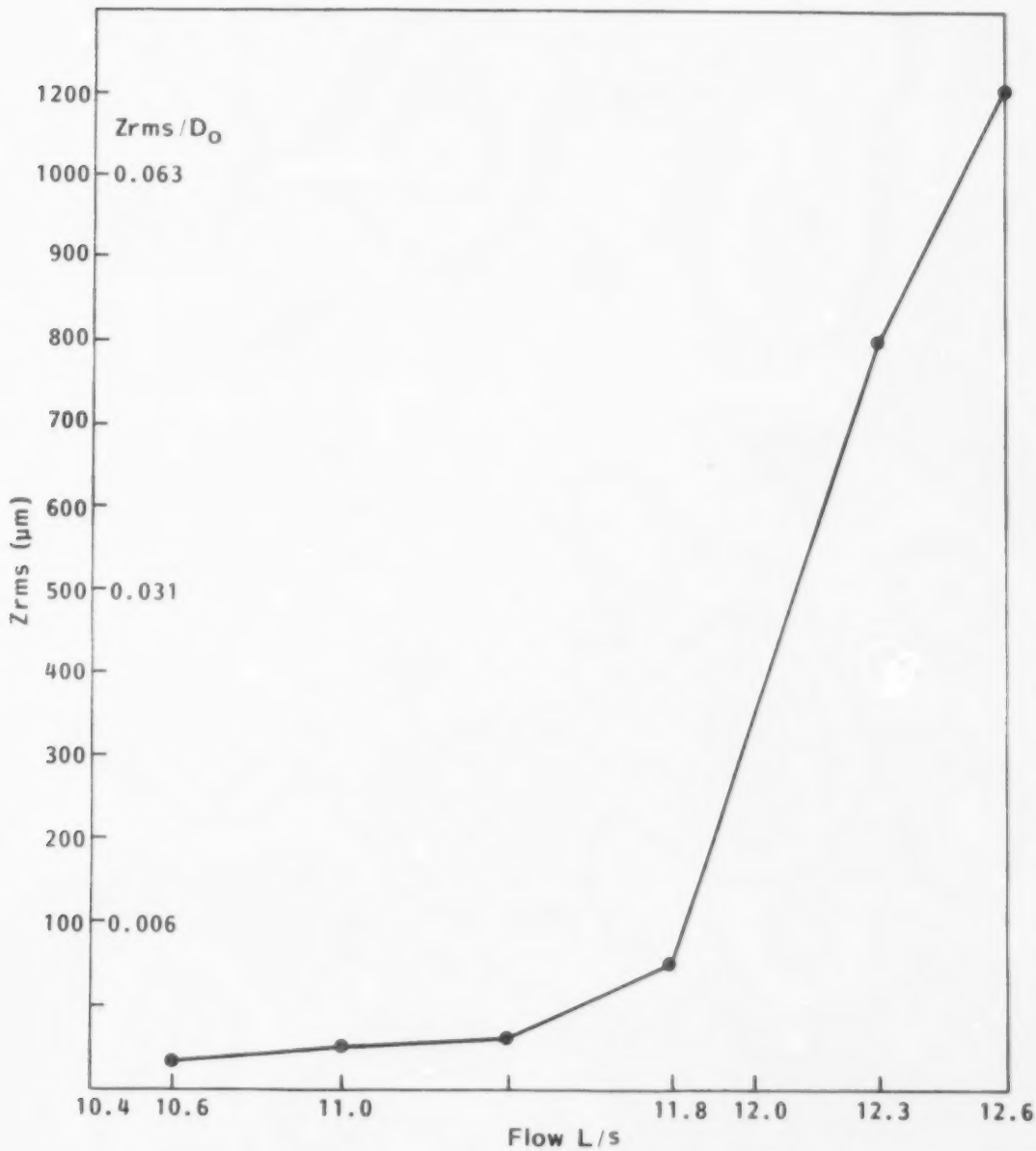

Figure 42: Phase IV Tests
Tube B-4 Displacement vs Flow for the 90° U Bend Position, Low Flow

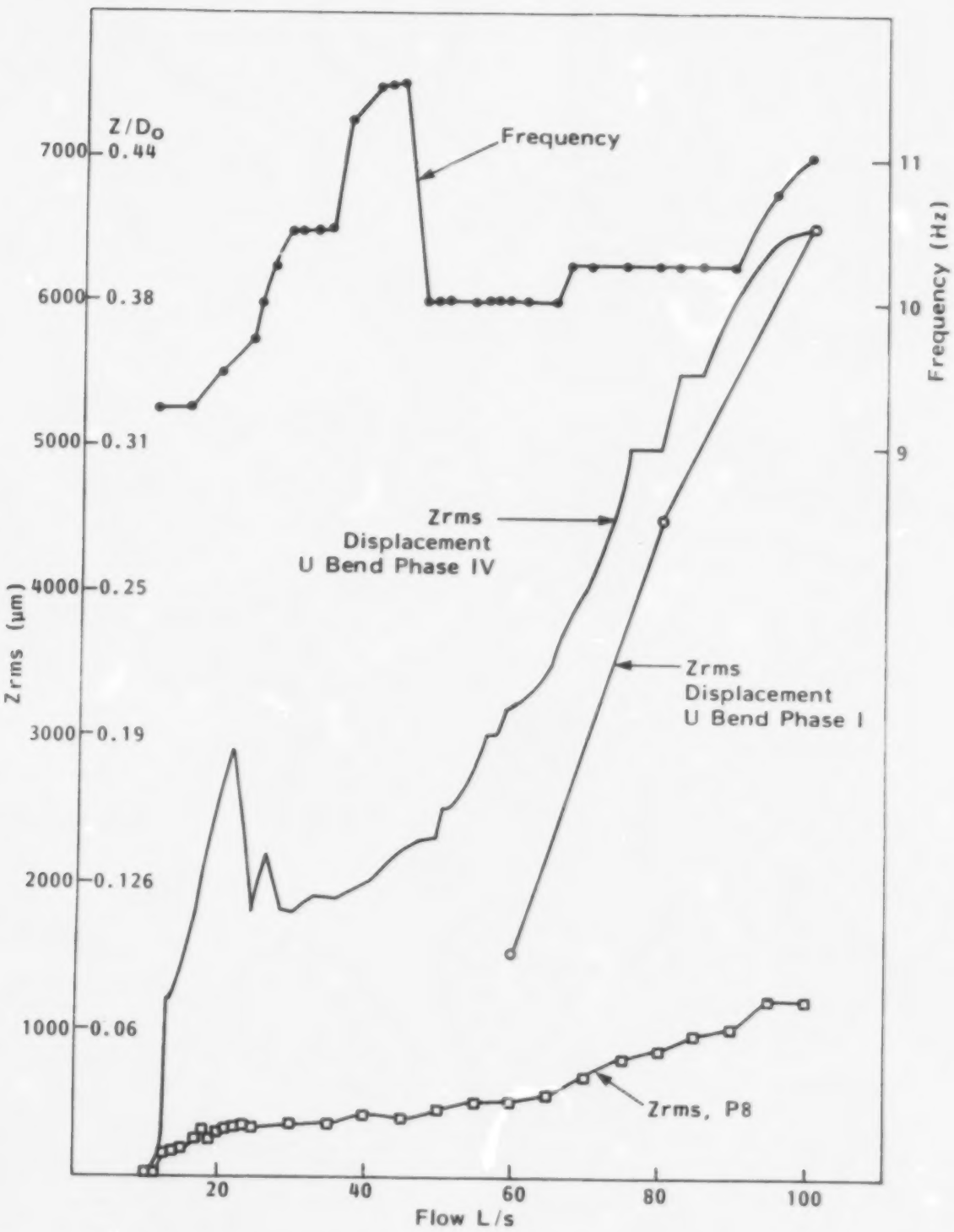

Figure 43: Phase IV Tests
Tube B-4 Displacement & Frequency vs Flow for
90° U Bend Position

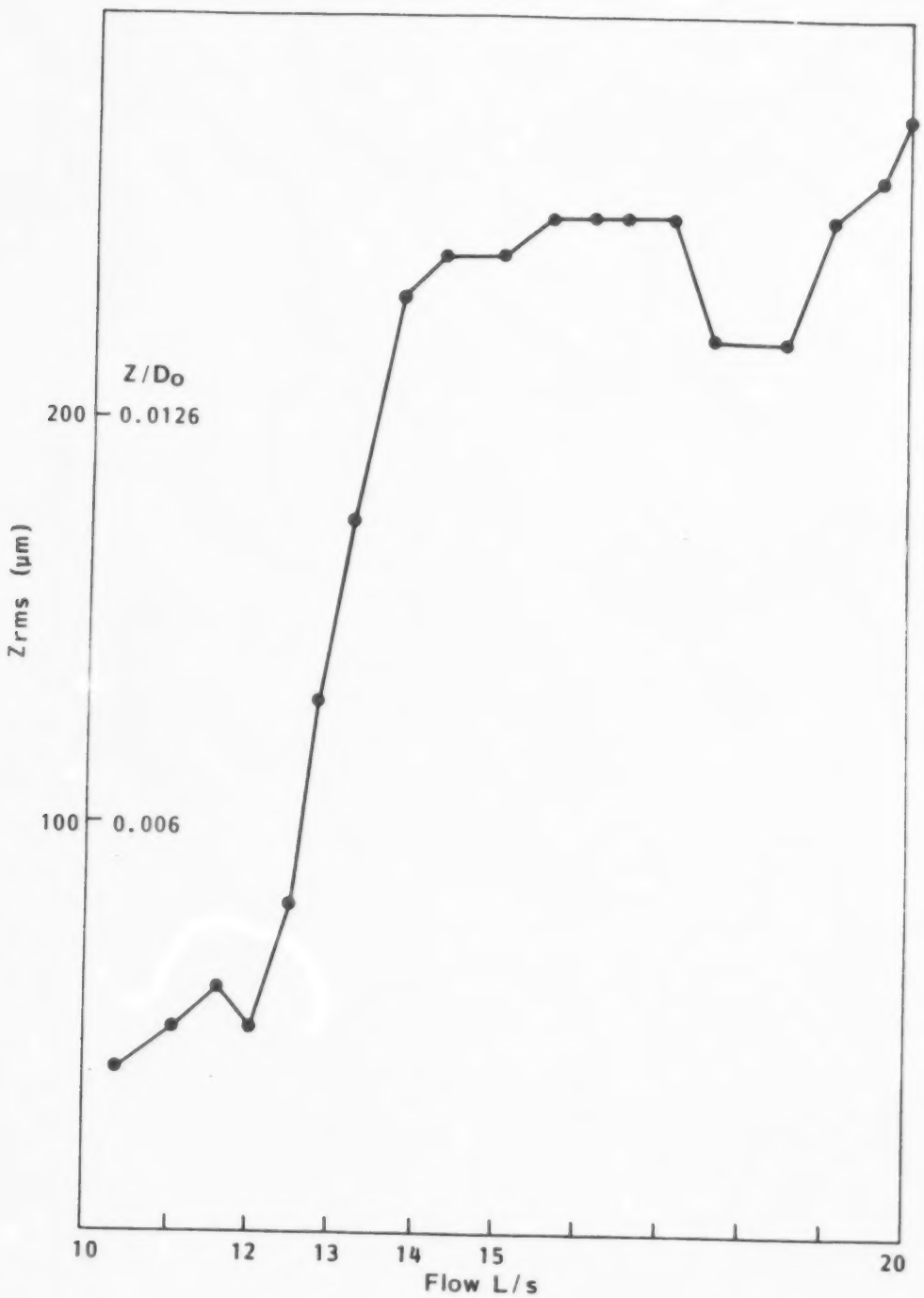

Figure 44: Test Phase IV
Zrms Displacement in Tube C-3 U Bend, 90° Position

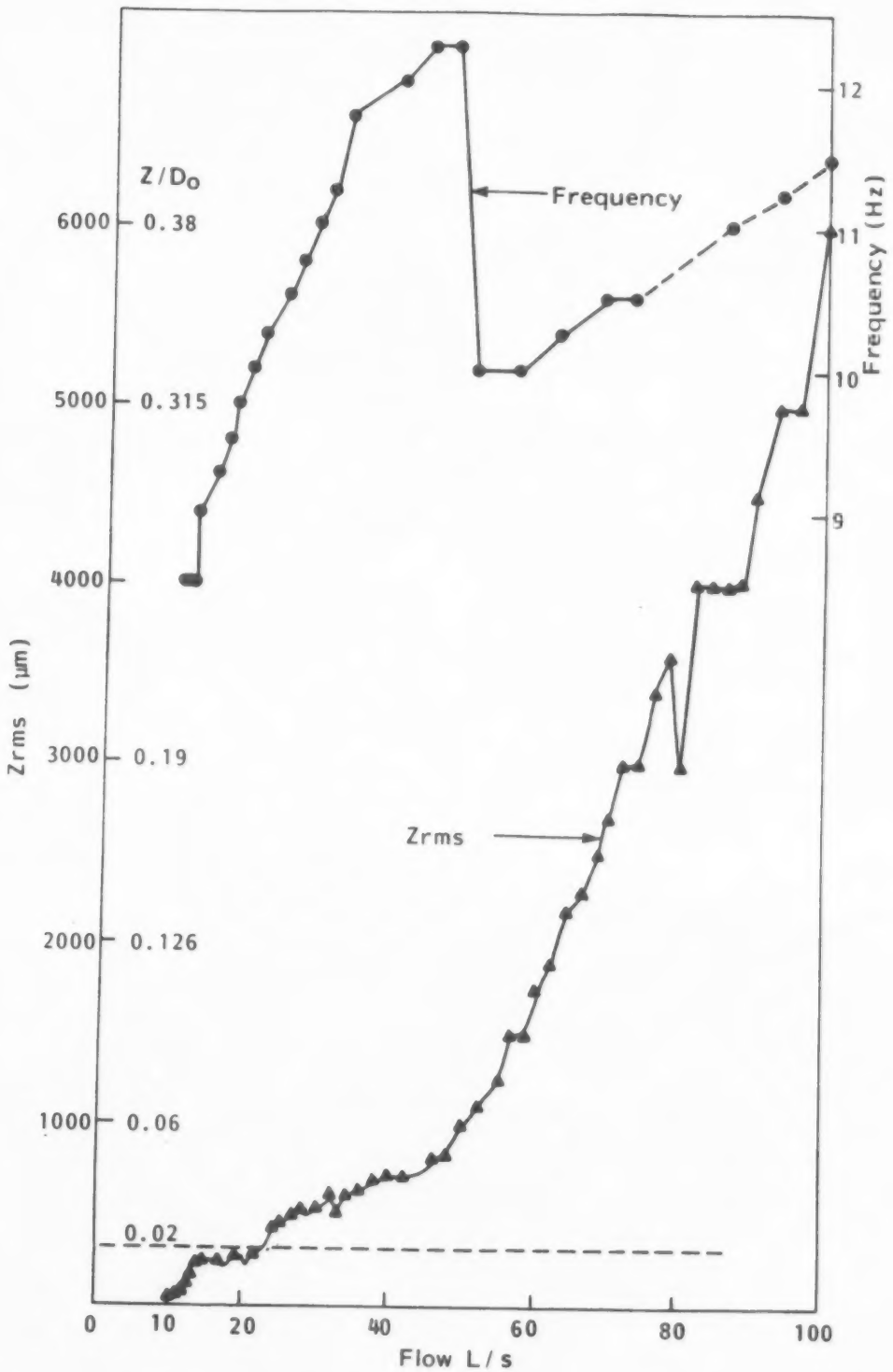

Figure 45: Phase IV
Zrms Displacement & Frequency in Tube C-3
U-Bend at the 90° Position

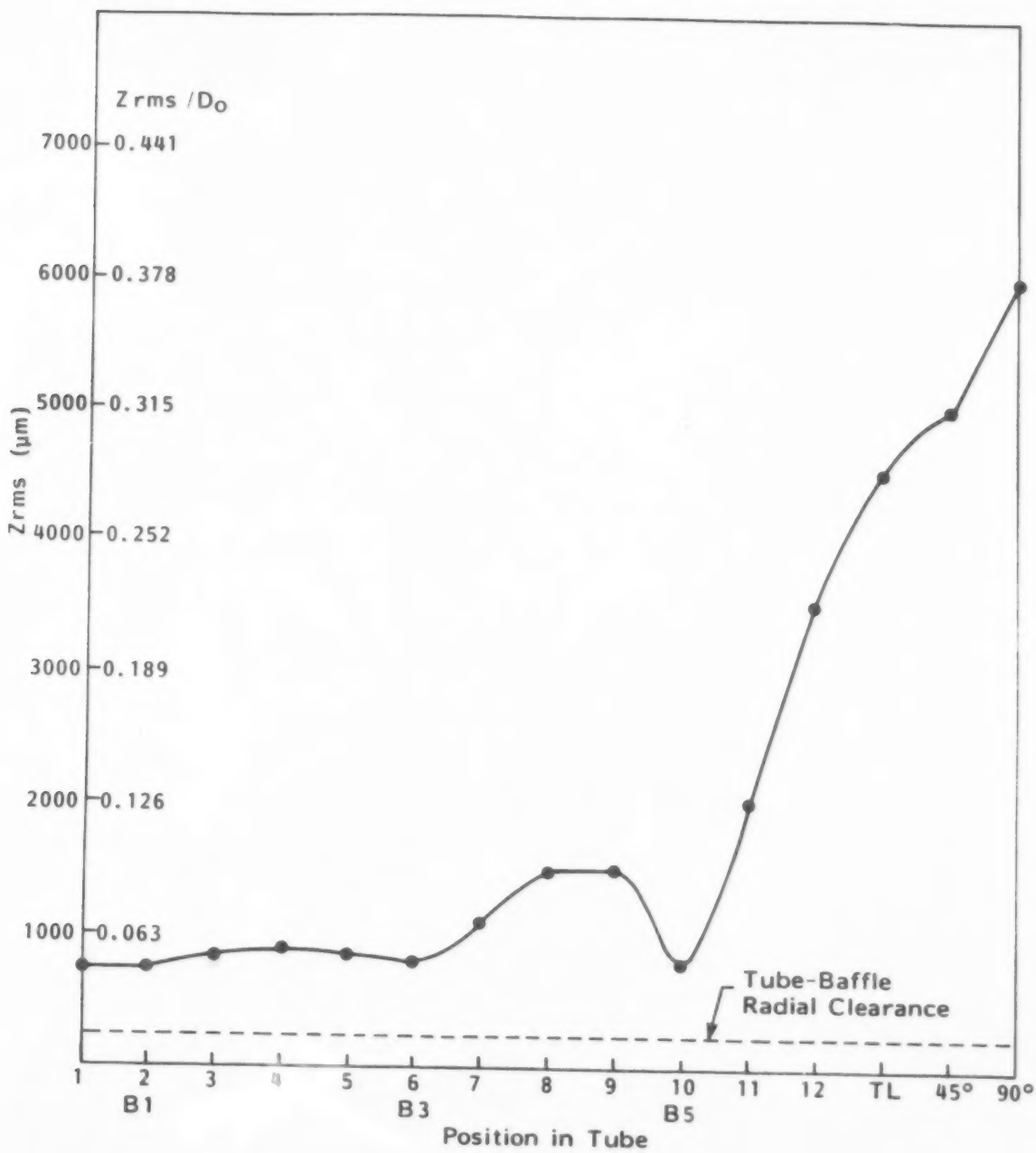

Figure 46: Phase IV
Tube C-3 Zrms Displacement @ 100 L/s

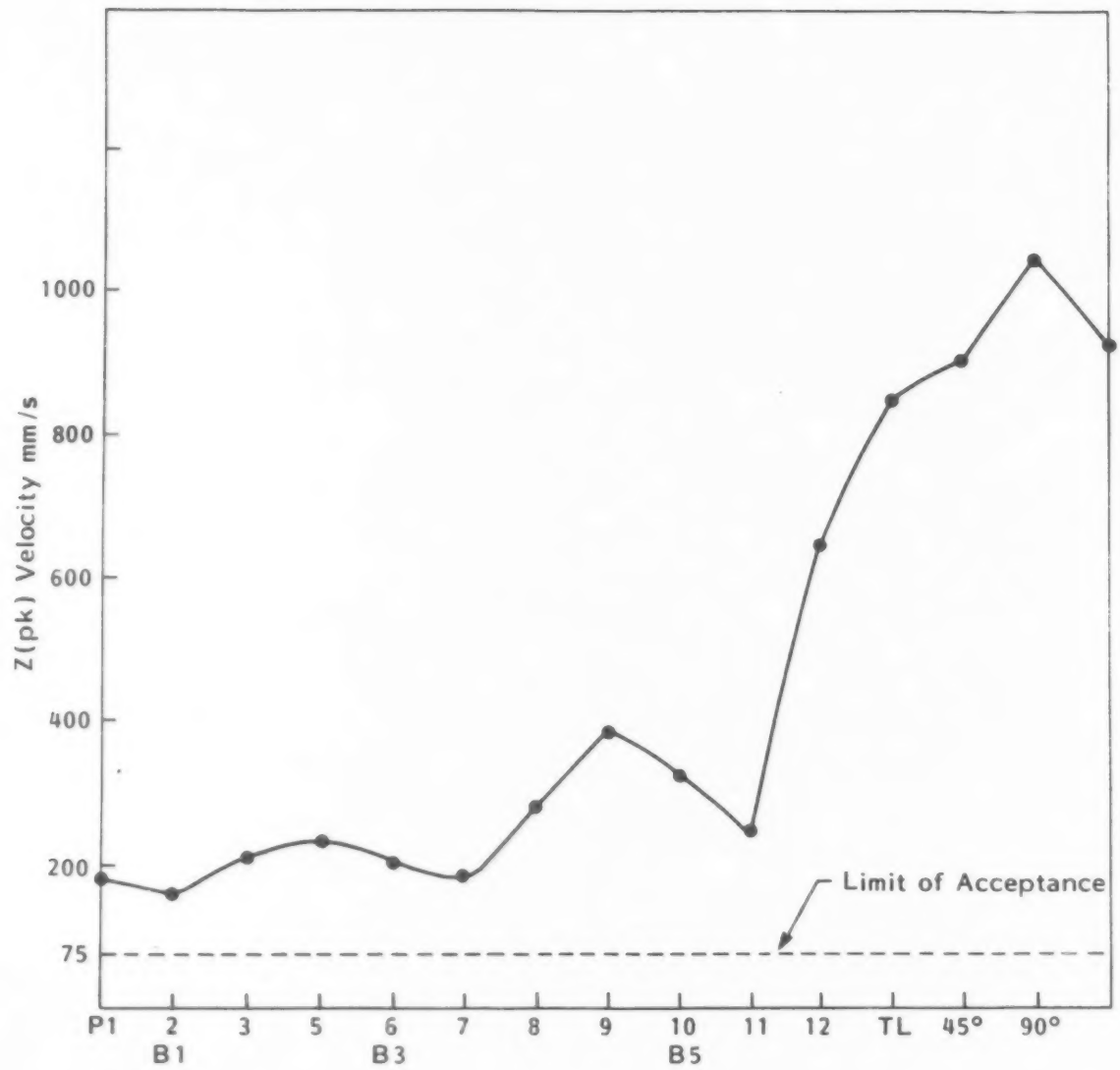

Figure 47: Phase IV
Z Peak Velocity in Tube C-3 at 100 L/s

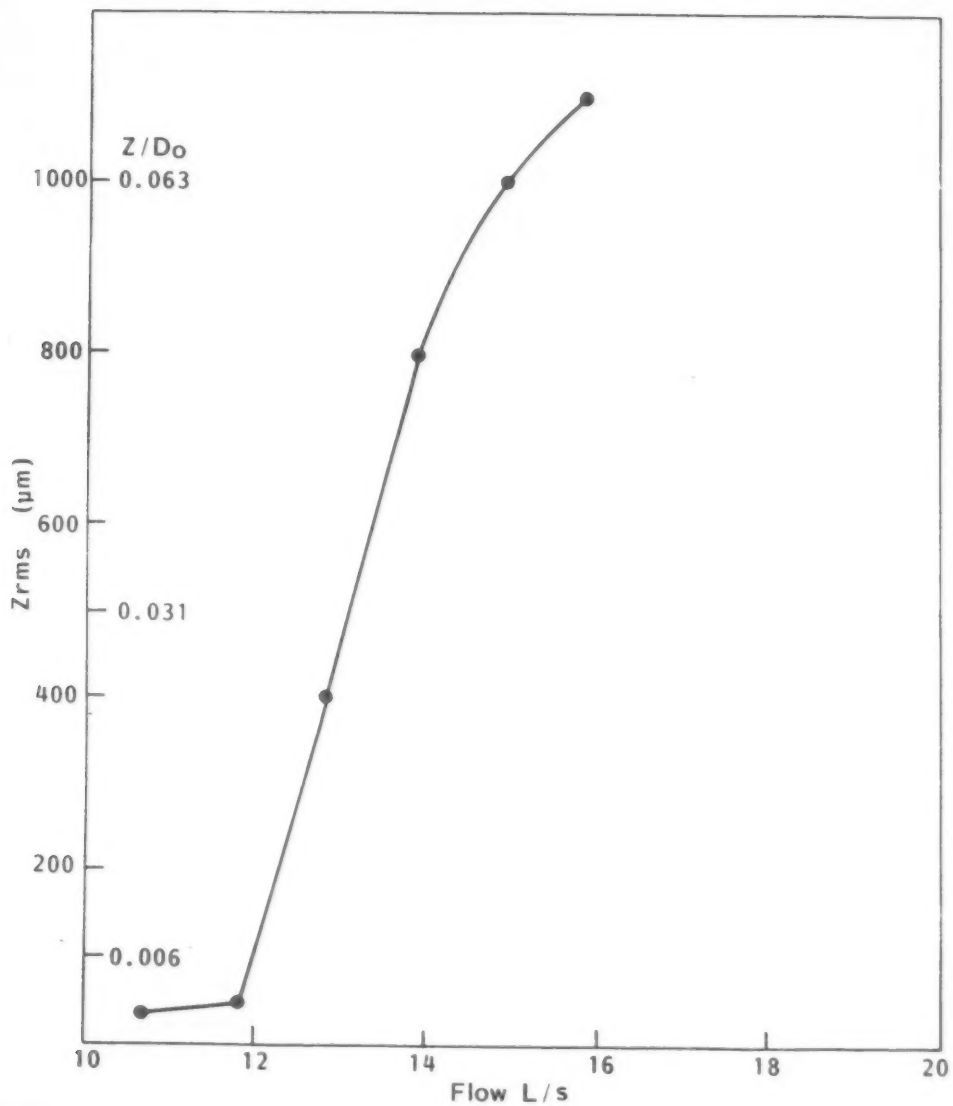

Figure 48: Phase IV
Tube D-4 U Bend Midspan Displacement vs Flow

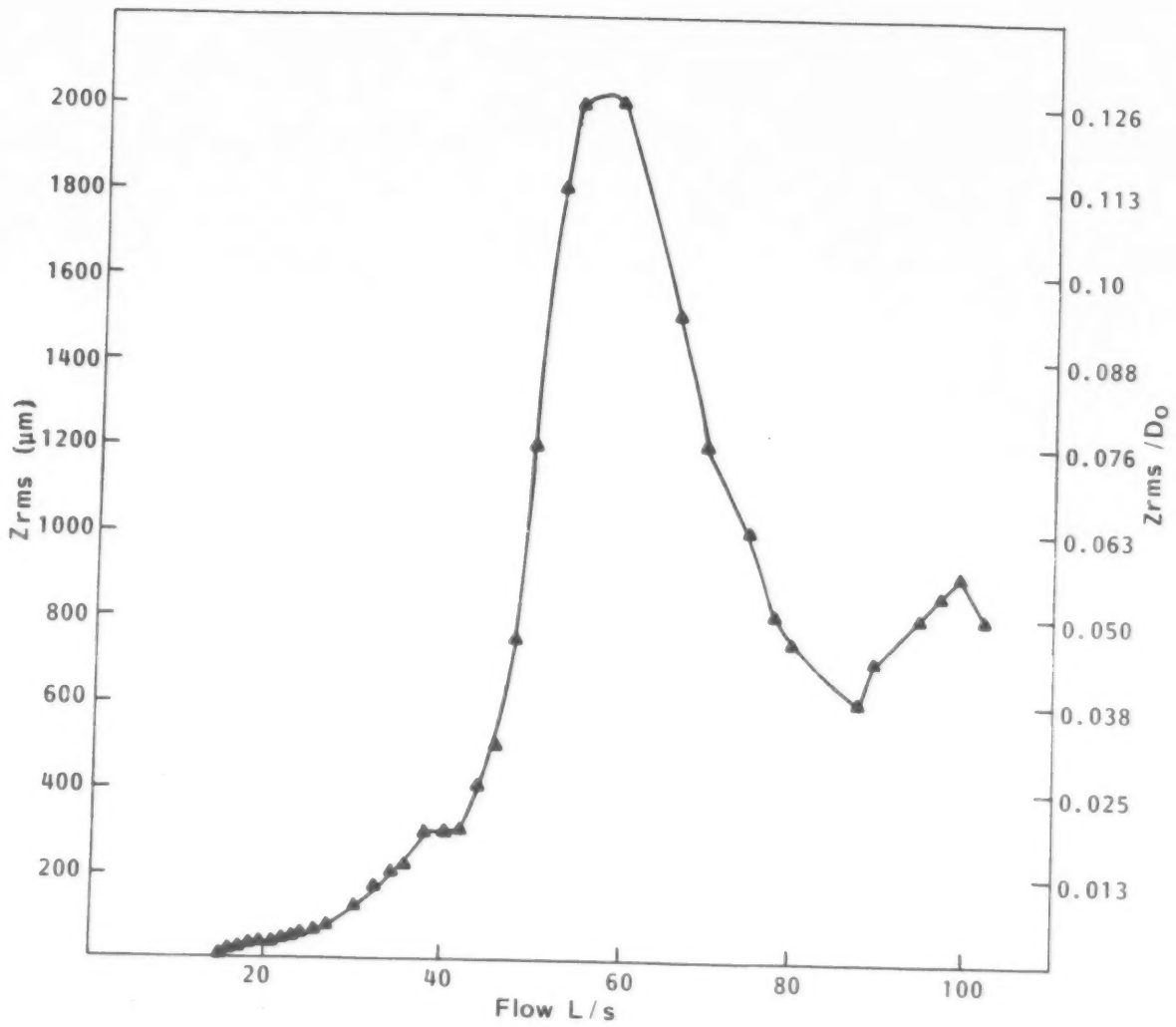

Figure 49: Phase IV
Displacement in Tube A-9 at the Tangent Line Position

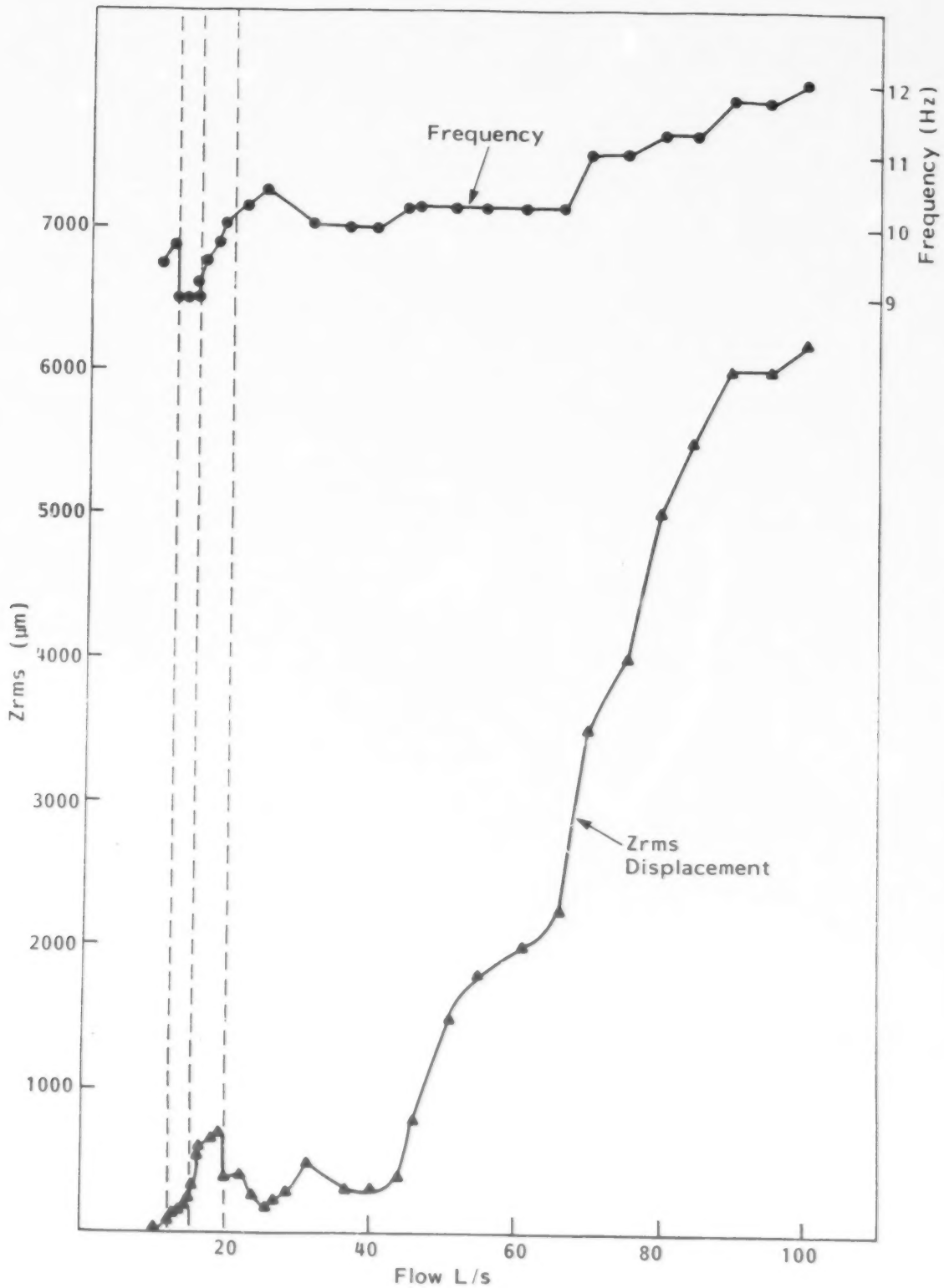

Figure 50: Phase IV Tests
Tube C-5 Zrms Displacement vs Flow for 90° U Bend Position

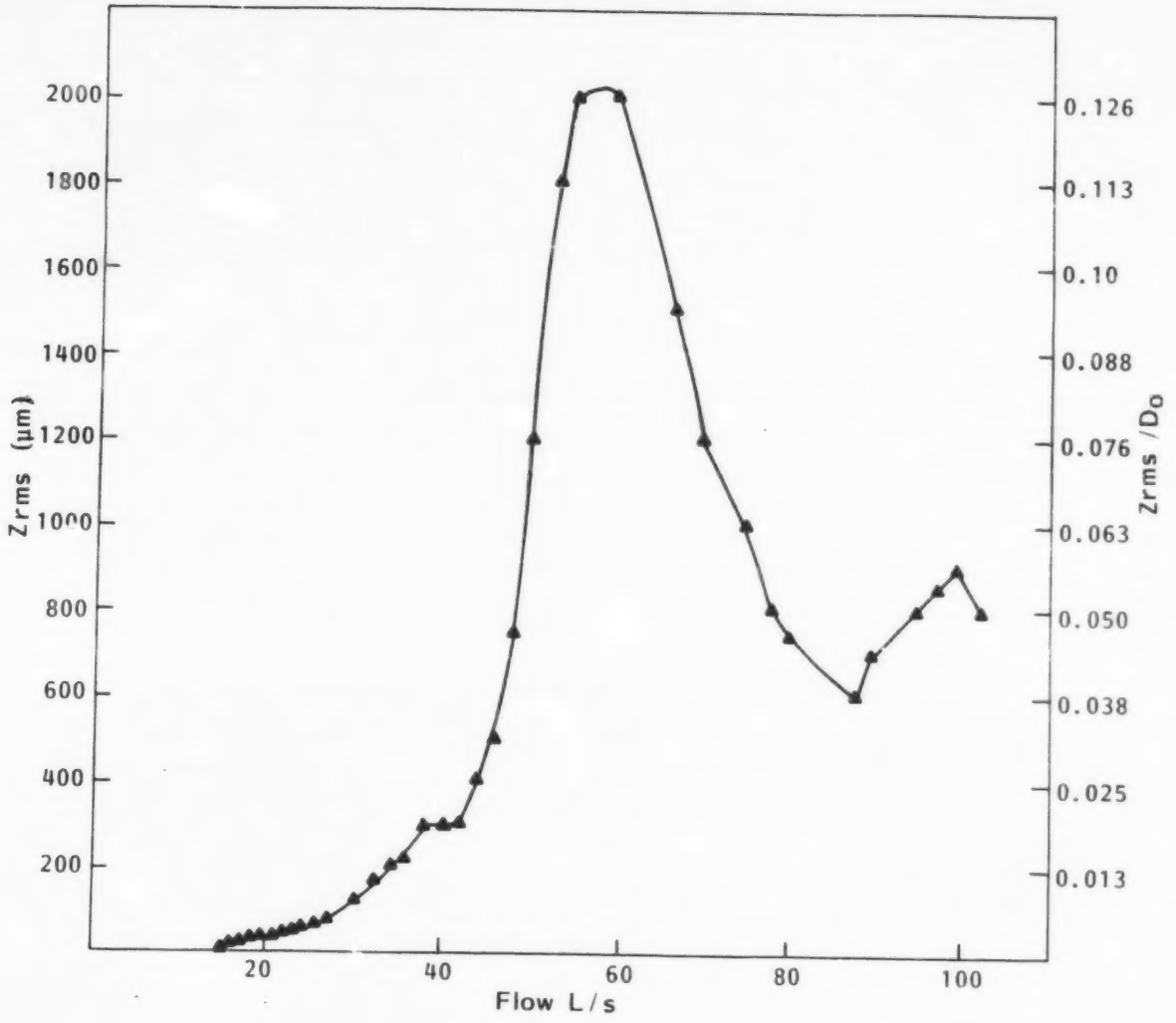

Figure 49: Phase IV
Displacement in Tube A-9 at the Tangent Line Position

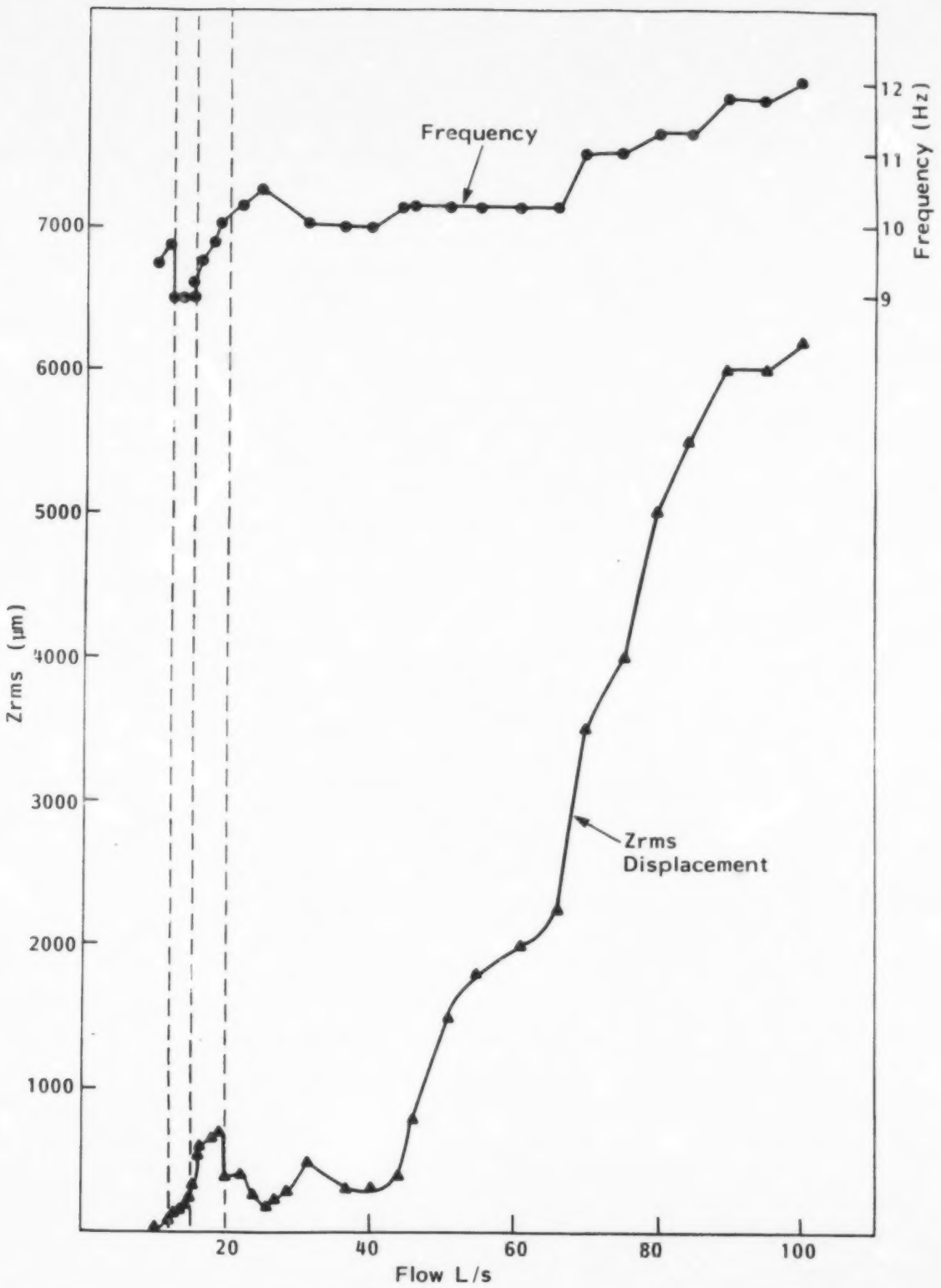

Figure 50: Phase IV Tests
Tube C-5 Zrms Displacement vs Flow for 90° U Bend Position

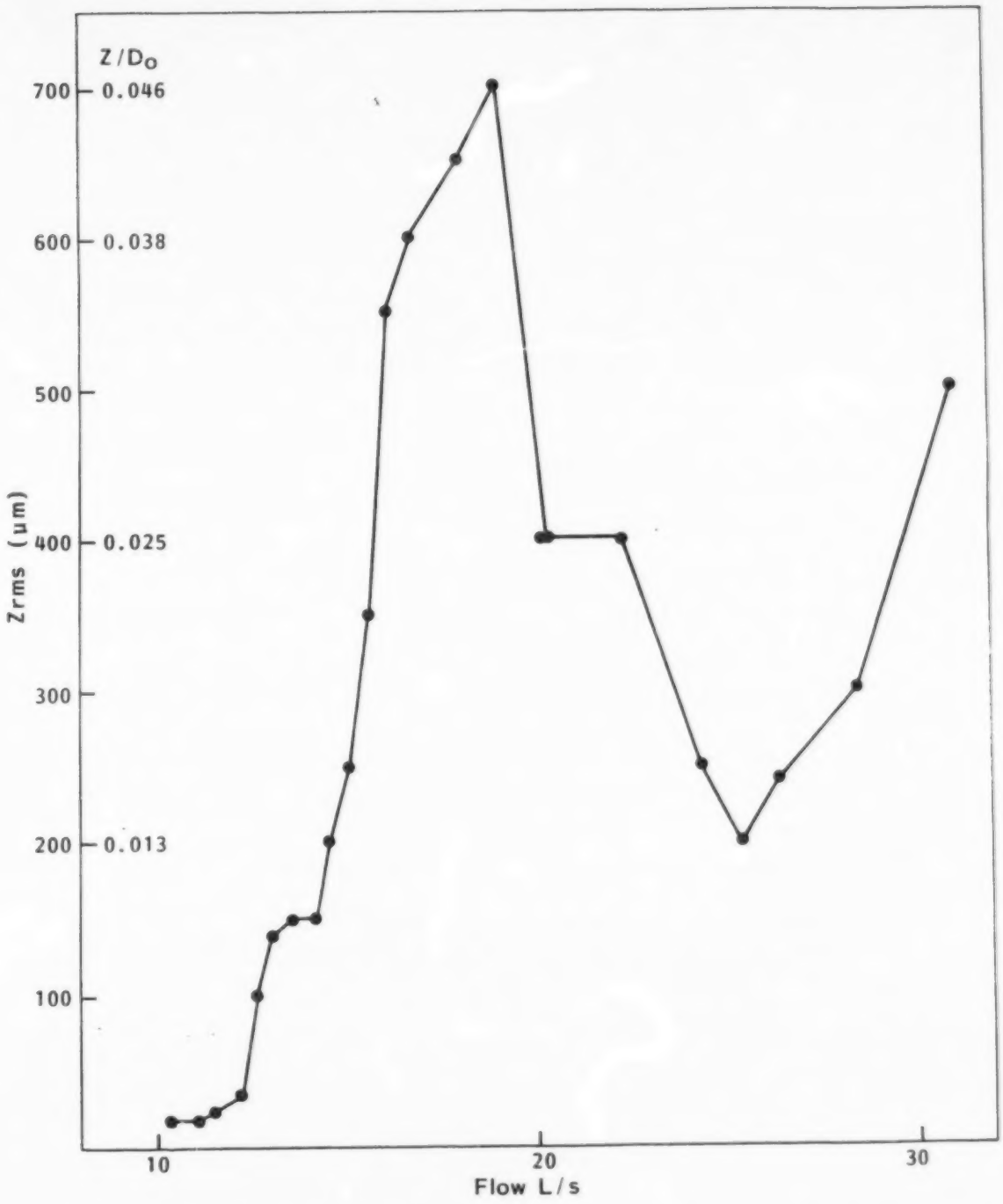

Figure 51: Phase IV Tests
Tube C-5 Zrms Displacement vs Flow at Low Flow for 90°
U Bend Position

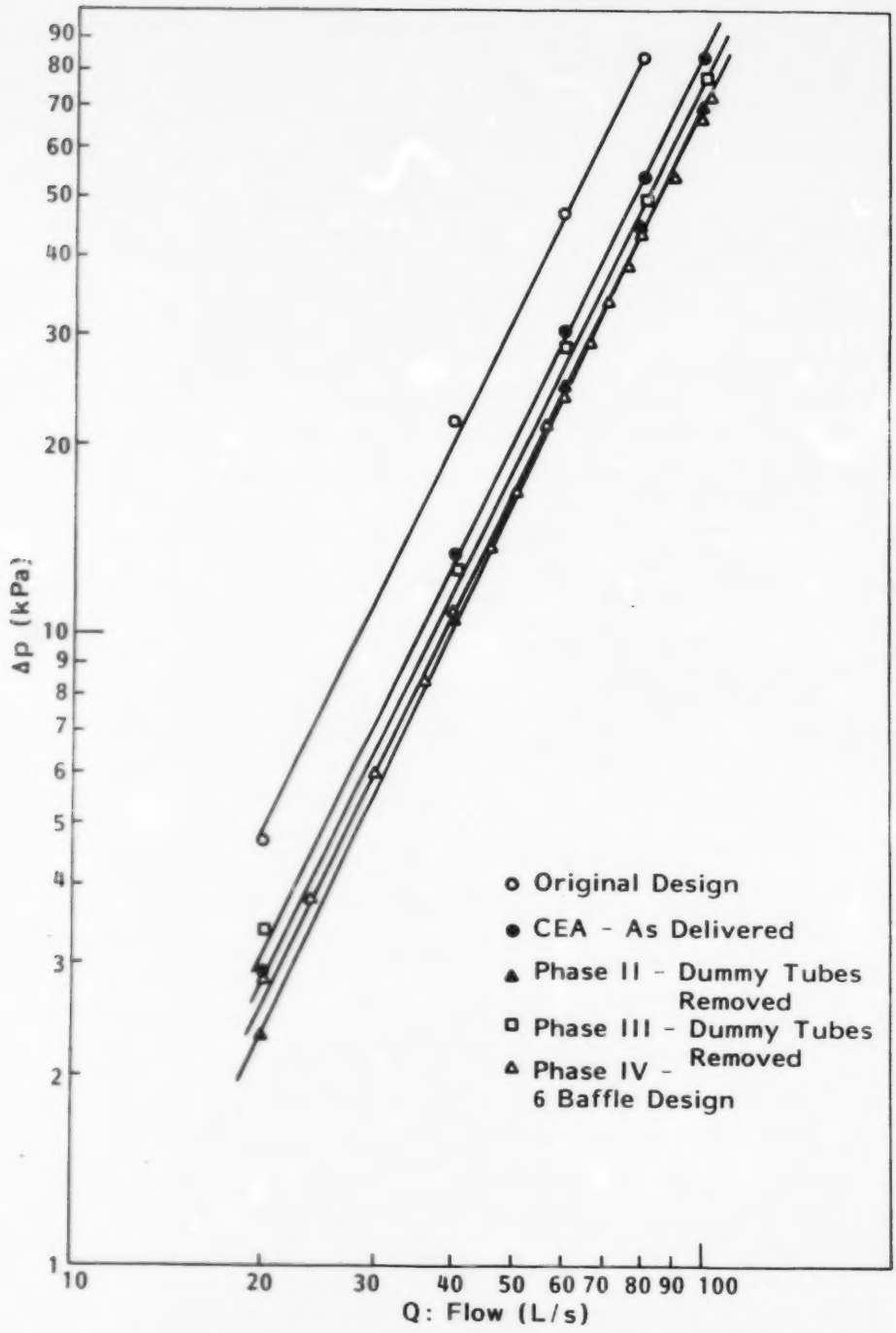

Figure 52: Overall Pressure Drop Logarithmic Plot

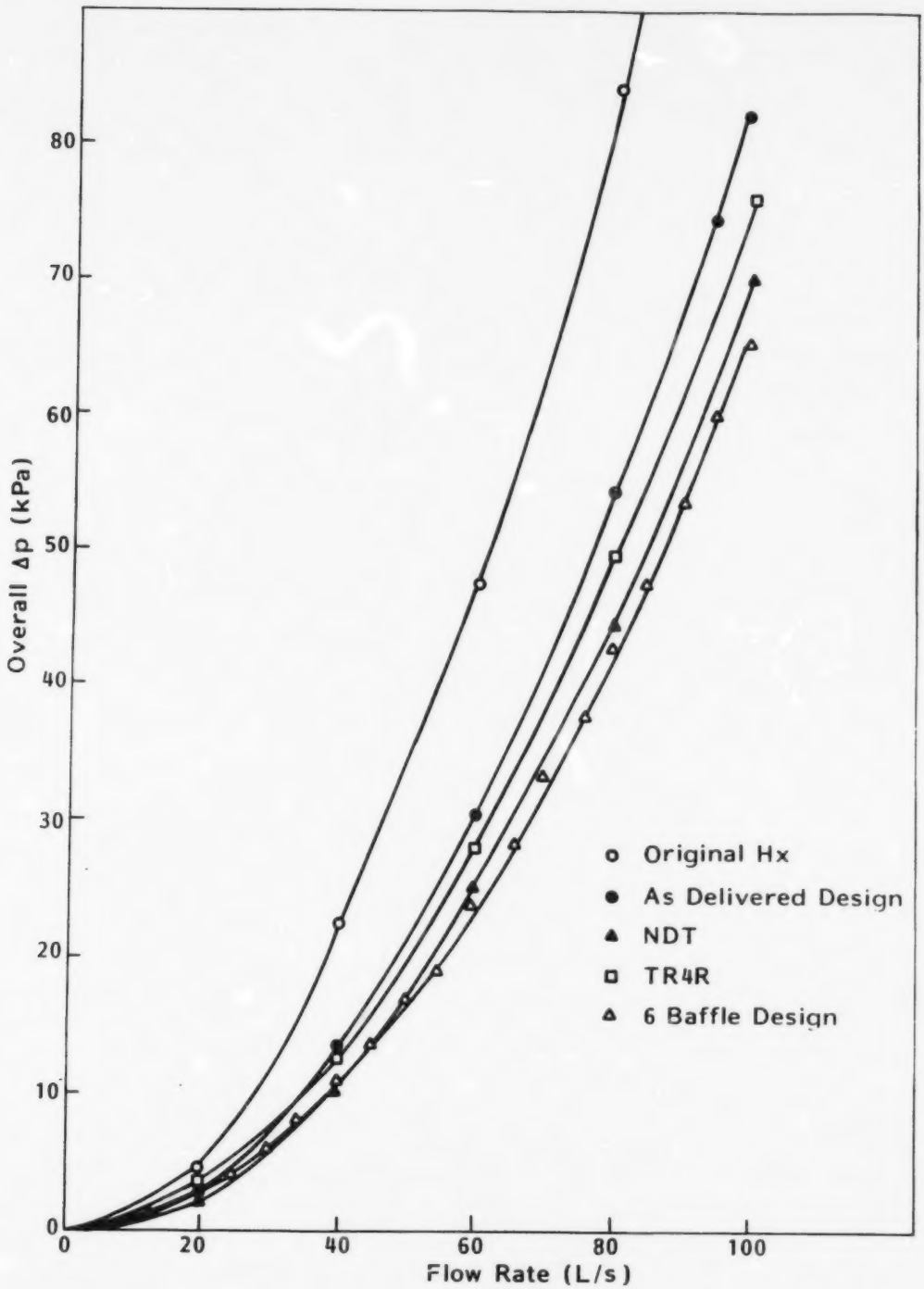

Figure 53: Plot of Overall Δp vs Flow Rate

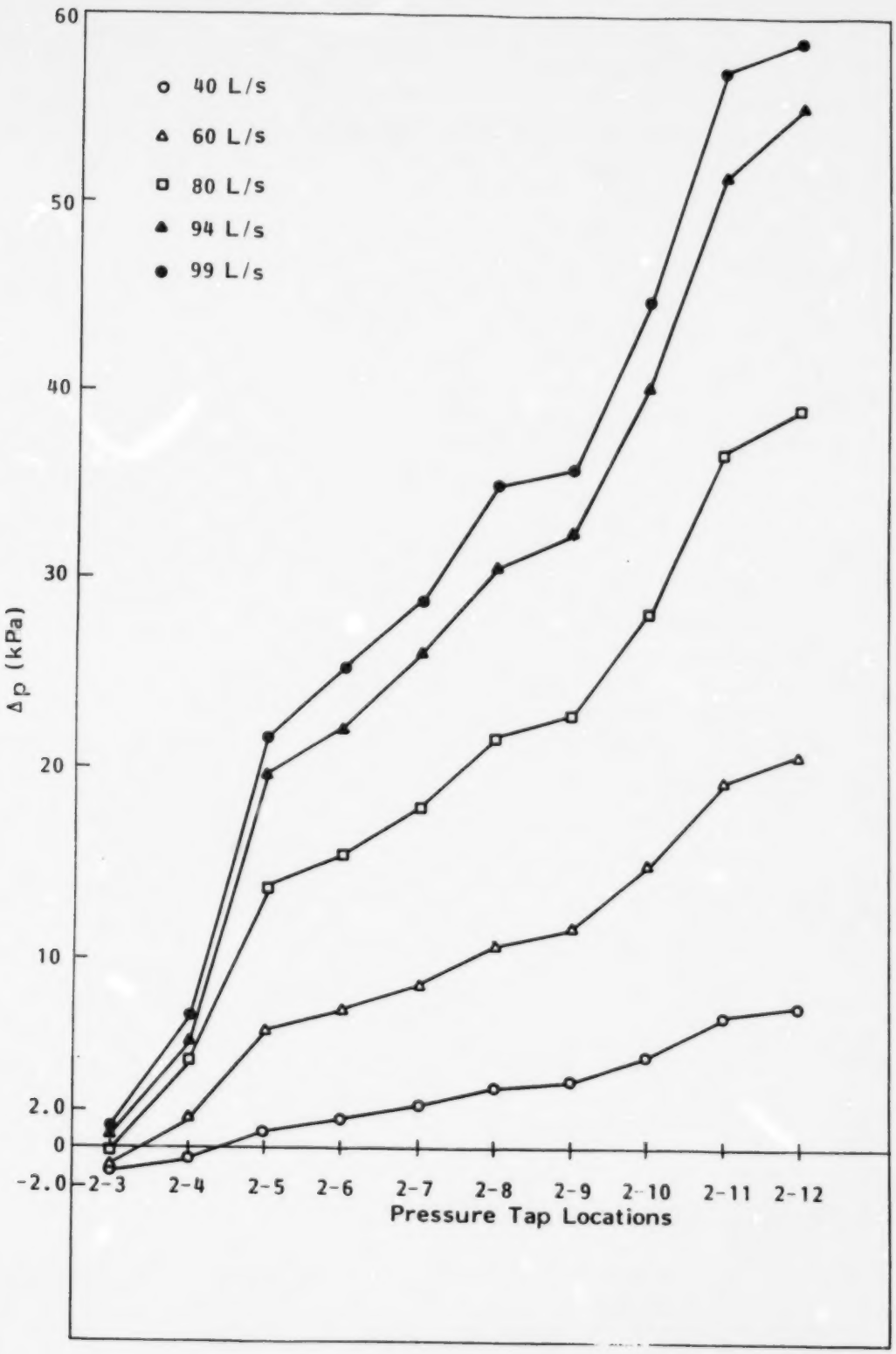

Figure 54: Phase I Tests
Baffle to Baffle Pressure Drop for all Flow Rates

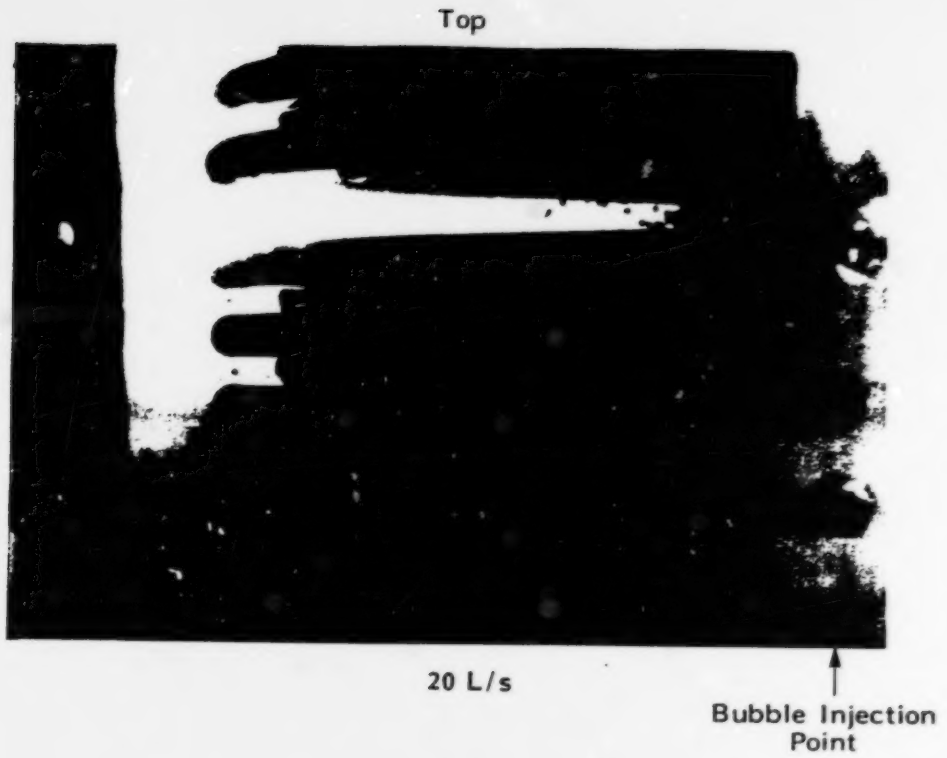

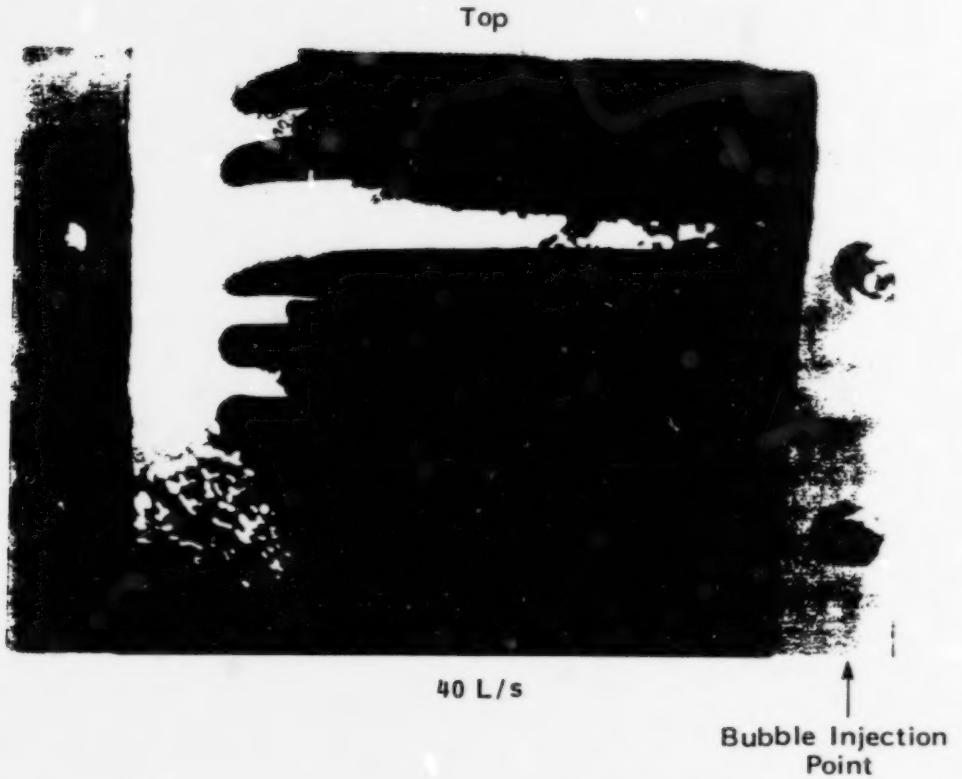

Figure 55: Flow Visualization Photographs

86-329
Cont'd

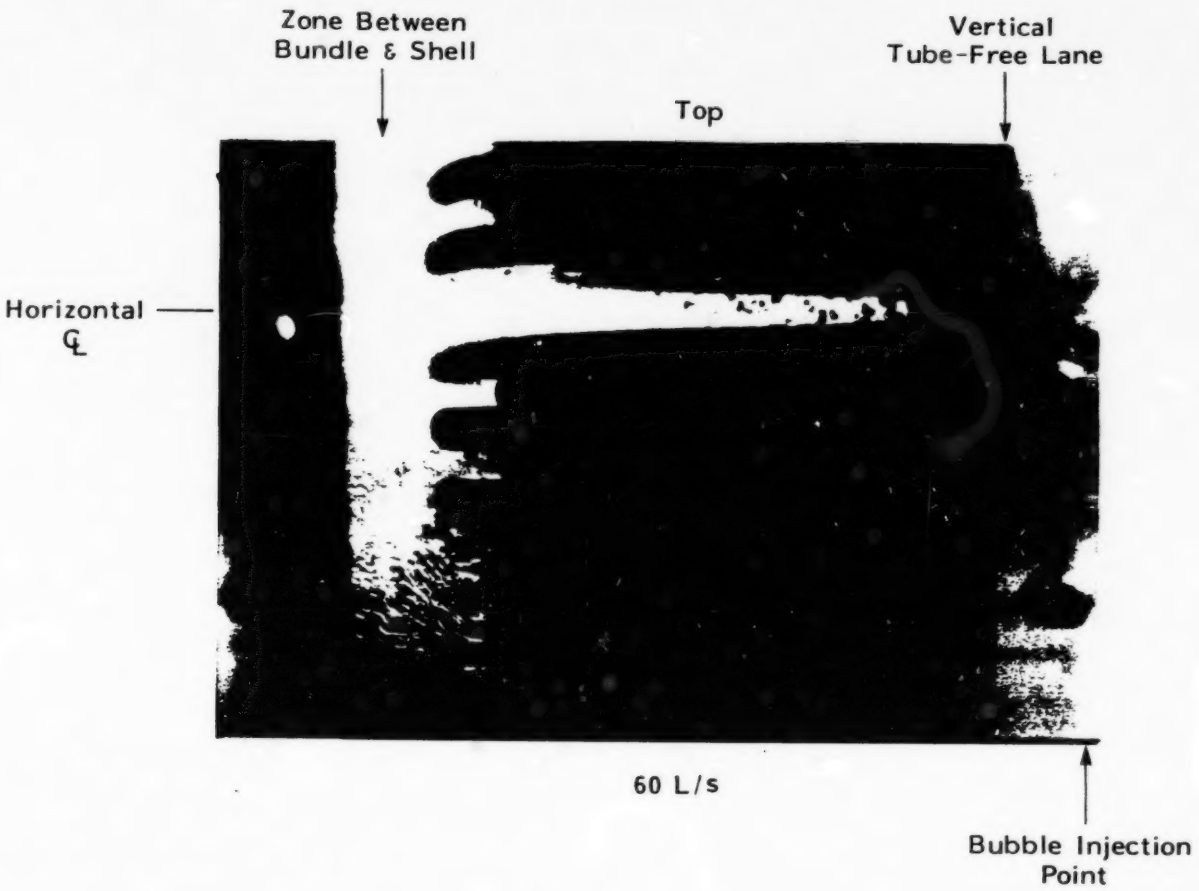

Figure 55 (Cont'd): Flow Visualization Photographs

DISTRIBUTION

Dr. D. Mills Professor M. Paidoussis	Director of Research Department of Mechanical Engineering McGill University 817 Sherbrooke W Montreal, Quebec H3A 2K6
Mr. M. Pettigrew	Chalk River Nuclear Laboratories Chalk River K0J 1J0
Dr. C.C. Gentry	Principal Process Engineer Heat Transfer 11 A2 Phillips Building Phillips Petroleum Co. Bartlesville, Oklahoma USA 74004
Mr. J. Graham	Technical & Training Serv, A7G2
Mr. H. Paetzold	Technical & Training Serv, A7F3
Mr. M. Valcic	Design & Dev - Gen, H10D10
Mr. R. Souve	Design & Dev,- Gen, H10F8
Mr. O. Nigol	Electrical Research
Mr. F. Perricone	Mechanical Research
Ms. H.L. Anderson (5)	Mechanical Research
Section File	KR277

Public Reference Centre
Editorial Section (2)
Office Copies (2)
Extra Copies (3)